



BNL-99596-2013-TECH

C-A/AP/452;BNL-99596-2013-IR

# Spin tracking simulations in AGS based on ray-tracing methods - bare lattice, no snakes -

F. Meot

July 2012

Collider Accelerator Department  
**Brookhaven National Laboratory**

**U.S. Department of Energy**

USDOE Office of Science (SC)

Notice: This technical note has been authored by employees of Brookhaven Science Associates, LLC under Contract No. DE-AC02-98CH10886 with the U.S. Department of Energy. The publisher by accepting the technical note for publication acknowledges that the United States Government retains a non-exclusive, paid-up, irrevocable, world-wide license to publish or reproduce the published form of this technical note, or allow others to do so, for United States Government purposes.

## **DISCLAIMER**

This report was prepared as an account of work sponsored by an agency of the United States Government. Neither the United States Government nor any agency thereof, nor any of their employees, nor any of their contractors, subcontractors, or their employees, makes any warranty, express or implied, or assumes any legal liability or responsibility for the accuracy, completeness, or any third party's use or the results of such use of any information, apparatus, product, or process disclosed, or represents that its use would not infringe privately owned rights. Reference herein to any specific commercial product, process, or service by trade name, trademark, manufacturer, or otherwise, does not necessarily constitute or imply its endorsement, recommendation, or favoring by the United States Government or any agency thereof or its contractors or subcontractors. The views and opinions of authors expressed herein do not necessarily state or reflect those of the United States Government or any agency thereof.

# **Spin tracking simulations in AGS based on ray-tracing methods - bare lattice, no snakes -**

**F. Meot, L. Ahrens, J. Glenn, H. Huang,  
A. Luccio, W. W. MacKay, T. Roser, N. Tsoupas**



**Collider-Accelerator Department  
Brookhaven National Laboratory  
Upton, NY 11973**

Notice: This document has been authorized by employees of Brookhaven Science Associates, LLC under Contract No. DE-AC02-98CH10886 with the U.S. Department of Energy. The United States Government retains a non-exclusive, paid-up, irrevocable, world-wide license to publish or reproduce the published form of this document, or allow others to do so, for United States Government purposes.

**Spin tracking simulations in AGS based on ray-tracing methods  
- bare lattice, no snakes -**

A work performed at BNL in September and October 2009, in collaboration with L. Ahrens, J. Glenn, H. Huang, A. Luccio, W. W. MacKay, T. Roser, N. Tsoupas

**Abstract**

This Note reports on the first simulations of and spin dynamics in the AGS using the ray-tracing code Zgoubi.

It includes lattice analysis, comparisons with MAD, DA tracking, numerical calculation of depolarizing resonance strengths and comparisons with analytical models, etc. It also includes details on the setting-up of Zgoubi input data files and on the various numerical methods of concern in and available from Zgoubi.

This work has been followed by further spin dynamics studies in presence of the AGS helical snakes, see Note CAD/AP/453.

## Contents

<b>1</b>	<b>Introduction</b>	<b>4</b>
<b>2</b>	<b>Preliminary data, working hypothesis</b>	<b>4</b>
2.1	Lattice . . . . .	4
2.1.1	A remark concerning the closed orbit length . . . . .	7
2.2	DA. Long term tracking . . . . .	7
2.2.1	Maximum stable amplitudes . . . . .	7
2.2.2	Dynamic aperture . . . . .	7
2.2.3	Symplecticity tests . . . . .	7
2.3	Quantities and formulas used in these spin tracking studies . . . . .	10
2.3.1	Working hypotheses . . . . .	10
2.3.2	Asymptotic depolarization . . . . .	10
2.3.3	Depolarization, static . . . . .	10
2.3.4	Weak resonance, Fresnel integral approximation . . . . .	11
2.3.5	Resonance strength, theoretical . . . . .	11
<b>3</b>	<b>Inventory of spin resonances, including spin tracking results</b>	<b>12</b>
3.1	Intrinsic resonances . . . . .	13
3.2	Imperfection resonances . . . . .	14
<b>4</b>	<b>Tracking through resonances</b>	<b>17</b>
4.1	Intrinsic resonances . . . . .	17
4.1.1	$\gamma G = \nu_z$ (3.648013 GeV) . . . . .	17
	$\epsilon_z/\pi = 0.01 \cdot 10^{-6}$ . . . . .	18
	$\epsilon_z/\pi = 0.05 \cdot 10^{-6}$ . . . . .	19
4.1.2	$\gamma G = 24 - \nu_z$ (7.82892 GeV) . . . . .	23
	$\epsilon_z/\pi = 0.1 \cdot 10^{-6}$ . . . . .	24
4.1.3	$\gamma G = 12 + \nu_z$ (7.82892 GeV) . . . . .	25
	$\epsilon_z/\pi = 0.002 \cdot 10^{-6}$ . . . . .	26
	$\epsilon_z/\pi = 2 \cdot 10^{-6}$ . . . . .	27
4.1.4	$\gamma G = 23 + \nu_z$ (15.68487 GeV) . . . . .	28
4.1.5	$\gamma G = 24 + \nu_z$ (16.20822 GeV) . . . . .	29
	$\epsilon_z/\pi = 2 \cdot 10^{-6}$ . . . . .	30
	$\epsilon_z/\pi = 30 \cdot 10^{-6}$ . . . . .	31
4.1.6	$\gamma G = 36 - \nu_z$ (13.31575 GeV) . . . . .	32
4.1.7	$\gamma G = 48 - \nu_z$ (19.59585 GeV) . . . . .	35
	$\epsilon_z/\pi = 0.125 \cdot 10^{-6}$ . . . . .	36
	$\epsilon_z/\pi = 0.25 \cdot 10^{-6}$ . . . . .	37
	$\epsilon_z/\pi = 0.5 \cdot 10^{-6}$ . . . . .	38
	$\epsilon_z/\pi = 10^{-6}$ . . . . .	39
	$\epsilon_z/\pi = 2 \cdot 10^{-6}$ . . . . .	40
4.1.8	$\gamma G = 48 - \nu_z$ , bare lattice (all bends' sextu off, all quads off) . . . . .	41
	$\epsilon_z/\pi = 10^{-6}$ . . . . .	42
4.1.9	$\gamma G = 36 + \nu_z$ (22.48832 GeV) . . . . .	43
	$\epsilon_z/\pi = 0.002 \cdot 10^{-6}$ . . . . .	44
	$\epsilon_z/\pi = 0.02 \cdot 10^{-6}$ . . . . .	45
4.2	Imperfection resonances . . . . .	47
4.2.1	$\gamma G = 9$ (3.77180 GeV) . . . . .	47
	$\hat{z}_{co} = 2.77$ mm . . . . .	48
4.2.2	$\gamma G = 12$ (5.341830 GeV) . . . . .	50
4.2.3	$\gamma G = 13$ (5.865171 GeV) . . . . .	53

4.2.4	$\gamma G = 23$ (11.09859 GeV) . . . . .	56
4.2.5	$\gamma G = 27$ (13.19196 GeV) . . . . .	59
4.2.6	$\gamma G = 45$ (22.61211 GeV) . . . . .	62
<b>5</b>	<b>Static neighboring of resonances</b>	<b>65</b>
5.1	Intrinsic resonances . . . . .	65
5.1.1	$\gamma G = \nu_z$ (3.648013 GeV) . . . . .	65
	$\epsilon_z/\pi = 0.0019 \cdot 10^{-6}$ . . . . .	66
	$\epsilon_z/\pi = 0.017 \cdot 10^{-6}$ . . . . .	68
5.1.2	$\gamma G = 48 - \nu_z$ (19.59585 GeV) . . . . .	70
	$\epsilon_z/\pi = 0.125 \cdot 10^{-6}$ . . . . .	71
	$\epsilon_z/\pi = 2 \cdot 10^{-6}$ . . . . .	73
5.1.3	$\gamma G = 36 + \nu_z$ (22.48832 GeV) . . . . .	75
	$\epsilon_z/\pi = 0.0017 \cdot 10^{-6}$ . . . . .	76
	$\epsilon_z/\pi = 0.17 \cdot 10^{-6}$ . . . . .	78
<b>6</b>	<b>Fresnel integrals approximation of weak resonances</b>	<b>80</b>
	$\gamma G = \nu_z, \epsilon_z/\pi = 0.002 \cdot 10^{-6}$ . . . . .	80
	$\gamma G = \nu_z, \epsilon_z/\pi = 0.01 \cdot 10^{-6}$ . . . . .	80
	$\gamma G = 36 + \nu_z, \epsilon_z/\pi = 0.0001 \cdot 10^{-6}$ . . . . .	81
	$\gamma G = 9, z_{CO} = 1.3$ mm . . . . .	81
	$\gamma G = 45, z_{CO} = 0.028$ mm . . . . .	81
<b>7</b>	<b><math>\vec{n}_0</math> spin vector, AGS bare lattice</b>	<b>82</b>
	<b>Appendix</b>	<b>84</b>
<b>A</b>	<b>MAD files</b>	<b>84</b>
A.1	Command file . . . . .	84
A.2	“print” file . . . . .	84
<b>B</b>	<b>Zgoubi data file specimen</b>	<b>85</b>
B.1	1-turn first order mapping calculation . . . . .	85
B.2	Zgoubi files, $\vec{n}_0$ vector search using FIT . . . . .	86
B.3	Zgoubi files, ring closed orbit search using FIT . . . . .	87

## 1 Introduction

Simulations of crossing and neighboring of spin resonances in AGS ring, bare lattice, without snake, have been performed, in order to assess the capabilities of Zgoubi in that matter, and are reported here. This yields a rather long document. The two main reasons for that are, on the one hand the desire of an extended investigation of the energy span, and on the other hand the fact that in doing so, it has been discovered that the agreement with DEPOL values for the resonance strengths is not good for weak resonances, thus entailing even more systematic exploration of the effects.

As to this disagreement in the resonance strengths, whether the weak reasoning is in Zgoubi or in DEPOL needs be determined, this is being worked at.

Section 2 details the working hypothesis : AGS lattice data, formulae used for deriving various resonance related quantities from the ray-tracing based “numerical experiments”, etc.

Section 3 gives inventories of the intrinsic and imperfection resonances together with the strengths derived from the ray-tracing.

Section 4 and Section 4.2 give the details of the numerical simulations of resonance crossing, including behavior of various quantities (close orbit, synchrotron motion, etc.) aimed at controlling that the conditions of particle and spin motions are correct.

In a similar manner Section 5 gives the details of the numerical simulations of spin motion in the static case : fixed energy in the neighboring of the resonance.

Section 7 shows the computation of the  $\vec{n}$  vector in the AGS lattice and tuning considered.

Many details on the numerical conditions as data files etc. are given in the Appendix Section, pages A and sqs.

## 2 Preliminary data, working hypothesis

This section details the working hypothesis, from both viewpoints of lattice data and of ray-tracing basic dynamics outputs.

### 2.1 Lattice

Tab. 1 displays the general optical parameters as obtained from MAD8, various input/output files of concern are reproduced in App. A.

Zgoubi optics file is translated from MAD8 “survey” output (a translator is available), parameter values so obtained are given in the middle col. (“Brute from MAD8) in Tab. 1 for comparison with MAD ones. A typical “zgoubi.dat” input file is displayed in App. B.1.

Note the  $\approx 3.2$  cm difference in orbit length (see below) and the  $\approx 9\%$  difference in  $D_x$ , to be explained.

Table 1: AGS parameters. The middle column “Brute from MAD8” gives the working conditions in the numerical experiments reported in the following sections. The right most column shows how some parameter have to evolve so to obtain zero closed orbit at main bend ends.

		MAD8	Ray-tracing <sup>1</sup> (Hard edge)	
			Brute from MAD8	Adjusted c.o. length <sup>5</sup>
Reference momentum	(relative)	1	1	1.00280
Orbit length <sup>4</sup>	(m)	807.07564	807.04378	807.07564
Perimeter of polygon <sup>(6)</sup>	(m)		807.06007	
Q <sub>x</sub> , Q <sub>y</sub>		8.71060, 8.76438	[8].71195, [8].76346 <sup>2</sup>	[8].65346, [8].76816
Q' <sub>x</sub> , Q' <sub>y</sub>		-22.7340, 1.7343	-20.9864, 1.7943	
$\alpha$ , $\sqrt{1/\alpha}$		0.01401, 8.44965	0.01400, 8.45102	
<i>Periodic functions at “Begin AGS” :</i>				
$\beta_x$ , $\beta_y$	(m)	19.785, 11.701	19.8432, 11.6751	
$\alpha_x$ , $\alpha_y$		-1.585, 1.037	-1.588, 1.033	
$D_x$ , $D'_x$	(m,-)	2.211, 0.154	2.034, 0.144	
closed orbit, $x_{co}$ , $x'_{co}$	mm, mrad	0, 0	-6.43 -0.50 <sup>1,3</sup>	$\approx 0$ , $\approx 0$

<sup>1</sup> Combined function dipoles are simulated using straight axis multipoles and  $d^n B/dx^n$  gradients, the “MULTIPOL” keyword, whereas MAD uses SBEND.

<sup>2</sup> Obtained from either coordinate interpolation or multiturn Fourier analysis.

<sup>3</sup> The c.o. is induced by straight axis dipole and multipole components.

<sup>4</sup> Note the substantial difference in orbit lengths - origin to be determined.

<sup>5</sup> Closed orbit adjusted using FIT procedure, zgoubi.dat data in App. B.3.

<sup>6</sup> Polygon is comprised of the axis of optical elements, all straight.

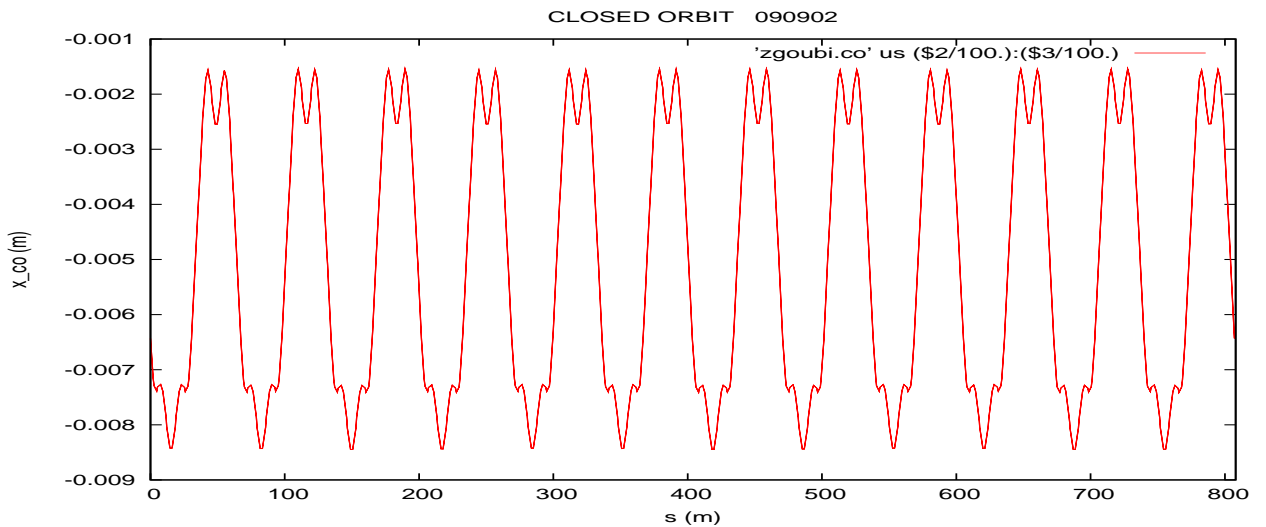
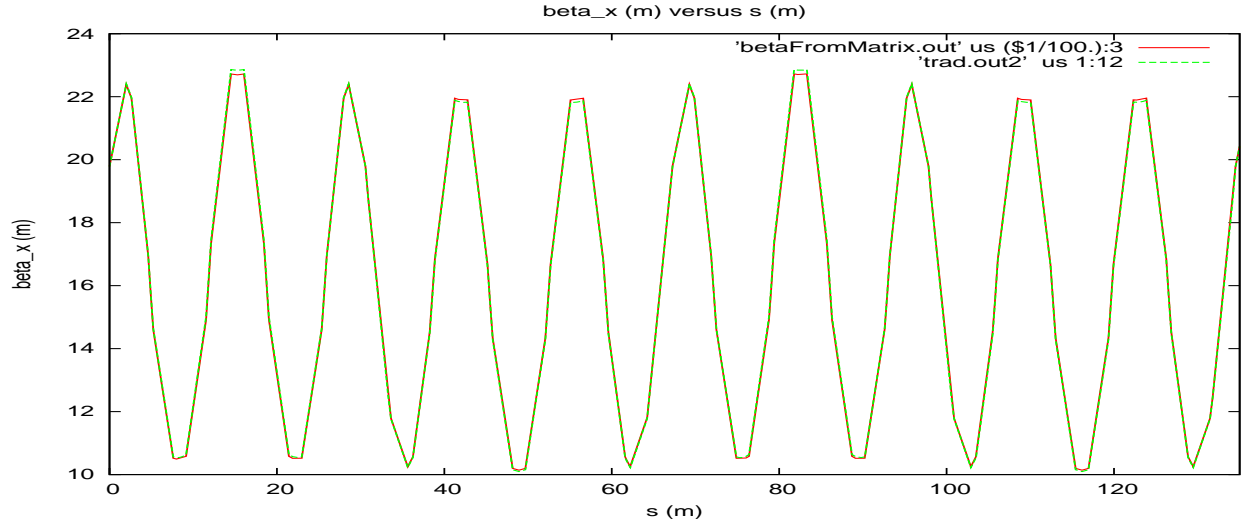
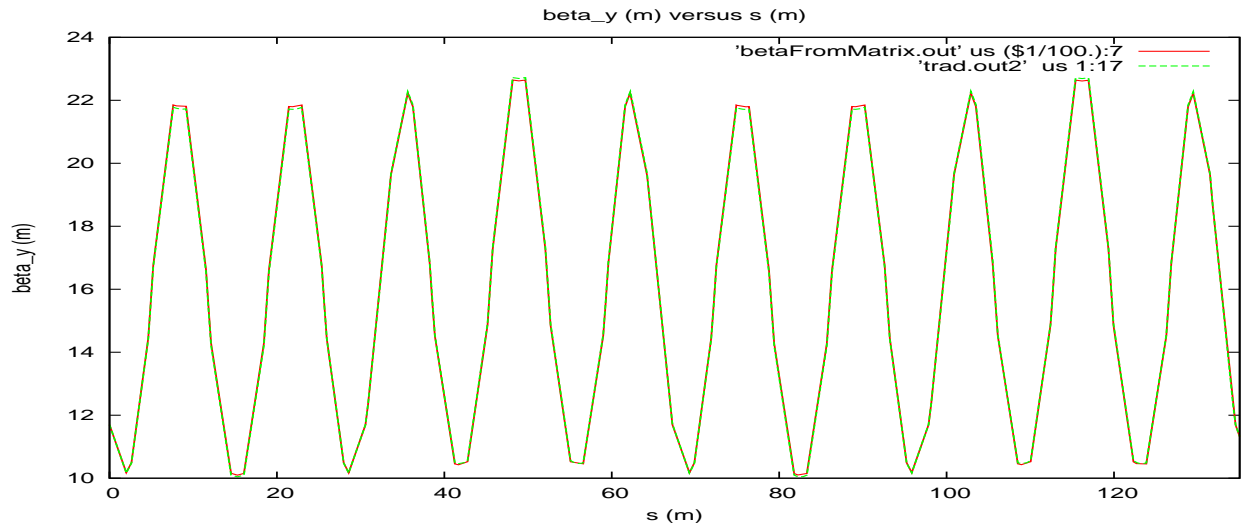
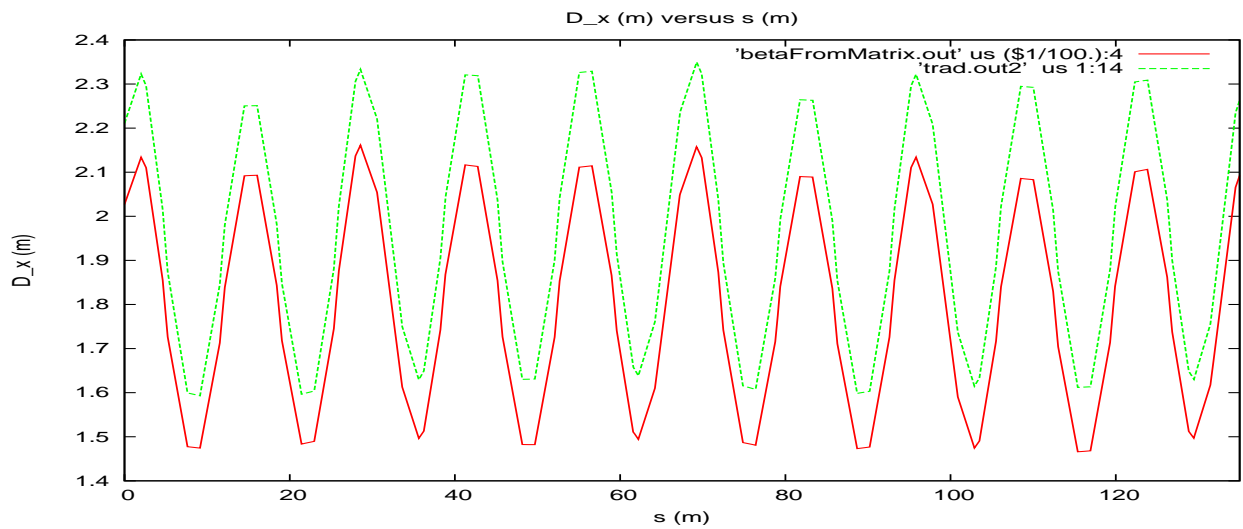


Figure 1: Closed orbit, induced by straight axis in bends (all hard-edge model).



## A superimposition of MAD/TWISS and Zgoubi outputs :

Figure 2:  $\beta_x$  over the first two superperiods.Figure 3:  $\beta_y$  over the first two superperiods.Figure 4:  $D_x$  over the first two superperiods.

### 2.1.1 A remark concerning the closed orbit length

The problem is the following : brute translation from MAD8 yields 3.2 cm shorter on-momentum closed orbit length from zgoubi (807.04378 m/zgoubi compared to 807.075641/MAD8, see cols. 1, 2 in Tab. 1.

Getting identical lengths can be achieved by changing the reference momentum, according to

$$\Delta\mathcal{L}/L = \alpha \delta p/p$$

$\alpha = 0.01400$ , an increase of  $\Delta\mathcal{L}/L = (807.075641 - 807.04378)/807.04378$  (Tab. 1), indicate that increasing the reference momentum in zgoubi by  $dp/p \approx 2.8 \cdot 10^{-3}$  is required.

However the closed orbit needs be found again for that new reference momentum value, so we use the FIT procedure to take care of both operations. The result in zgoubi.res is reproduced in App. B.3. (Note that, would tunes be matched using possible main bend windings, tune constraints could be added in the FIT.)

Tunes then change due to chromaticity mostly, according to

$$\Delta\nu_x = \xi_x \delta p/p \approx -0.059 \Rightarrow \nu_x \approx 8.653$$

$$\Delta\nu_y = \xi_y \delta p/p \approx \Rightarrow \nu_y \approx 8.769$$

this is confirmed by the ray-tracing values (rightmost column in Tab. 1).

## 2.2 DA. Long term tracking

Considering the importance of a good model of the ring dynamics if spin is to be tracked, we push further the investigation on the lattice we are working with, and of the ray-tracing outputs, by checking large excursion behavior, in terms of maximum stable amplitudes and DA. Long term tracking behavior is also tested.

### 2.2.1 Maximum stable amplitudes

Figs. 5, 6 show sample results of maximum stable amplitude tracking, 1000 turns.

It can be observed that the numerical integration in the horizontal case (Fig. 5) does not exhibit noticeable spiraling, an indication of correct symplectic behavior.

In the case of the vertical stability limit tracking (Fig. 6), coupling induces large horizontal motion, at the origin of spreading of the vertical invariant into a donut phase portrait ; the origin (e.g., width of non-linear coupling resonance, lack of tracking precision...) remains to be determined.

### 2.2.2 Dynamic aperture

Fig. 8 gives the dynamic aperture of the ring for  $\delta p/p = 0, \pm 1, \pm 2, \pm 3\%$ . These  $(x, z)$  limits are obtained by scanning the x-axis, step size 3 cm, and looking, at each  $x$ -step, for the maximum vertical stable amplitude upon 1000-turn tracking (namely, doing what is illustrated in Fig. 6), with 2 mm precision on that  $z$ -limit. The operation is performed repeatedly for the various momenta.

### 2.2.3 Symplecticity tests

Long term tracking may be required in assessing depolarizing effects in AGS or RHIC. Fig. 9 displays some sample results, showing very good behavior. The integration step size is  $\sim 1$  cm in all optical elements.

In the case of RHIC, *it the step size can be a little larger* given that the dipoles are not combined function. It has been checked that 1.5 cm at top energy (where spin moves the fastest in the dipoles) does ensure in addition convergence of the solution of  $\vec{S}' = \vec{x}\vec{\omega}$ .

Spin has been tracked in AGS step by step as well during this  $n \approx 5 \cdot 10^5$ -turn motion tracking. Zgoubi calculates independently the three components,  $S_x, S_y, S_z$ . It comes out that  $|\vec{S}|^2 = S_x^2 + S_y^2 + S_z^2 \equiv 1$ , from beginning to end. Similar behavior in RHIC at top energy with 1.5 cm step size.

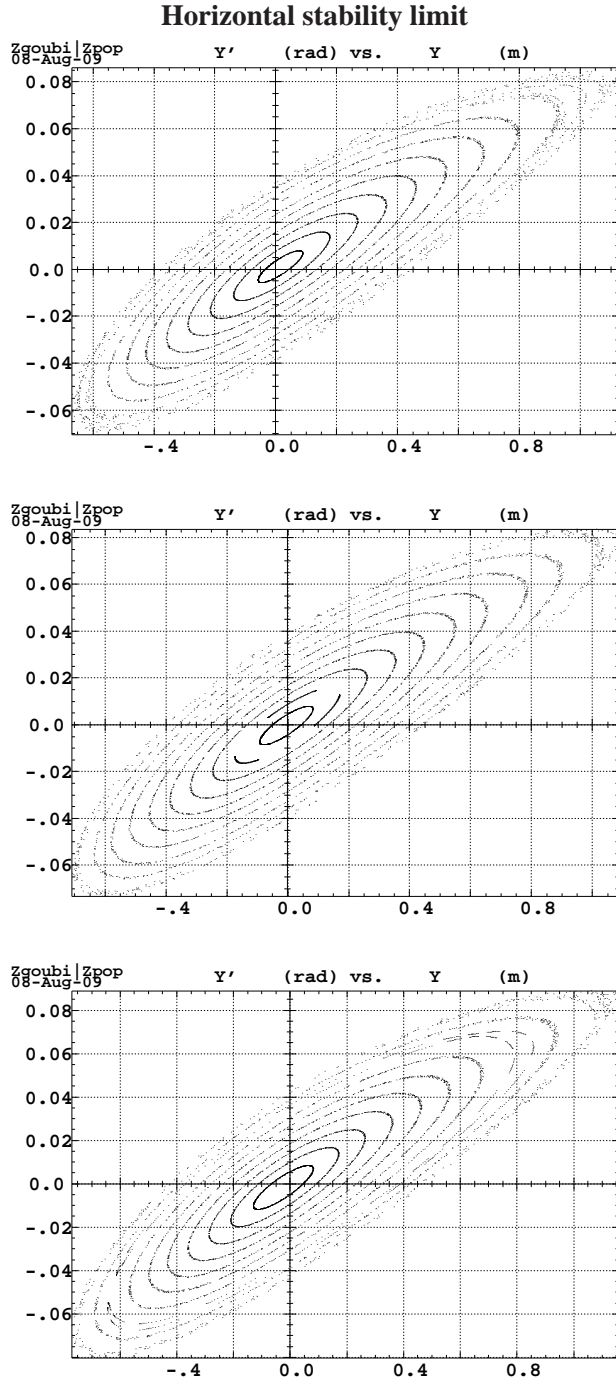


Figure 5: Maximum horizontal stable amplitude, 1000 turns in the ring, case of zero vertical emittance. From top to bottom :  $\delta p/p = +0.01, 0, -0.01$ . Hard edge optical elements.

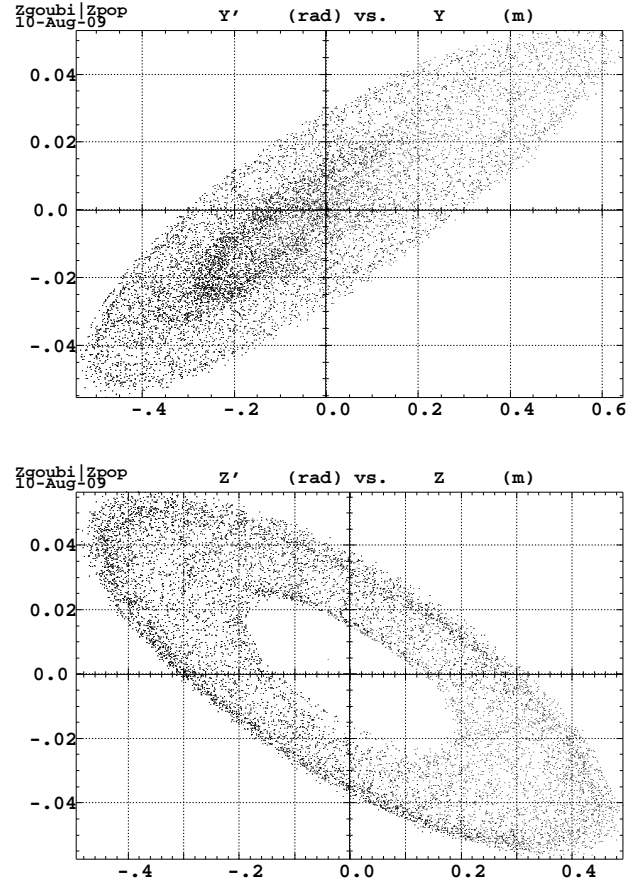


Figure 6: Maximum vertical stable amplitude, 1000 turns, showing H-V emittance exchange,  $\delta p/p = 0$ . Top plot : coupling induced x-motion ; bottom plot : vertical donut at maximum stable amplitude. Hard edge optical elements.

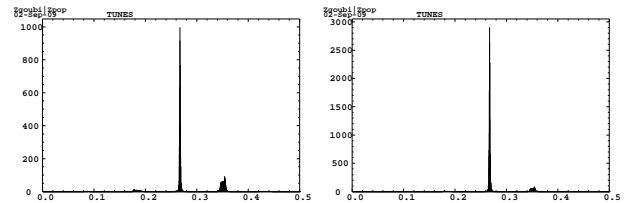


Figure 7: x-x' and z-z' spectra (left, right), exhibiting coupling.

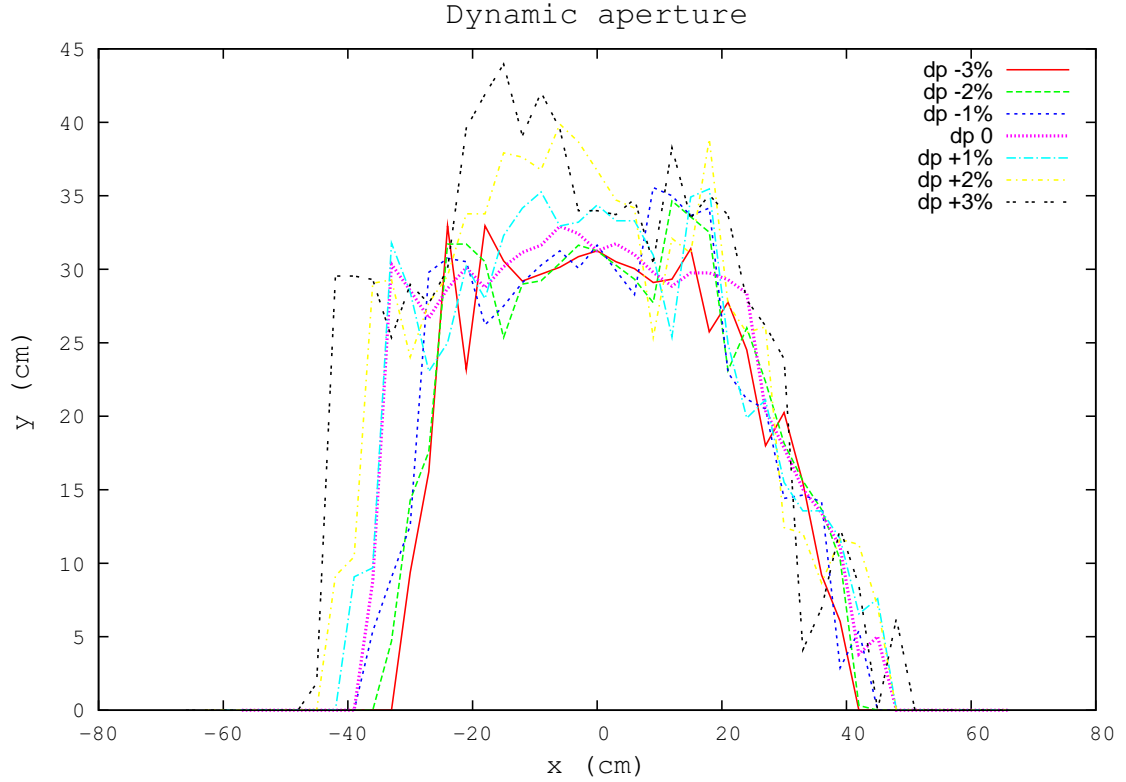


Figure 8: Dynamical apertures at  $\delta p/p = 0, \pm 1, \pm 2, \pm 3\%$ . 3 cm step in  $x$ , 2 mm precision on 1000-turn maximum vertical stable amplitude. Hard edge optical elements.

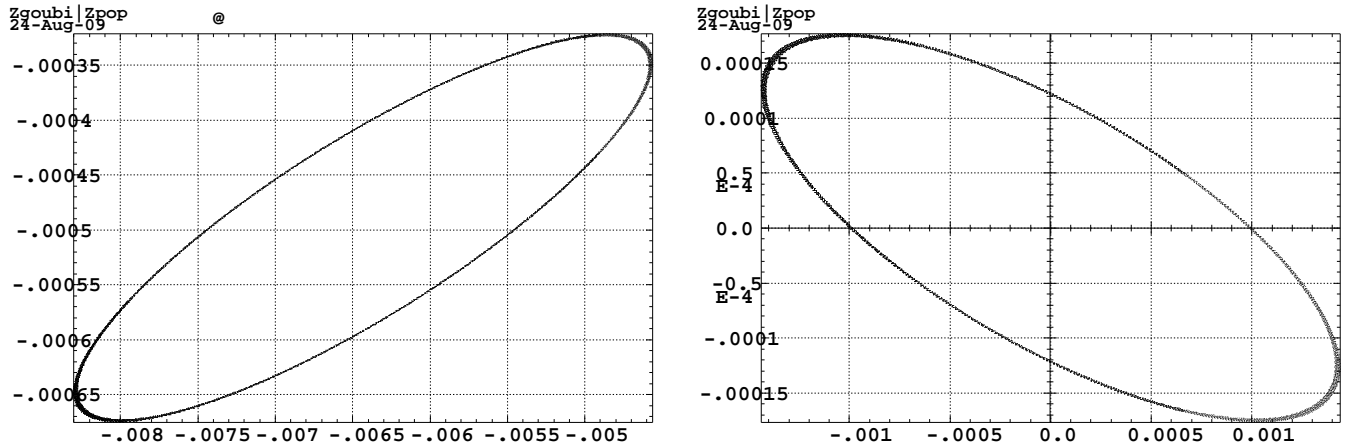


Figure 9:  $4 \cdot 10^5$ -turn tracking for a particle launched on  $\epsilon_x/\pi = \epsilon_z/\pi = 0.35$  mm.mrad, at fixed rigidity, observed at “Begin AGS”.

There is no substantial broadening of the invariants, nor visible spiraling.

Note : a matching of optical functions yields,  $\beta_x = 19.8$  m,  $\alpha_x = -1.58$ ,  $\beta_z = 11.7$  m,  $\alpha_z = 1.03$ , consistent with Tab. 1 data.

Hard edge optical elements.

### 2.3 Quantities and formulas used in these spin tracking studies

Classical formulae which will be used in the “numerical experiments” to follow are recalled below, together with various numerical data values<sup>1</sup>.

#### 2.3.1 Working hypotheses

The crossing speed writes

$$\alpha = G \frac{d\gamma}{d\theta} = G \frac{1}{2\pi} \frac{\Delta E}{M_0} \quad (1)$$

with  $M_0 = 938.27203$  MeV,  $G = 1.7928474$ . In the numerical simulations we take

$$\hat{V} = 290 \text{ kV}$$

$$\phi_s = 30 \text{ degrees or } 150 \text{ degrees}$$

hence

$$\Delta E = 145 \text{ keV/turn} \quad \text{and} \quad \alpha = 4.4096356 \cdot 10^{-5}$$

Besides,

$$\dot{B} = \Delta E / (2\pi R\rho) = \Delta E / (C\rho)$$

The ring circumference is (Tab. 1)

$$C = 807.04378 \text{ m}$$

whereas  $1/\rho = B/B\rho = 0.01171255$  (see dipole component in 'SBEN' type of magnets, zgoubi.dat file in App. B.1). (Note :  $\rho = 85.378504$ , packing factor  $R/\rho = 9.4525406$ ). This yields

$$\dot{B} = 2.104 \text{ T/s}$$

#### 2.3.2 Asymptotic depolarization

Crossing of an isolated resonance entails asymptotic depolarization given by the Froissard-Stora formula,

$$\frac{p_{final}}{p_{initial}} = 2 \exp(-A^2) - 1 = 2 \exp\left(-\frac{\pi}{2} \frac{|J_n|^2}{\alpha}\right) - 1 \quad (2)$$

#### 2.3.3 Depolarization, static

Free oscillation of polarization vector  $\vec{S}$  around arbitrary local precession vector  $\vec{\omega}$ , at fixed energy, starting with  $\vec{S} \equiv \vec{S}_z$ , satisfies

$$\frac{(-)}{\sqrt{1-|C|^2}} \frac{dC}{d\theta} = J_n e^{j\Delta\theta} \quad \text{with } C \text{ of the form } e^{j\mu\theta} \text{ and } \rho = \text{constant} \text{ yielding } \rho^2 = \frac{1}{1 + \Delta^2/|J_n|^2} \quad (3)$$

with

$$\begin{aligned} \Delta &= \text{distance to the resonance} = \gamma G - (n \times M - \nu_z) \\ \bar{S}_z^2 &= 1 - |\rho|^2 \quad \text{yields} \quad \bar{S}_z^2 = \frac{1}{1 + |J_n|^2/\Delta^2} \end{aligned} \quad (4)$$

with  $\bar{S}_z$  the average value of  $S_z$ . This allows computing  $|J_n|$  from the numerical value of  $S_z$ , following

$$|J_n|^2 = \Delta^2 / \left( \frac{1}{\rho^2} - 1 \right) \quad (5)$$

In particular,

1% depolarization ( $\bar{S}_z = 0.99$ ) corresponds to  $\Delta = \gamma G - n = 7|J_n|$  (an energy band  $\pm\delta\gamma = \pm 7|J_n|/G$ )

86.6% depolarization ( $\rho = 0.5$ ) corresponds to  $\Delta = \gamma G - n = \sqrt{3}|J_n|$

<sup>1</sup>Ref. Gérard Leleux, Traversée des résonances de dépolarisation, unpublished, SATURNE, Saclay, 15 Février 1992.

### 2.3.4 Weak resonance, Fresnel integral approximation

Reference : Gérard Leleux, Traversée des résonances de dépolarisation, unpublished, SATURNE, Saclay, 15 Février 1992.

Depolarization in the case of weak resonances (i.e.,  $p_f/p_i \approx 1$ ) is given by

- upstream of the resonance ( $\theta < 0$ ) :  $(p(\theta)/p_i)^2 = 1 - \frac{\pi}{\alpha} |J_n|^2 \left[ (0.5 - C(-\theta\sqrt{\frac{a}{\pi}}))^2 + (0.5 - S(-\theta\sqrt{\frac{a}{\pi}}))^2 \right]$  (6)
- downstream of the resonance ( $\theta > 0$ ) :  $(p(\theta)/p_i)^2 = 1 - \frac{\pi}{\alpha} |J_n|^2 \left[ (0.5 + C(\theta\sqrt{\frac{a}{\pi}}))^2 + (0.5 + S(\theta\sqrt{\frac{a}{\pi}}))^2 \right]$

where

$$C(x) = \int_0^x \cos\left(\frac{\pi}{2}t^2\right) dt, \quad S(x) = \int_0^x \sin\left(\frac{\pi}{2}t^2\right) dt$$

are the Fresnel integrals.

Note that

$$p(\theta)/p_i \xrightarrow{\theta \rightarrow \infty} 1 - \frac{\pi}{\alpha} |J_n|^2 \quad (7)$$

i.e., Froissard-Stora formula (Eq. 2) taken to first order in  $|J_n|^2/\alpha$ . The approximation holds in the limit that higher order terms can be neglected, i.e.  $\pi|J_n|^2/\alpha$  is small enough compared to 1.

In Section 6, Zgoubi is tested against the weak-resonance approximation.

### 2.3.5 Resonance strength, theoretical

It can be computed from MAD type of output, this allows comparison with ray-tracing results. The following formulae hold.

Imperfection, thin lens approximation :

$$J_n = \frac{1 + \gamma G}{2\pi} \sum_{Qpoles} \left\{ \begin{array}{l} \cos(\gamma G \alpha_i) \\ \sin(\gamma G \alpha_i) \end{array} \right\} (KL)_i z_{co,i} \quad (8)$$

with  $\alpha_i$  cumulated bend angle,  $z_{co,i}$  the closed orbit amplitude, at quadrupole  $i$  with strength  $(KL)_i$ .

Intrinsic, thin lens approximation :

$$J_n^\pm = \frac{1 + \gamma G}{4\pi} \sum_{Qpoles} \left\{ \begin{array}{l} \cos(\gamma G \alpha_i \pm \psi_i) \\ \sin(\gamma G \alpha_i \pm \psi_i) \end{array} \right\} (KL)_i \sqrt{\beta_{z,i} \epsilon_z / \pi} \quad (9)$$

with

$$\psi_i = \int_0^{\theta_i} \frac{ds}{\beta_z}, \quad ' + ' \text{ sign for } \gamma G + \nu_z - n = 0, \quad ' - ' \text{ sign for } \gamma G - \nu_z - n = 0$$

and  $(KL)_i$  strength of quadrupole  $i$  located at  $\theta_i$ .

### **3 Inventory of spin resonances, including spin tracking results**

Two inventories of the intrinsic resonances are given in Tables 2, 3 respectively, below. They include the numerical value of the resonance strengths as obtained for the numerical ray-tracing, in both dynamic (crossing) and static cases. The difference between both (a factor 3-4) remains to be elucidated.

### 3.1 Intrinsic resonances

Table 2: Intrinsic resonances.  $\nu_z = 8.76346$ ,  $M = 12$  superperiods.  $A^2 = \frac{\pi}{2} \frac{|J_n|^2}{\alpha}$ .

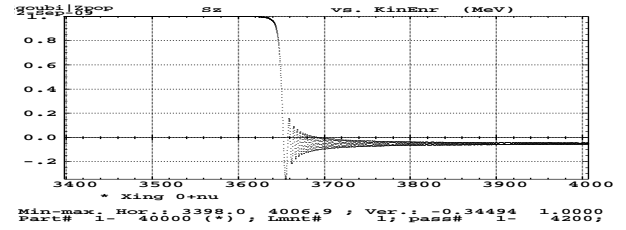
Intrinsic resonances, systematic, $kM \pm \nu_z$ , $M = 12$ , classed by energy.														
$kM \pm \nu_z$	$\gamma G$	kin. E (GeV)	$B\rho$ (T.m)	$\epsilon_z/\pi$ ( $10^{-6}$ )	$A^2$	$ J_n ^2$ ( $10^{-6}$ )	$\frac{A^2}{\epsilon_z/\pi}$ ( $10^6$ )	MAD	$\frac{ J_n ^2}{\epsilon_z/\pi}$ ZGOUBI dyn. stat. <sup>(a)</sup>	Final $P_z$ (dyn.)	$ 4\nu_z^2 - (kM)^2 $			
0 +qz	8.76345	3.64801	14.9746	0.0017	0.0071	0.200	3.5576	125	100.0 100.3	390	0.9858 0.9298	307		
				0.01	0.0357	1.003	3.5731							
				0.017										455
				0.05	0.1788	5.020	3.5765						100.4	0.6725
				0.2	0.7467	2.096	3.7338						104.8	-0.0522
24 -qz	15.2365	7.03564	26.4134	0.1	0.0011	0.0295	0.1051	0.30	0.30	0.9979	269			
12 +qz	20.7634	9.92811	36.1110	0.01	0.0026	0.072	1.2826	39	37	0.7590 -0.8428	163			
12 +qz	20.7634	9.92811	36.1110	0.1	0.1290	3.621	1.2897		37					
12 +qz	20.7634	9.92811	36.1110	2	2.5431	71.39	1.2716		37					
36 -qz	27.2365	13.3157	47.4432	0.05	0.5494	15.42	10.989	320	309	0.1545	989			
24 +qz	32.7634	16.2082	57.1088	2	0.0737	2.070	0.0368	0.90	1.04	0.857	269			
				30	1.0113	28.39	0.0337		0.95	-0.269				
48 -qz	39.2365	19.5958	68.4229	0.125	0.0463	1.299	0.3704	4.90	10.4 ?	27	0.9095	1997		
				0.25	0.0986	2.768	0.3945		11.1	0.812				
				0.5	0.1913	5.370	0.3826		10.7	0.6515				
				1	0.3895	10.94	0.3895		10.9	0.3545				
				2	0.8073	22.67	0.4036		11.3	30	-0.1078			
36 +qz	44.7634	22.4883	78.0800	0.0001	0.0066	0.186	66.118	1950	1856	4997	0.9868	989		
				0.002	0.1329	3.733	66.480		1937	0.751				
				0.02	1.4318	40.19	71.592		2010	5560	-0.522			
60 -qz	51.2365	25.8759	89.3879					73400			3293			

(a) Emittances in static case may slightly differ from that given in the ' $\epsilon_z/\pi$ ' column, exact values can be found in Sec. 5.

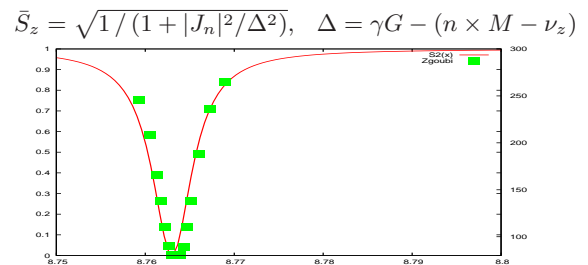
MAD, data obtained using :

$$J_n^\pm = \frac{1+\gamma G}{4\pi} \sum_{Qpoles} \left\{ \begin{array}{l} \cos(\gamma G \alpha_i \pm \psi_i) \\ \sin(\gamma G \alpha_i \pm \psi_i) \end{array} \right\} (KL)_i \sqrt{\beta_{z,i} \epsilon_z / \pi}$$

ZGOUBI , data obtained using :



or





### **3.2 Imperfection resonances**

A closed orbit is excited using a vertical kicker (DVCA02) ; the fourth column in Tab. 3 gives the maximum amplitude of the resulting closed orbit around AGS.

Table 3: Closed orbit resonances.

$\gamma G$	kin. E (GeV)	$B\rho$ (T.m)	$\hat{z}$ (mm)	$A^2$	$ J_n ^2$ ( $10^{-5}$ )	$A^2/\hat{z}^2$	$ J_n ^2/\hat{z}^2$		Final $P_z$
							MAD	Zgoubi dyn.	
5	1.678437	8.147990							
6	2.201779	9.995557							
7	2.725121	11.81217							
8	3.248463	13.61023							
9	3.771804	15.39624	.139 2.77	1.224737	3.4381555	159618	4.75	4.48	-0.412
10	4.295146	17.17396							
11	4.818487	18.94571							
12	5.341830	20.71305	13.84	0.6379532	1.7909011	3330	.031	0.094	0.05674
13	5.865171	22.47699	13.84	0.5469143	1.5353313	2855	.019	0.080	0.15745
14	6.388514	24.23830							
15	6.911855	25.99749							
16	7.435197	27.75499							
17	7.958539	29.51107							
18	8.481881	31.26600							
19	9.005222	33.01994							
20	9.528564	34.77305							
21	10.05191	36.52545							
22	10.57525	38.27723							
23	11.09859	40.02848	13.84	1.734326	4.868705	905437	.082	0.25	-0.6468
24	11.62193	41.77927							
25	12.14527	43.52964							
26	12.66861	45.27966							
27	13.19196	47.02935	1.384	0.8763353	2.460102	457507	11.3	12.8	-0.167355
28	13.71530	48.77875							
29	14.23864	50.52790							
30	14.76198	52.27681							
31	15.28532	54.02551							
32	15.80867	55.77403							
33	16.33201	57.52238							
34	16.85535	59.27057							
35	17.37869	61.01860							
36	17.90203	62.76652							
37	18.42537	64.51430							
38	18.94872	66.26198							
39	19.47206	68.00956							
40	19.99540	69.75704							
41	20.51874	71.50443							
42	21.04208	73.25175							
43	21.56543	74.99899							
44	22.08877	76.74614					9.0		
45	22.61211	78.49324	0.028 0.275	0.2047056	0.57466214	2706852	68.3	76.0	0.99596 0.62962
46	23.13545	80.24029					4.3		

**MAD**, data obtained using :

$$J_n = \frac{1 + \gamma G}{2\pi} \sum_{Qpoles} \left\{ \begin{array}{l} \cos(\gamma G \alpha_i) \\ \sin(\gamma G \alpha_i) \end{array} \right\} (KL)_{i z_{co,i}} \quad (10)$$

## I built a “Xing factory” from all that material, applicable to AGS and RHIC :

- Starting from a MAD/TWISS file, a sheet is produced, which containing strengths, vertical closed orbit etc. :

n	+/-Qz	$J_n^2/z\alpha^2$	$N_n^2/\epsilon_z/\pi$	zmax	vkick	2pi-2pi
0	+8.7648	0.0	127.3933	0.0000E+00	0.0000E+00	0.2032E-10
12	+8.7648	0.0	39.2391	0.0000E+00	0.0000E+00	0.2032E-10
24	-8.7648	0.0	0.3019	0.0000E+00	0.0000E+00	0.2032E-10
24	+8.7648	0.0	0.9011	0.0000E+00	0.0000E+00	0.2032E-10
36	-8.7648	0.0	321.0361	0.0000E+00	0.0000E+00	0.2032E-10
36	+8.7648	0.0	1937.6307	0.0000E+00	0.0000E+00	0.2032E-10
48	-8.7648	0.0	4.87452	0.0000E+00	0.0000E+00	0.2032E-10

Strengths from lattice functions are computed using the regular thin-lens modelling :

$$\text{- closed orbit : } (J_n/\hat{z}) = \frac{1+\gamma G}{2\pi} \sum_{Qpoles} \left\{ \begin{array}{l} \cos(\gamma G \alpha_i) \\ \sin(\gamma G \alpha_i) \end{array} \right\} (KL)_i z_{co,i} / \hat{z}$$

$$\text{- intrinsic : } (J_n^\pm / \sqrt{\epsilon_z/\pi}) = \frac{1+\gamma G}{4\pi} \sum_{Qpoles} \left\{ \begin{array}{l} \cos(\gamma G \alpha_i \pm \psi_i) \\ \sin(\gamma G \alpha_i \pm \psi_i) \end{array} \right\} (KL)_i \sqrt{\beta_{z,i}}$$

Note that the long combined function AGS bends need be split into 4 pieces at least so to get the strengths in that table converged.

- Taking  $n \pm \nu_z$  from that sheet, and including in addition working conditions for the tracking,
  - under the form of a template zgoubi.dat file obtained from MAD translation,
  - with specific values for  $\hat{V}$ ,  $\phi_s$ , etc.

then Zgoubi will perform a scan of all resonances, one after the other.

Initial particle conditions are taken to be :

$$\text{- closed orbit : } \hat{z}_{co} = \sqrt{8 \cdot 10^{-6}} / (J_n / \hat{z}_{co})$$

$$\text{- intrinsic : } \epsilon_y / \pi = \sqrt{8 \cdot 10^{-6}} / (J_n / \epsilon_y)$$

with  $\sqrt{8 \cdot 10^{-6}}$  in there just because  $2 \exp(-\frac{\pi}{2} \frac{|J_n|^2}{\alpha}) - 1 \approx 0.5$  (given  $\alpha \approx 4.41 \cdot 10^{-5}$ ) is a convenient value for appropriate accuracy when drawing  $p_f/p_i$  from the tracking data.

The distance  $\Delta$  upstream of the resonance where to start from is given by (in units of  $J_n$ )

$$\Delta / |J_n| = S_z / \sqrt{1 - S_z^2}$$

taking for instance  $S_z = 1 - 10^{-4}$ , which translates into a number of turns using  $\gamma G = \Delta + (n \pm \nu_z)$  and the acceleration rate,  $dE$  per turn.

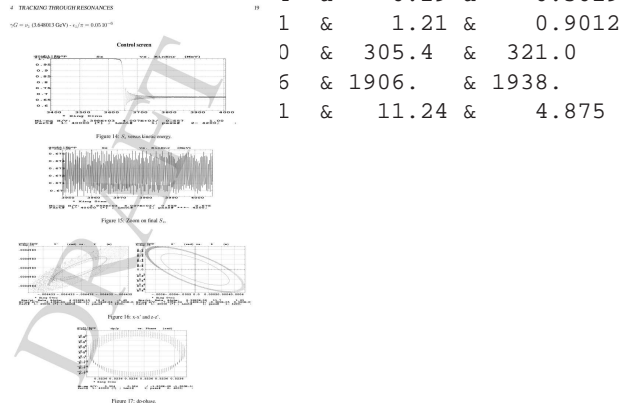
This tool produces the typical following table :

& Energy & Qz & e_z/pi & p_init & p_final &  J_n ^2 &  J_n ^2/ez } \\
& (GeV) & & (1e-6) & & & (1e-6) & ZGOUBI & MAD \\
0+Qz & 4.2359 & 0.76345 & 3.604E-02 & 1.000 & 0.7434 & 3.855 & 107.0 & 127.4
12+Qz & 10.516 & 0.76345 & 0.123 & 1.000 & 0.6995 & 4.571 & 37.15 & 39.24
24-Qz & 7.6222 & 0.76490 & 15.8 & 0.9994 & 4.574 & 0.29 & 0.3019
24+Qz & 16.796 & 0.76331 & 5.42 & 0.9972 & 1 & 1.21 & 0.9012
36-Qz & 13.902 & 0.76346 & 1.516E-02 & 1.000 & 0 & 305.4 & 321.0
36+Qz & 23.076 & 0.76346 & 2.537E-03 & 1.000 & 6 & 1906. & 1938.
48-Qz & 20.182 & 0.76343 & 1.01 & 0.9992 & 1 & 11.24 & 4.875

which includes provision for comparison between MAD and output data.

Tunes and emittances are “measured” in the vicinity of the crossing gamma, namely, considering a few hundred turns around  $(n \pm \nu_z) / G$ .

This tool also produces a “control panel” :



## 4 Tracking through resonances

### 4.1 Intrinsic resonances

#### 4.1.1 $\gamma G = \nu_z$ (3.648013 GeV)

##### Tracking data

Zgoubi.dat, excerpts :

```
Xing 0+nu
'OBJET'
14.12163e3
8
 1 1 1
-0.64319816e-2 -0.49829722e-3 0.0 0.0E+00 0.0E+00 1. 'p'
-1.588 19.843 0.
1.033 11.675 0.01 to 0.2e-6 =epsilon_z/pi
0 1 0.
'SCALING'
1 2
MULTIPOL SBEN
-1
14.12163
1
MULTIPOL QUAD
-1
14.12163
1
'PARTICUL'
938.27203d0 1.602176487d-19 1.7928474d0 0. 0.
.....
'CAVITE'
2.1
807.043778118095 12.
290.d3 0.5235987755982988731 9cavitiesx32kV, phi_s=30deg
'MARKER' #End
'REBELOTE'
4199 0.2 99
'END'
```

-----  
From zgoubi.res :

```
Particle properties :
  Mass      = 938.272      MeV/c2
  Charge    = 1.602176E-19 C
  G factor  = 1.79285
Reference data :
  rigidity (kG.cm) : 14121.6
  mass (MeV/c2)    : 938.272
  momentum (MeV/c) : 4233.56
  energy, total (MeV) : 4336.29
  energy, kinetic (MeV) : 3398.01
  beta = v/c      : 0.9763099040
  gamma          : 4.621565007
  beta*gamma     : 4.512079688
```

### Strengths

From Figs. 10-23 one gets

$\epsilon_z/\pi$ ( $10^{-6}$ )	$A^2$	$ J_n ^2$ ( $10^{-5}$ )	$A^2/\epsilon_z/\pi$	$ J_n ^2/\epsilon_z/\pi$	$P_{init}$	$P_{final}$
0.01	0.0357308	1.0030567	3573080	100.3057	1	0.9298
0.05	0.1788277	5.0201593	3576553	100.4032	1	0.6725
0.2	0.7467644	2.0963627	3733822.	104.8181	0.9999	-5.22E-02

$$\gamma G = \nu_z (3.648013 \text{ GeV}) - \epsilon_z / \pi = 0.01 \cdot 10^{-6}$$

Control screen

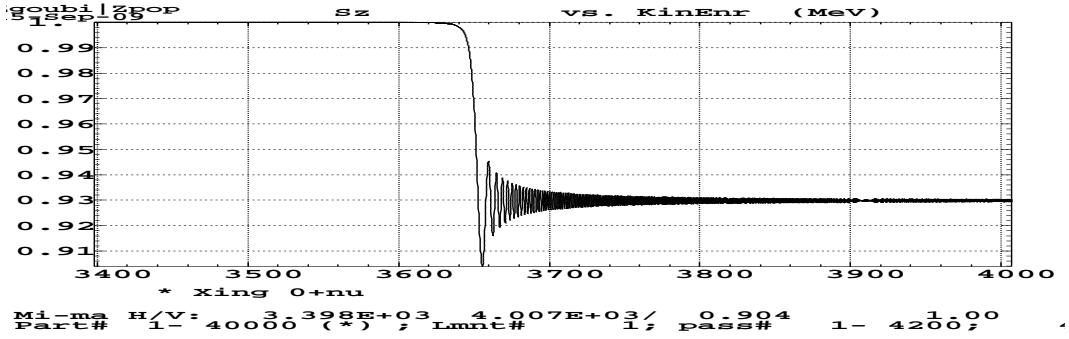


Figure 10:  $S_z$  versus kinetic energy.

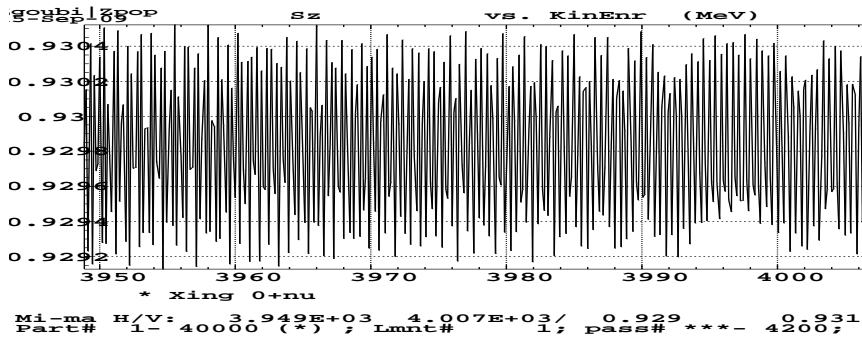


Figure 11: Zoom on final  $S_z$ .

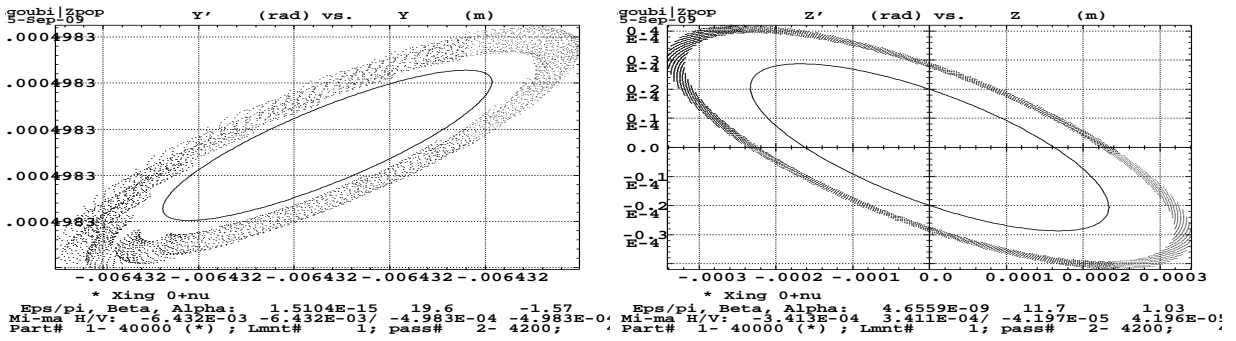


Figure 12:  $x-x'$  and  $z-z'$ .

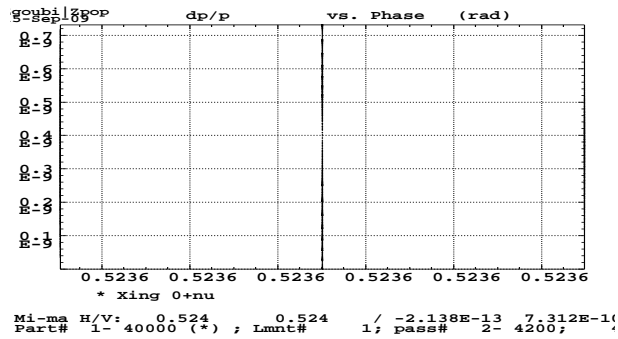


Figure 13:  $dp$ -phase.

$$\gamma G = \nu_z (3.648013 \text{ GeV}) - \epsilon_z/\pi = 0.05 \cdot 10^{-6}$$

Control screen

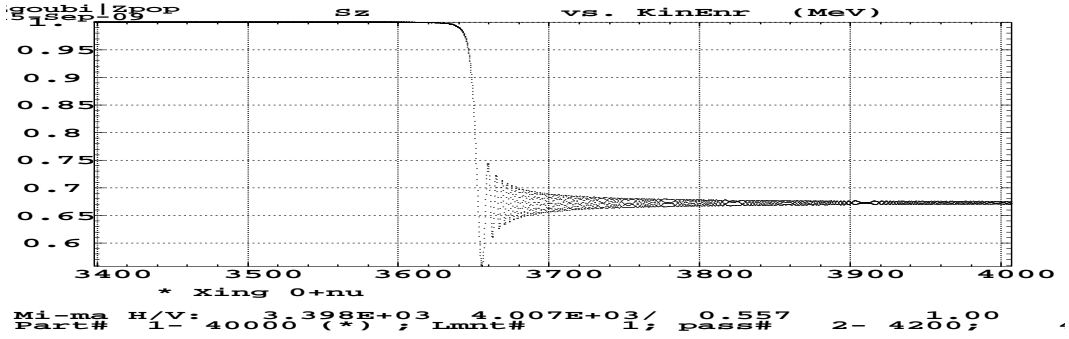


Figure 14:  $S_z$  versus kinetic energy.

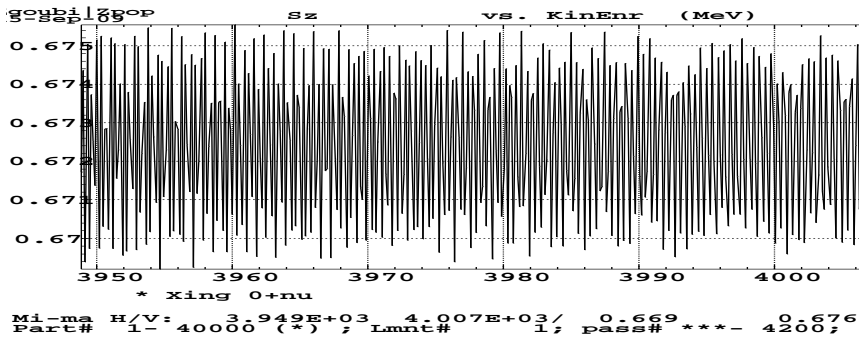


Figure 15: Zoom on final  $S_z$ .

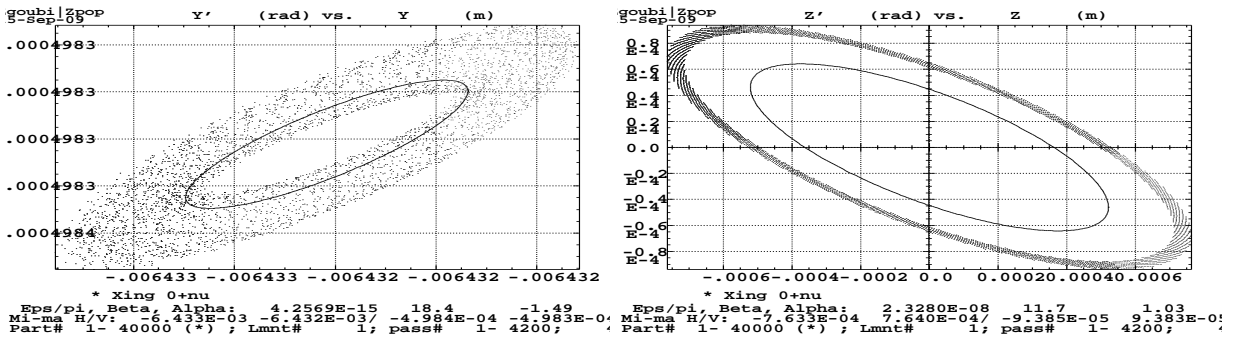


Figure 16:  $x-x'$  and  $z-z'$ .

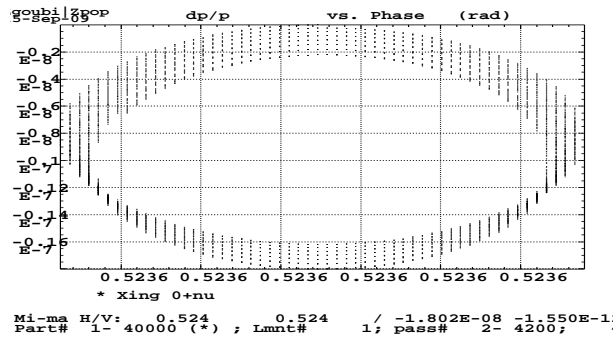


Figure 17:  $dp$ -phase.

$$\gamma G = \nu_z (3.648013 \text{ GeV}) - \epsilon_z / \pi = 0.2 \cdot 10^{-6}$$

Control screen

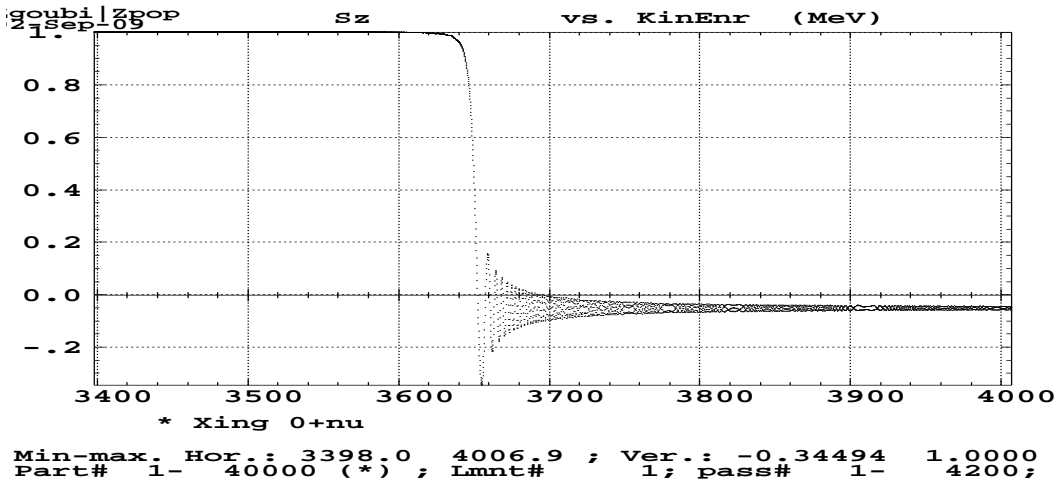


Figure 18:  $S_z$  versus kinetic energy.

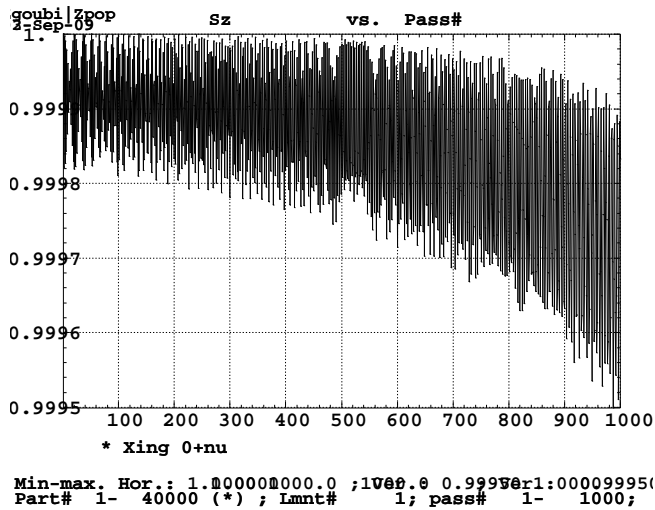


Figure 19: Zoom on initial  $S_z$ .

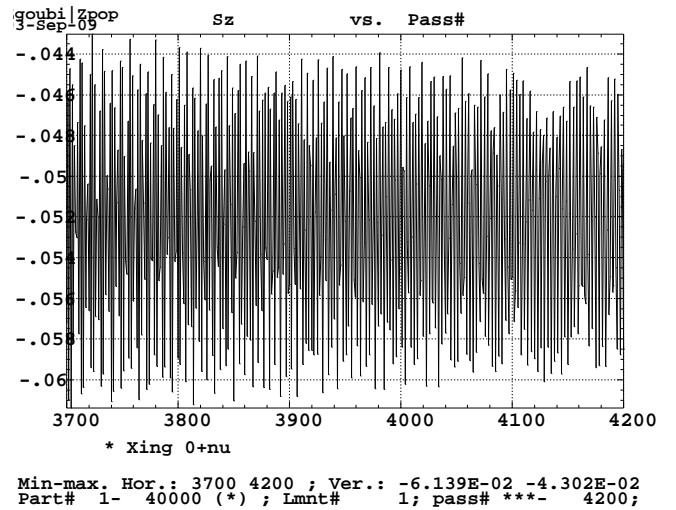


Figure 20: Zoom on final  $S_z$ .

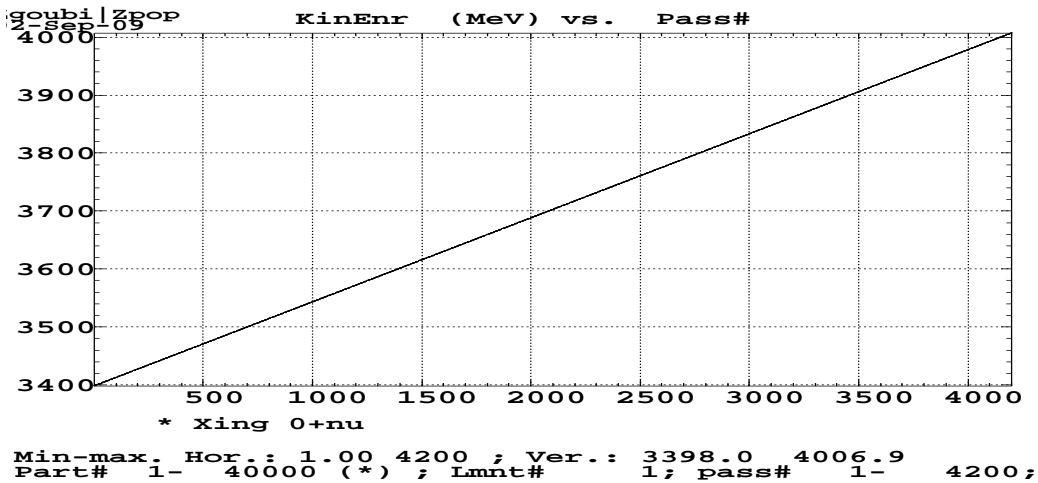


Figure 21: Kinetic E versus turn number.

$$\gamma G = \nu_z (3.648013 \text{ GeV}) - \epsilon_z / \pi = 0.2 \cdot 10^{-6}$$

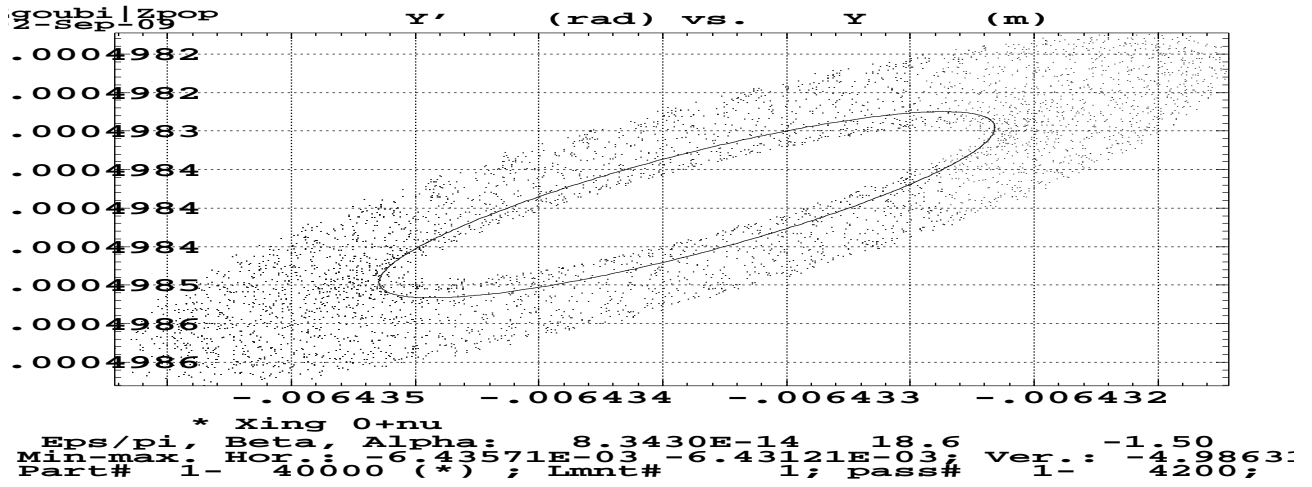


Figure 22: x-x'.

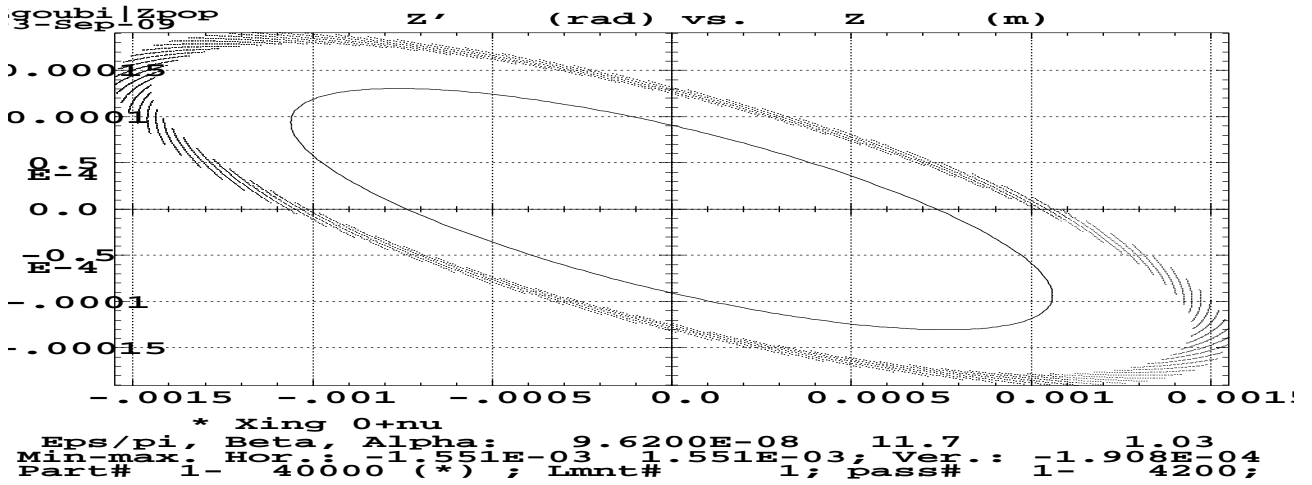


Figure 23: z-z'.

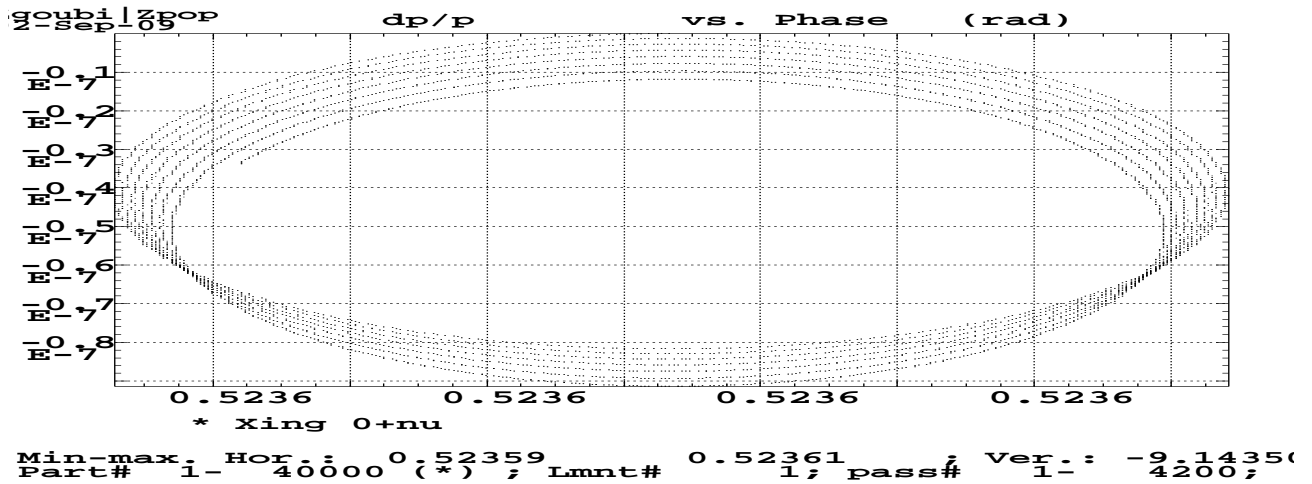


Figure 24: dp-phase.



### Testing possible effect of betatron phase

7 particles evenly spread on  $\epsilon_z/\pi = 0.2$  mm.mrad invariant are launched : no observable difference in spin dynamics.

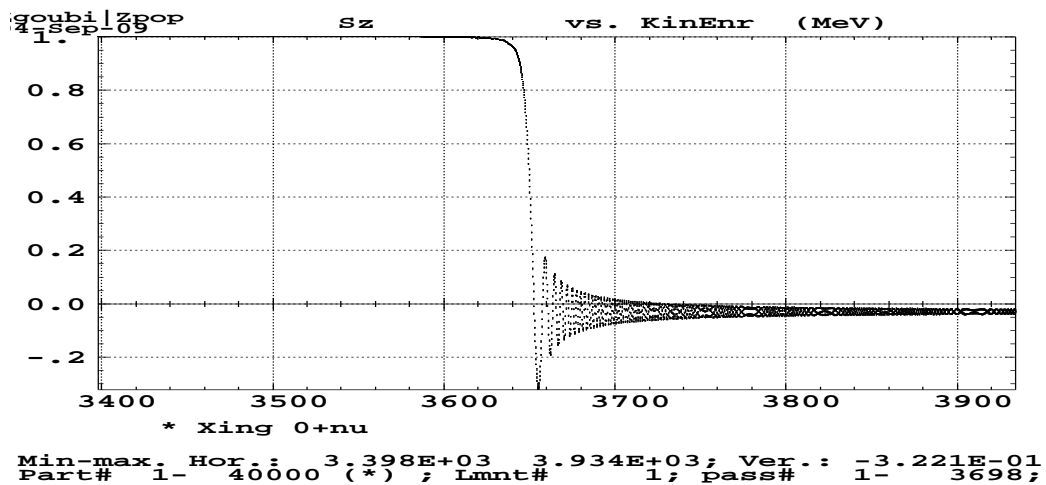


Figure 25:  $S_z$  versus kinetic energy, 7 particles evenly spread on  $\epsilon_z/\pi = 0.2$  mm.mrad invariant.

### 4.1.2 $\gamma G = 24 - \nu_z$ (7.82892 GeV)

#### Tracking data

Zgoubi.dat, excerpts :

```
Xing 24-nu. Data generated by geneZGDat4Xing
'OBJET'
 25.92623852d3
 8
 1 1 1
-0.64319816e-2 -0.49829722e-3 0.0 0.0E+00 0.0E+00 1. 'p'
-1.588 19.843 0.
 1.033 11.675 .1e-6
 0 1 0.
'PARTICUL'
 9.382720300E+02 1.602176487E-19 1.792847400E+00 0. 0.
'SPNTRK'
 3
'FAISCEAU'
'SCALING'
 1 2
MULTIPOL SBEN
-1
 25.92623852
 1
MULTIPOL QUAD
-1
 25.92623852
 1
'PICKUPS'
 1
#Start
'SPNSTORE'
 b_zgoubi.spn #Start
 1
'FAISTORE'
 b_zgoubi.fai #End
 1
'MARKER' #Start
'MARKER' MARK BSUPERA
'MULTIPOL' SBEN ALBF
0 .Dip
200.6554 10.00 0.11712499 0.04848519 -0.00050563 0.0 0.0 0.0 0.0 0.0 0.0 0.0
0. 0. 10.00 4.0 0.800 0.00 0.00 0.00 0.00 0. 0. 0. 0.
.....
'CAVITE'
 2 .1
 807.04377811810 12.00
 2.900000000E+05 2.617993877991E+00
'MARKER' #End
'REBELOTE'
 2500 0.2 99
```

#### Strengths

$\epsilon_z/\pi$ ( $10^{-6}$ )	$A^2$	$ J_n ^2$ ( $10^{-6}$ )	$A^2/\epsilon_z/\pi$	$ J_n ^2/\epsilon_z/\pi$	$p_{init}$	$p_{final}$
0.1	1.050547E-03	2.94915967E-2	10505	0.29491597	1.	0.997900

$$\gamma G = 24 - \nu_z (7.82892 \text{ GeV}) - \epsilon_z / \pi = 0.1 \cdot 10^{-6}$$

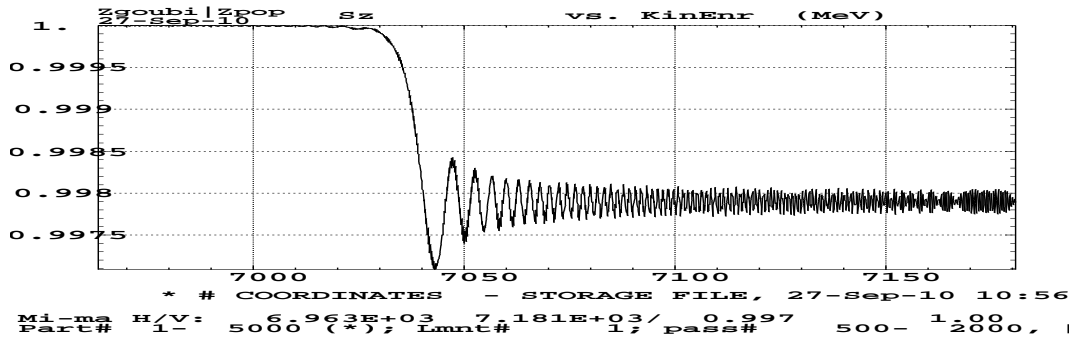


Figure 26:  $S_z$  versus kinetic energy.

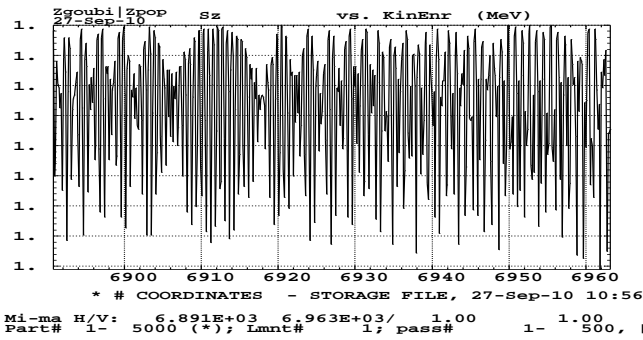


Figure 27: Zoom on initial  $S_z$ .

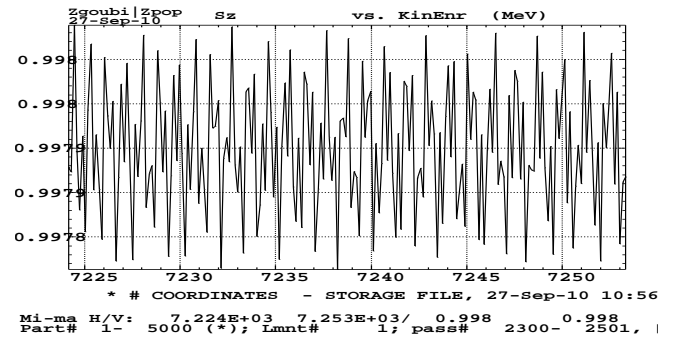


Figure 28: Zoom on final  $S_z$ .

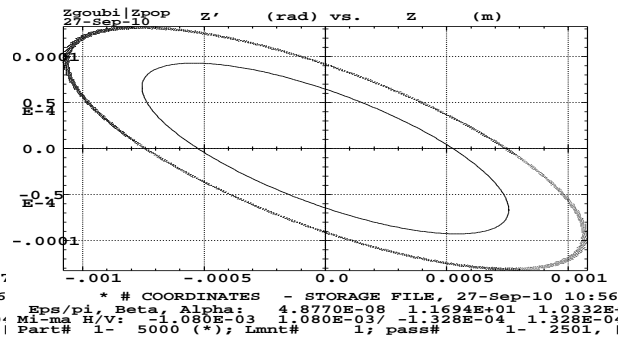
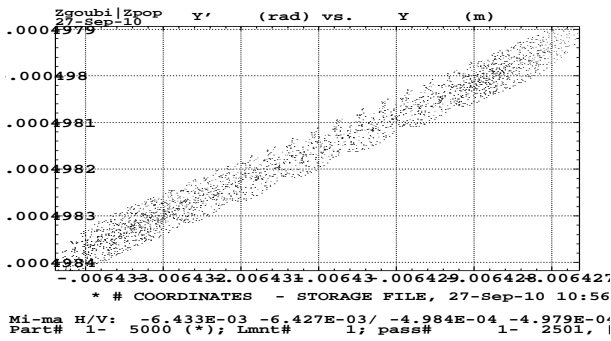


Figure 29:  $x-x'$  and  $z-z'$ .

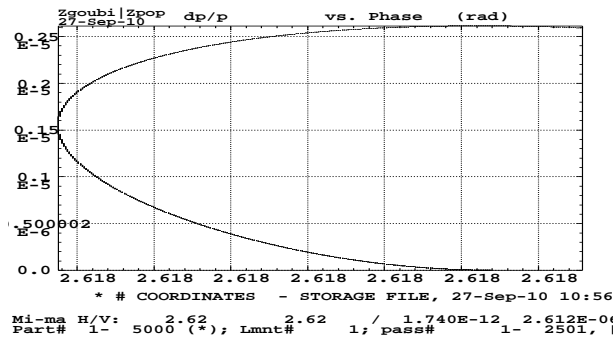


Figure 30:  $dp$ -phase.

4.1.3  $\gamma G = 12 + \nu_z$  (7.82892 GeV)

## Tracking data

Zgoubi.dat, excerpts :

```

Xing 12+nu. Data generated by geneZGDat4Xing
'OBJET'
 35.38271465d3
 8
   1 1 1
  -0.64319816e-2 -0.49829722e-3 0.0 0.0E+00 0.0E+00 1. 'p'
  -1.588 19.843 0.
  1.033 11.675 .1e-6
   0 1 0.
'PARTICUL'
 9.382720300E+02 1.602176487E-19 1.792847400E+00 0. 0.
'SPNTRK'
 3
'FAISCEAU'
'SCALING'
 1 2
MULTIPOL SBEN
-1
35.38271465
1
MULTIPOL QUAD
-1
35.38271465
1
'PICKUPS'
1
#Start
'SPNSTORE'
 b_zgoubi.spn #Start
 1
'FAISTORE'
 b_zgoubi.fai #End
 1
'MARKER' #Start
'MARKER' MARK BSUPERA
'MULTIPOL' SBEN ALBF
0 .Dip
200.6554 10.00 0.11712499 0.04848519 -0.00050563 0.0 0.0 0.0 0.0 0.0 0.0 0.0
0. 0. 10.00 4.0 0.800 0.00 0.00 0.00 0.00 0. 0. 0. 0.
4 .1455 2.2670 -.6395 1.1558 0. 0. 0.
0. 0. 10.00 4.0 0.800 0.00 0.00 0.00 0.00 0. 0. 0. 0.
4 .1455 2.2670 -.6395 1.1558 0. 0. 0.
0. 0. 0. 0. 0. 0. 0. 0. 0. 0. 0. 0.
#20|200|20 Dip ALBF
3 0.000000000000000 0.000000000000000 -1.175115045000000E-002
.....
'CAVITE'
 2 .1
 807.04377811810 12.00
 2.900000000E+05 2.617993877991E+00
'MARKER' #End
'REBELOTE'
 3000 0.2 99

```

## Strengths

$\epsilon_z/\pi$ ( $10^{-6}$ )	$A^2$	$ J_n ^2$ ( $10^{-6}$ )	$A^2/\epsilon_z/\pi$	$ J_n ^2/\epsilon_z/\pi$	$p_{init}$	$p_{final}$
0.002	0.00256527	0.07201394	1282637	36.006969	1.	0.994876
0.1	0.12897037	3.62053515	1289703	36.205349	1.	0.7590
2	2.5431926	71.3940608	1271596	35.697029	1.	-0.842770

$$\gamma G = 12 + \nu_z (7.82892 \text{ GeV}) - \epsilon_z/\pi = 0.002 \cdot 10^{-6}$$

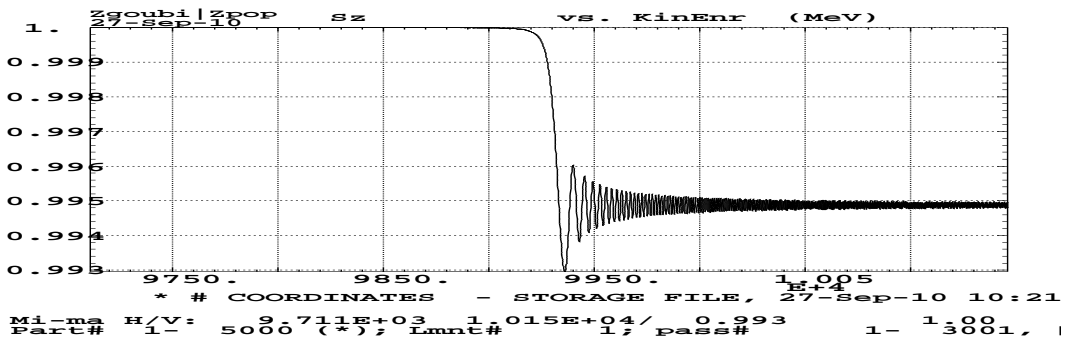


Figure 31:  $S_z$  versus kinetic energy.

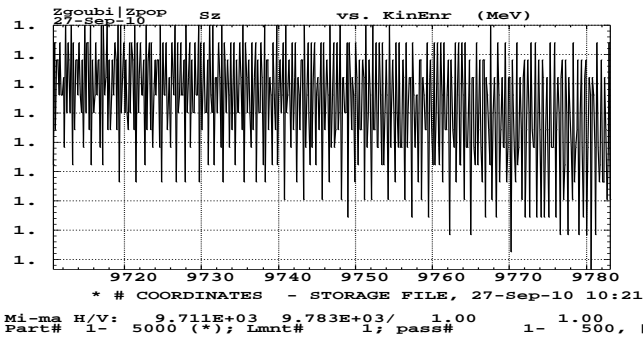


Figure 32: Zoom on initial  $S_z$ .

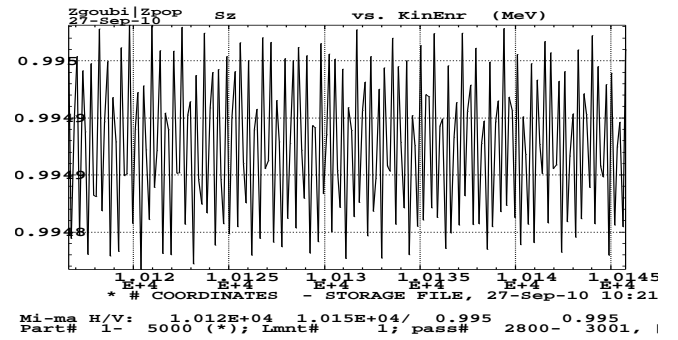


Figure 33: Zoom on final  $S_z$ .

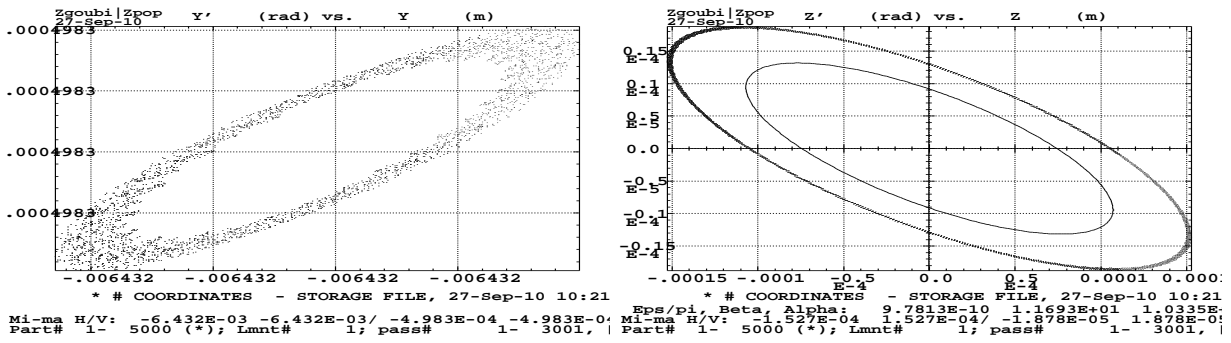


Figure 34:  $x-x'$  and  $z-z'$ .

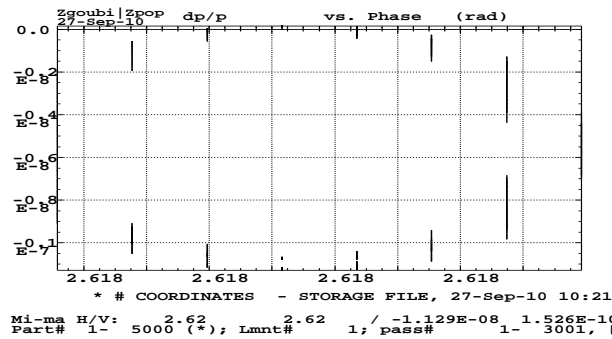


Figure 35:  $dp$ -phase.

$$\gamma G = 12 + \nu_z (7.82892 \text{ GeV}) - \epsilon_z/\pi = 2 \cdot 10^{-6}$$

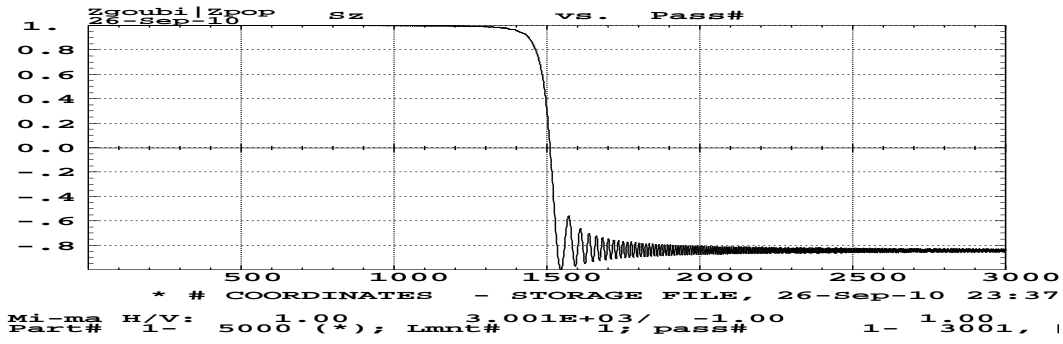


Figure 36:  $S_z$  versus kinetic energy.

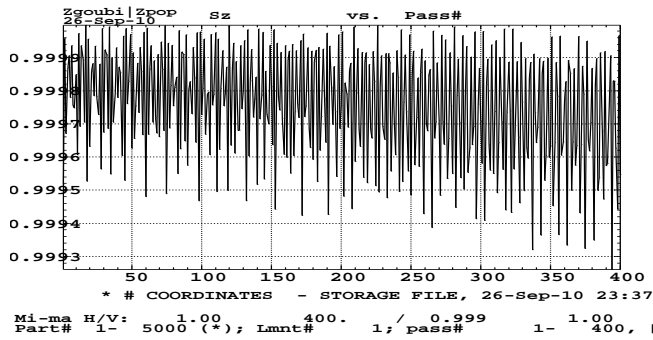


Figure 37: Zoom on initial  $S_z$ .

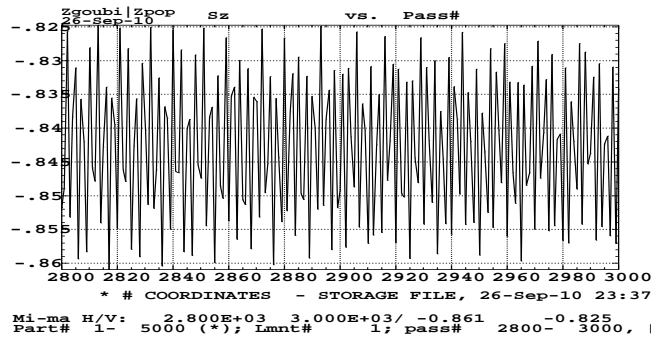


Figure 38: Zoom on final  $S_z$ .

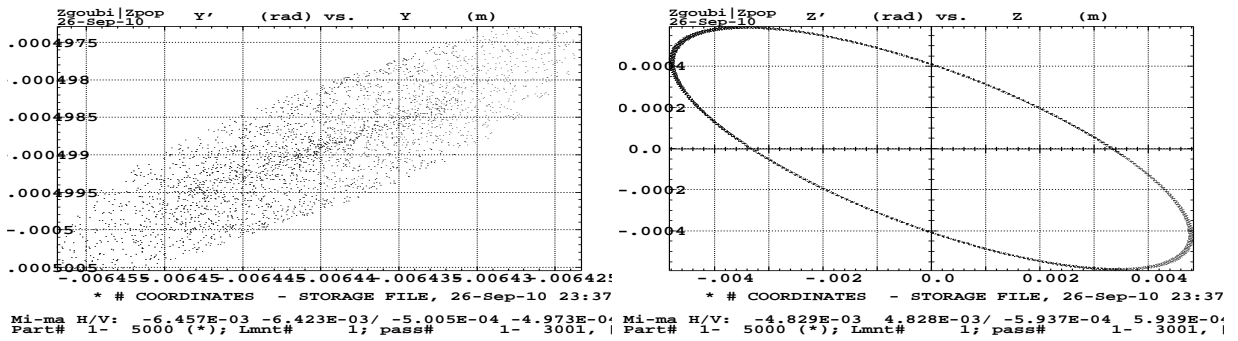


Figure 39:  $x-x'$  and  $z-z'$ .

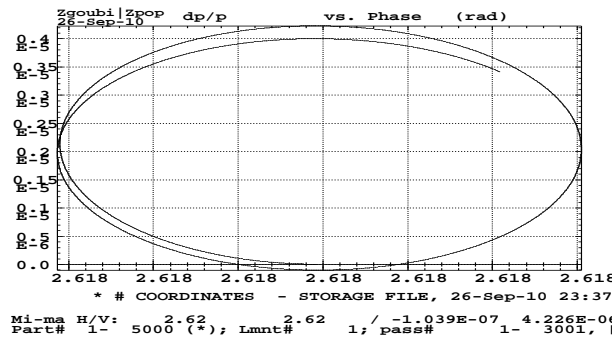


Figure 40:  $dp$ -phase.

#### 4.1.4 $\gamma G = 23 + \nu_z$ (15.68487 GeV)

##### Tracking data

Zgoubi.dat, excerpts :

```
Xing 23+nu
'OBJET'
54.92333e3
8
  1  1  1
-0.64319816e-2 -0.49829722e-3  0.0 0.0E+00  0.0E+00  1.  'p'
-1.588  19.843  0.
1.033  11.675  10e-4
  0  1  0.
'FAISCEAU'
'SCALING'
1  2
MULTIPOL SBEN
-1
54.92333
1
MULTIPOL QUAD
-1
54.92333
1
```

##### Strength

No visible resonance,  $S_z \simeq 1$ ,  $\forall G\gamma$ , up to unreasonable V emittances...

4.1.5  $\gamma G = 24 + \nu_z$  (16.20822 GeV)

## Tracking data

Zgoubi.dat, excerpts :

```

Xing 24+nu
'OBJET'
56.67175e3
8
  1  1  1
-0.64319816e-2 -0.49829722e-3  0.0 0.0E+00  0.0E+00  1.  'p'
-1.588  19.843  0.
1.033  11.675  30e-6  to
  0  1  0.
'FAISCEAU'
'SCALING'
1  2
MULTIPOL SBEN
-1
56.67175
1
MULTIPOL QUAD
-1
56.67175
1
.....
'CAVITE'
2.1 .1 is to fill zgoubi.CAVITE.Out for plot using zpop/7/20
807.043778118095  12.
290.d3  2.617993877991494365  9cavitiesx32kV, phi_s=180-30deg

```

## Strengths

$\epsilon_z/\pi$ ( $10^{-6}$ )	$A^2$	$ J_n ^2$ ( $10^{-5}$ )	$A^2/\epsilon_z/\pi$	$ J_n ^2/\epsilon_z/\pi$	$p_{init}$	$p_{final}$
30	1.011348	2.83912	33711.59	0.9463723	0.987	-0.2690
2	0.0737230	0.20696	36861.53	1.034799	0.999	0.857



$$\gamma G = 24 + \nu_z (16.20822 \text{ GeV}) - \epsilon_z/\pi = 2 \cdot 10^{-6}$$

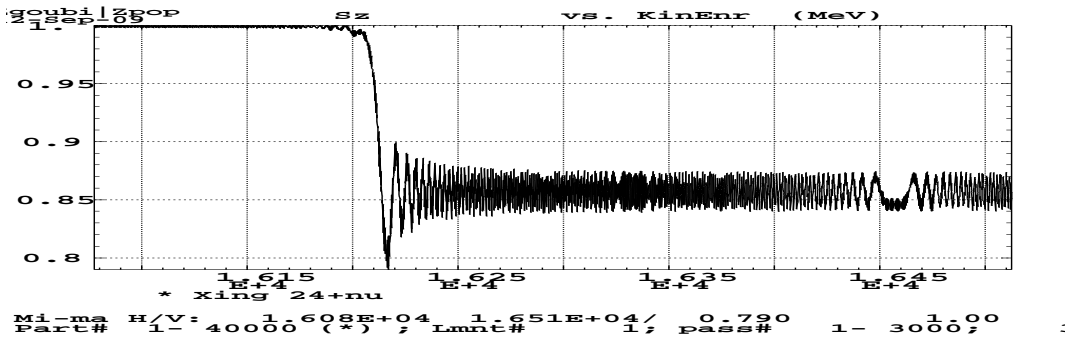


Figure 41:  $S_z$  versus kinetic energy.

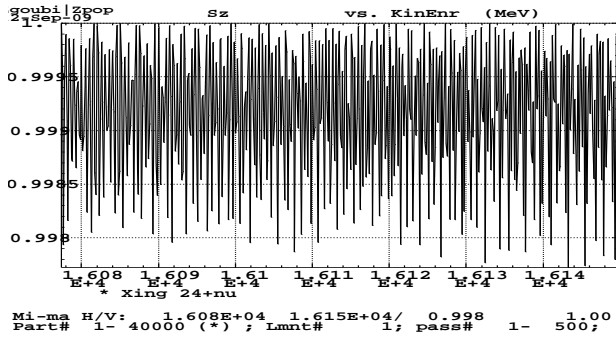


Figure 42: Zoom on initial  $S_z$ .

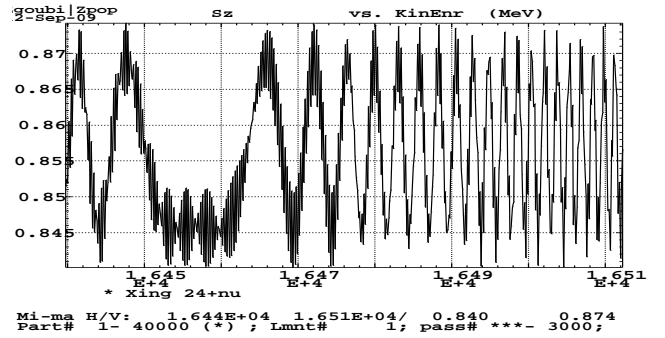


Figure 43: Zoom on final  $S_z$ .

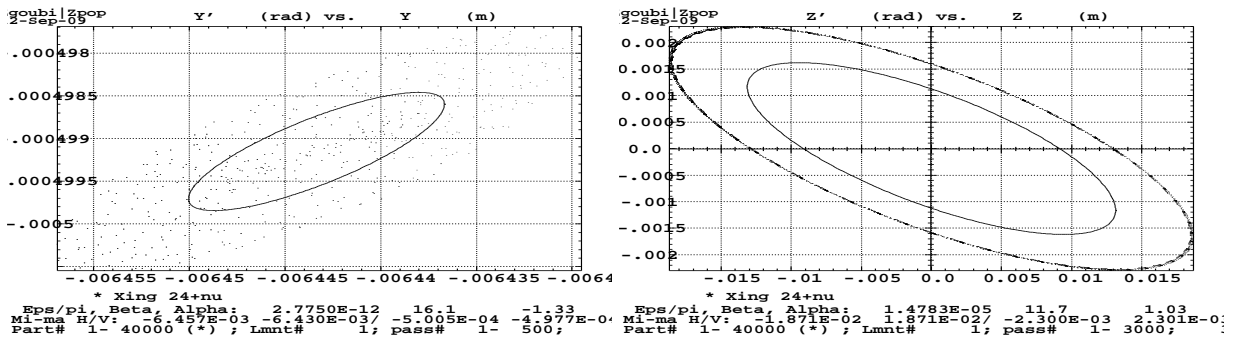


Figure 44:  $x-x'$  and  $z-z'$ .

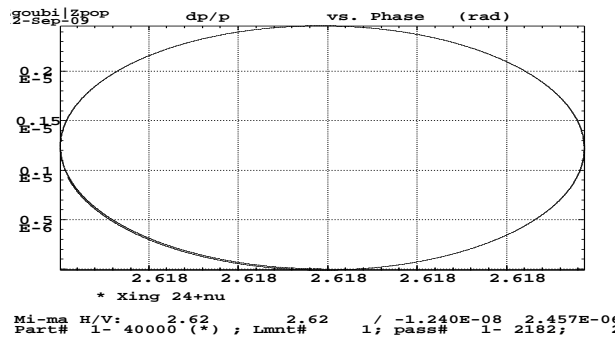


Figure 45:  $dp$ -phase.

$$\gamma G = 24 + \nu_z (16.20822 \text{ GeV}) - \epsilon_z/\pi = 30 \cdot 10^{-6}$$

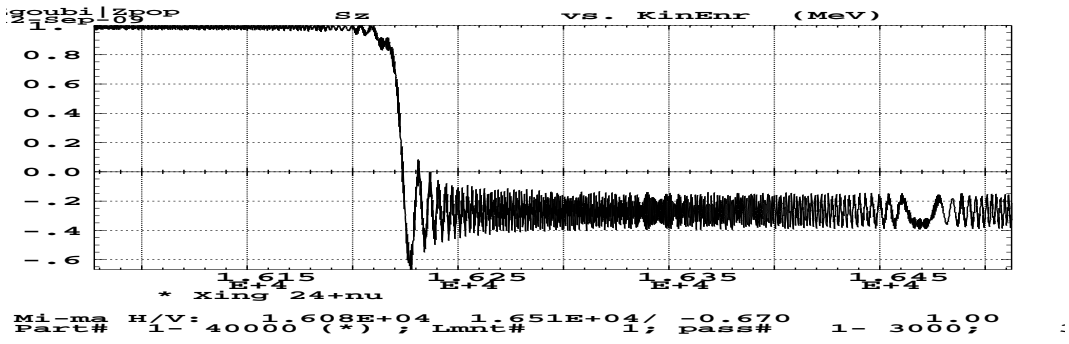


Figure 46:  $S_z$  versus kinetic energy.

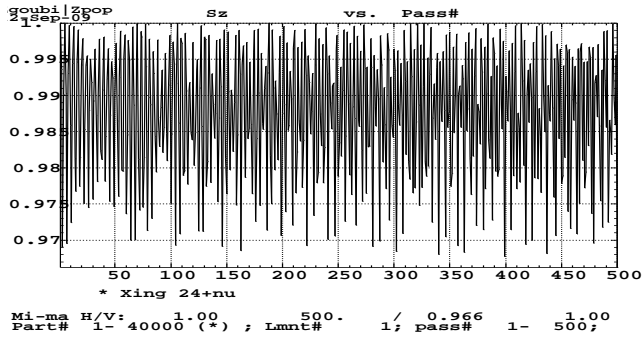


Figure 47: Zoom on initial  $S_z$ .

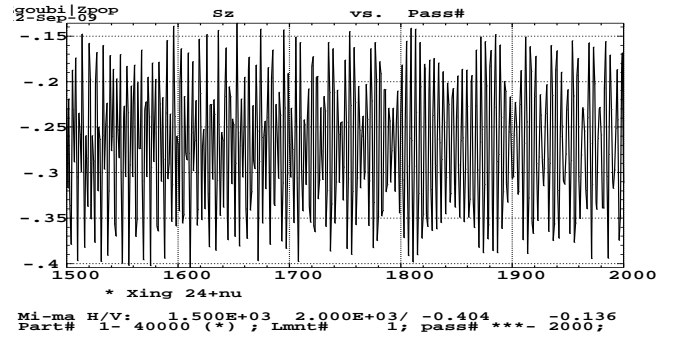


Figure 48: Zoom on final  $S_z$ .

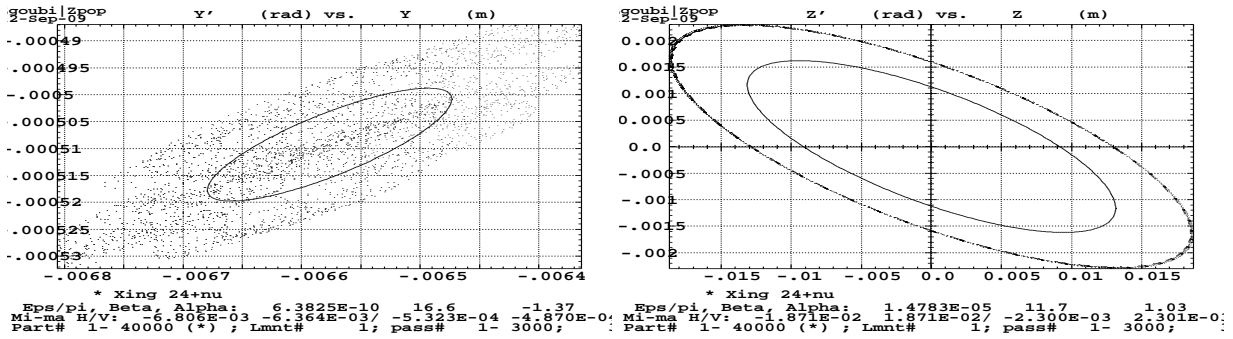


Figure 49:  $x-x'$  and  $z-z'$ .

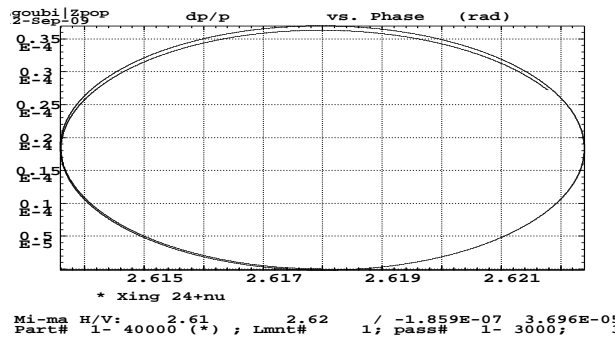


Figure 50:  $dp$ -phase.

### 4.1.6 $\gamma G = 36 - \nu_z$ (13.31575 GeV)

#### Tracking data

Zgoubi.dat, excerpts :

```
Xing 36-nu
'OBJET'
47.00580e3
8
  1  1  1
-0.64319816e-2 -0.49829722e-3  0.0 0.0E+00  0.0E+00  1.  'p'
-1.588  19.843  0.
1.033  11.675  .5e-7 =epsilon_z/pi
  0  1  0.
'SCALING'
1  2
MULTIPOL SBEN
-1
47.00580
1
MULTIPOL QUAD
-1
47.00580
1
'PARTICUL'
938.27203d0  1.602176487d-19  1.7928474d0  0.  0.
.....
'CAVITE'
2.1 .1 is to fill zgoubi.CAVITE.Out for plot using zpop/7/20
807.043778118095  12.
290.d3  2.617993877991494365  9cavitiesx32kV, phi_s=180-30deg
-----
```

From zgoubi.res :

```
Particle properties :
  Mass      = 938.272      MeV/c2
  Charge    = 1.602176E-19 C
  G factor  = 1.79285
```

```
Reference data :
  rigidity (kG.cm)      : 47005.8
  mass (MeV/c2)         : 938.272
  momentum (MeV/c)     : 14092.0
  energy, total (MeV)   : 14123.2
  energy, kinetic (MeV) : 13184.9
  beta = v/c           : 0.9977907636
  gamma                : 15.05233592
  beta*gamma           : 15.01908175
```

#### Strength

From Figs. 52, 53 one gets

$$p_{init} \approx 0.9998300, \quad p_{final} \approx 0.1545000$$

Eq. 2 yields

$$A^2 = 0.5494571$$

$$|J_n|^2 = 1.5424697E - 05$$

$$\gamma G = 36 - \nu_z \text{ (13.31575 GeV)}$$

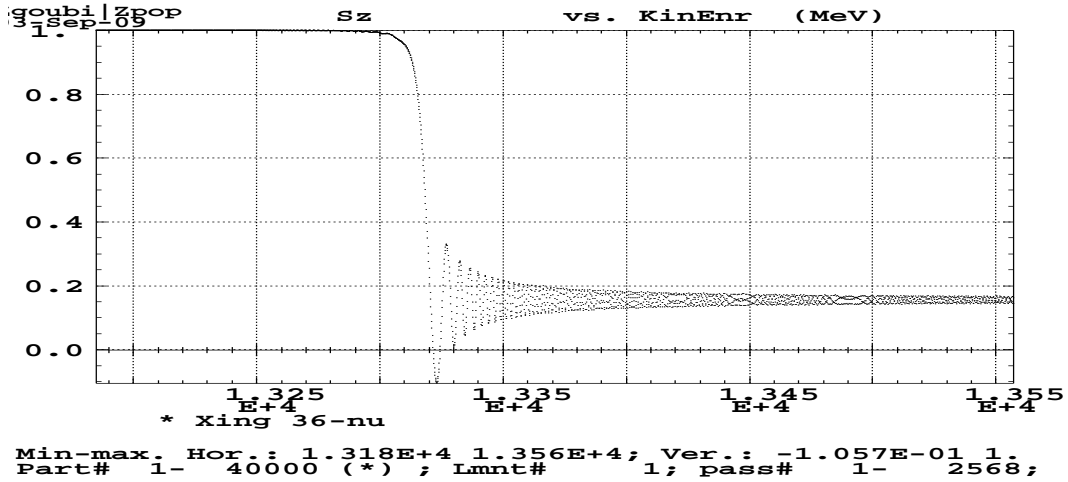


Figure 51:  $S_z$  versus kinetic energy.

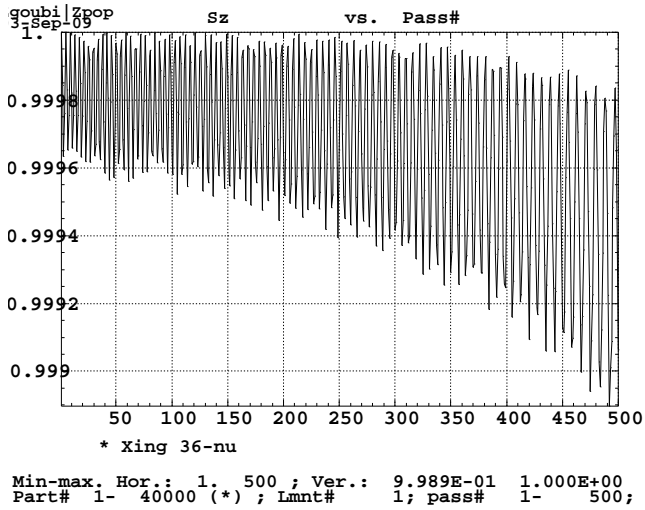


Figure 52: Zoom on initial  $S_z$ .

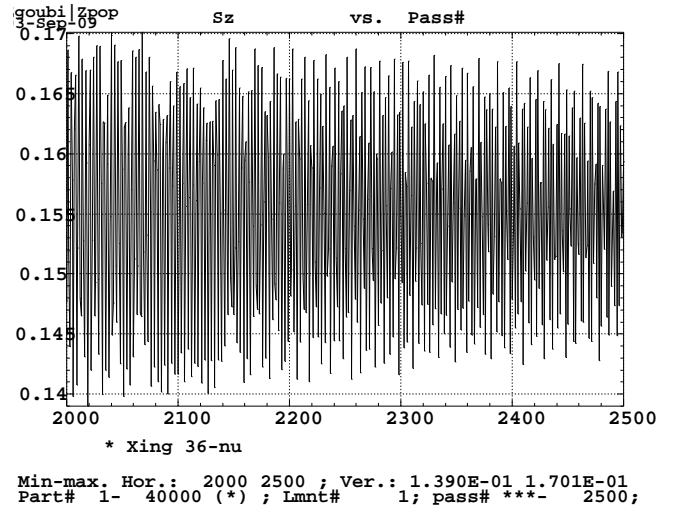


Figure 53: Zoom on final  $S_z$ .

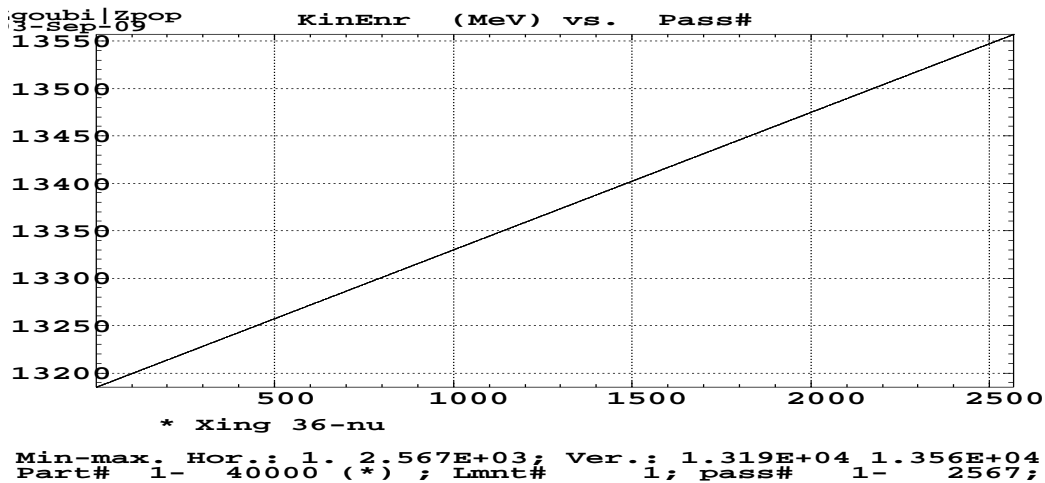


Figure 54: Kinetic E versus turn number.

$$\gamma G = 36 - \nu_z \text{ (13.31575 GeV)}$$

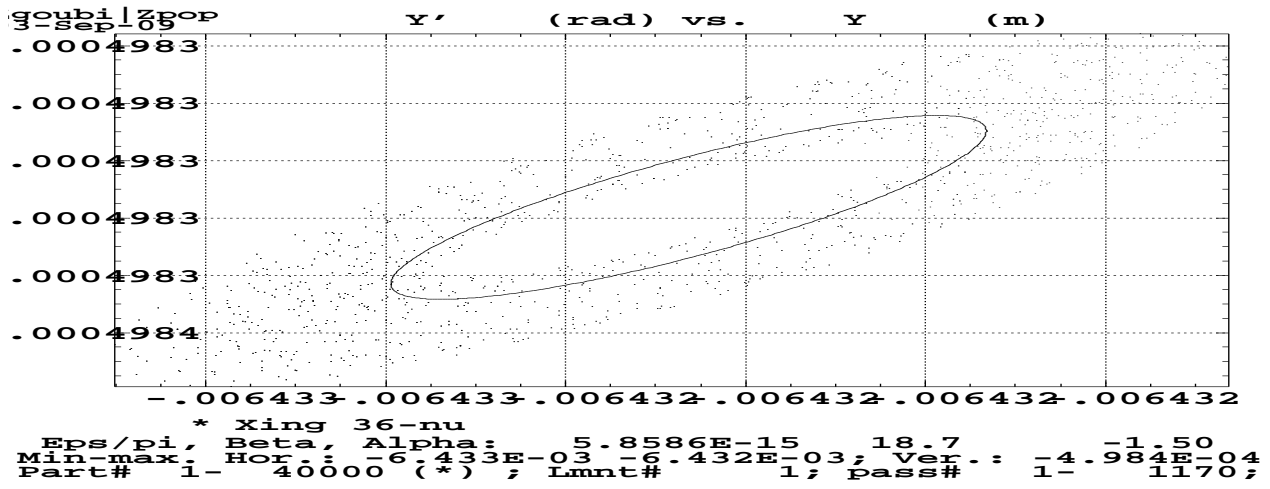


Figure 55: x-x'.

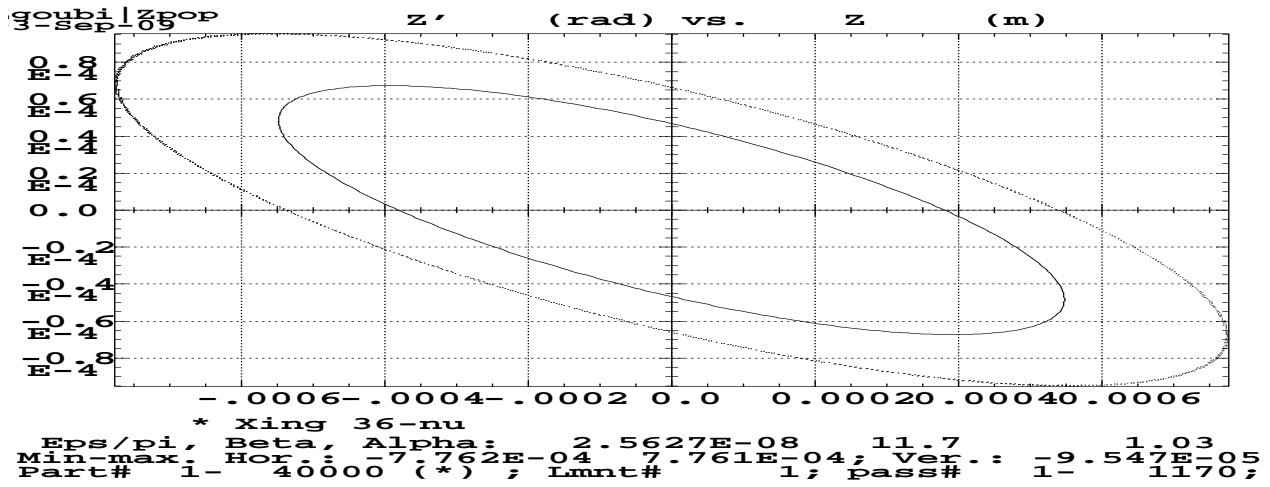


Figure 56: z-z'.

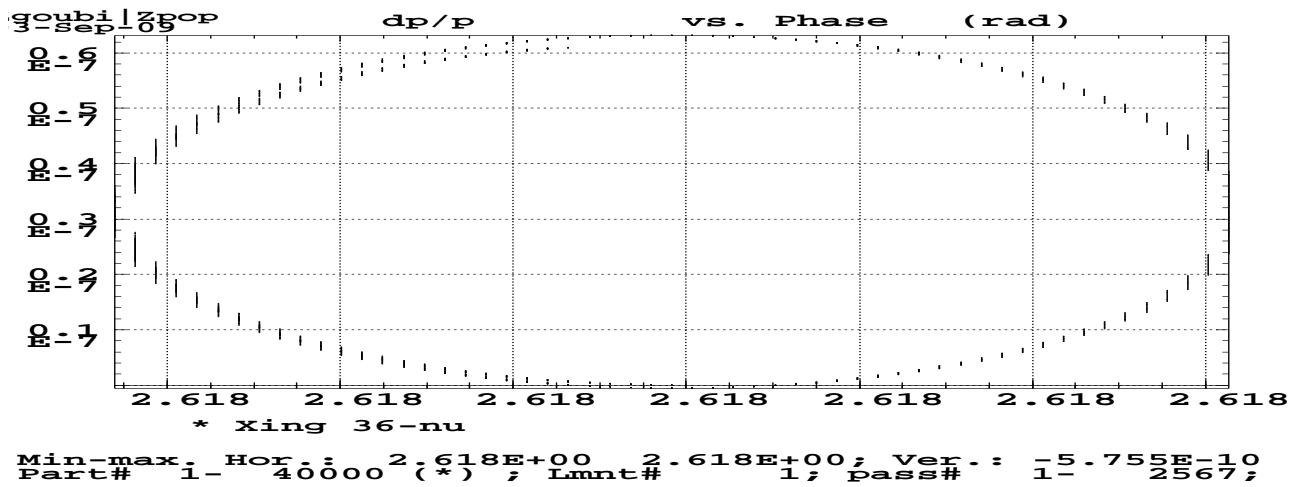


Figure 57: dp-phase.

### 4.1.7 $\gamma G = 48 - \nu_z$ (19.59585 GeV)

#### Tracking data

Zgoubi.dat, excerpts :

```
Xing 48-nu
'OBJET'
67.98605e3
8
  1  1  1
-0.64319816e-2 -0.49829722e-3  0.0 0.0E+00  0.0E+00  1.  'p'
-1.588  19.843  0.
1.033  11.675  0.5 to 2e-6
  0  1  0.
'SCALING'
1  2
MULTIPOL SBEN
-1
67.98605
1
MULTIPOL QUAD
-1
67.98605
1
```

3

#### Strength

Eq. 2 yields the results displayed in Tab. 4.

Table 4: Resonance strength for various vertical invariant values.

$\epsilon_z/\pi$ ( $\times 10^{-6}$ )	$A^2$	$ J_n ^2$	$A^2/\epsilon_z/\pi$	$ J_n ^2/\epsilon_z/\pi$	$p_{init}$	$p_{final}$
.125	0.04630575	1.2999233E-06	370446.0	10.39939	1	0.9095
.25	0.09862635	2.7686992E-06	394505.4	11.07480	0.9998	0.812
.5	0.1913054	5.3704412E-06	382610.8	10.74088	0.9996	0.6515
1	0.3895315	1.0935165E-05	389531.5	10.93517	0.9993	0.3545
2	0.8073937	2.2665648E-05	403696.8	11.33282	0.9985	-0.1078

$$\gamma G = 48 - \nu_z (19.59585 \text{ GeV}) - \epsilon_z/\pi = 0.125 \cdot 10^{-6}$$

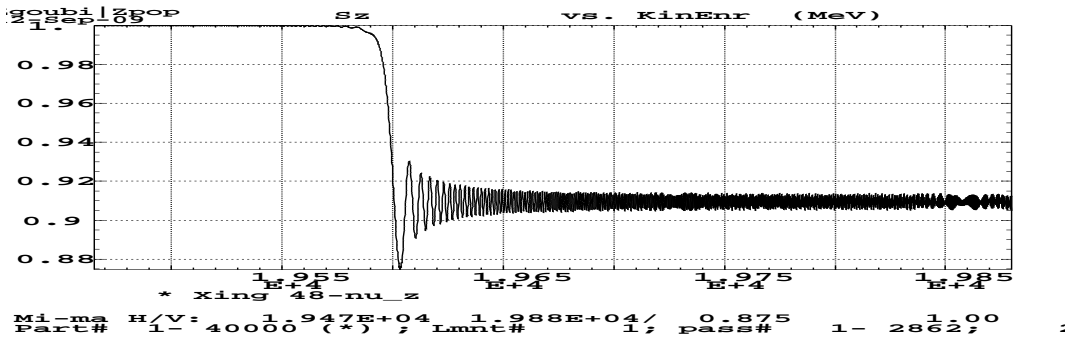


Figure 58:  $S_z$  versus kinetic energy.

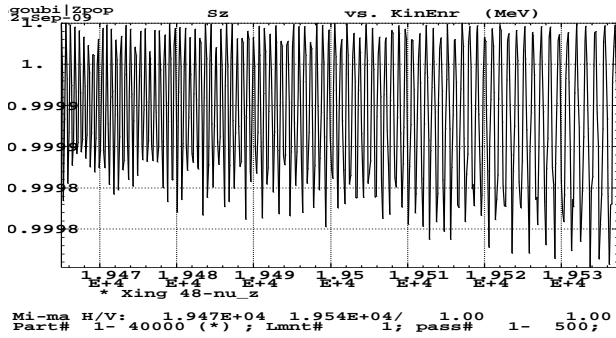


Figure 59: Zoom on initial  $S_z$ .

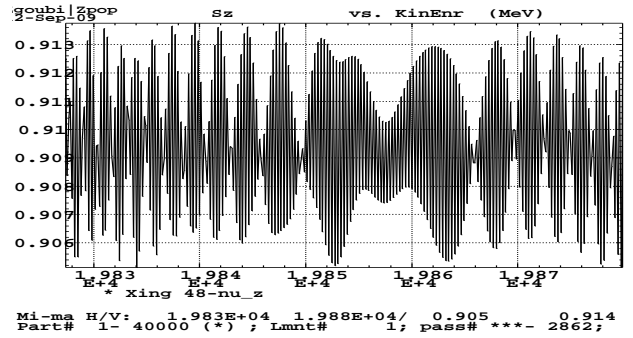


Figure 60: Zoom on final  $S_z$ .

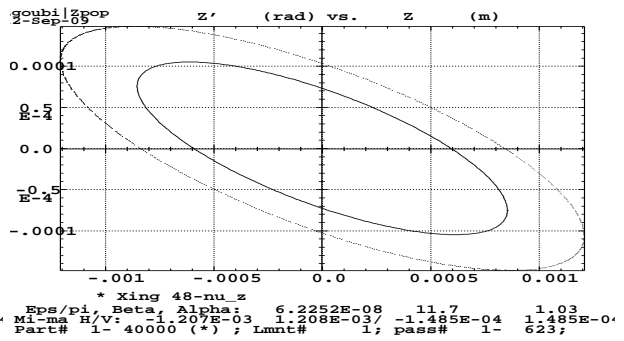
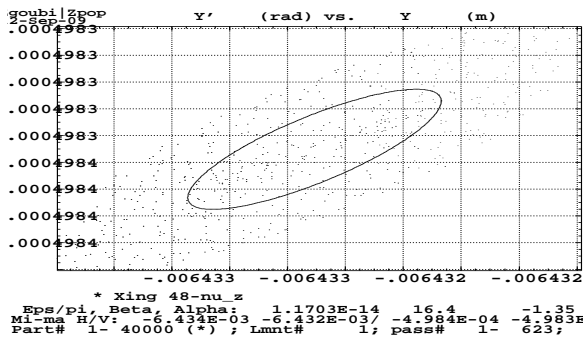


Figure 61:  $x-x'$  and  $z-z'$ .

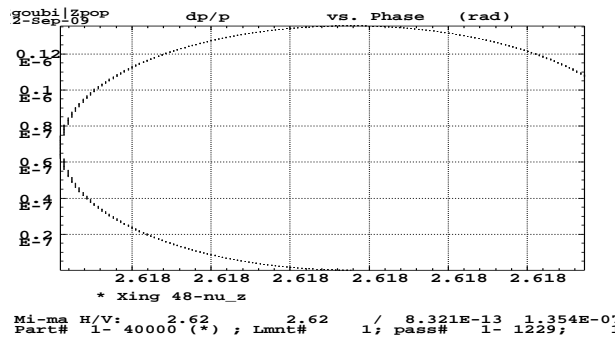


Figure 62:  $dp$ -phase (1350 turns).

$$\gamma G = 48 - \nu_z (19.59585 \text{ GeV}) - \epsilon_z/\pi = 0.25 \cdot 10^{-6}$$

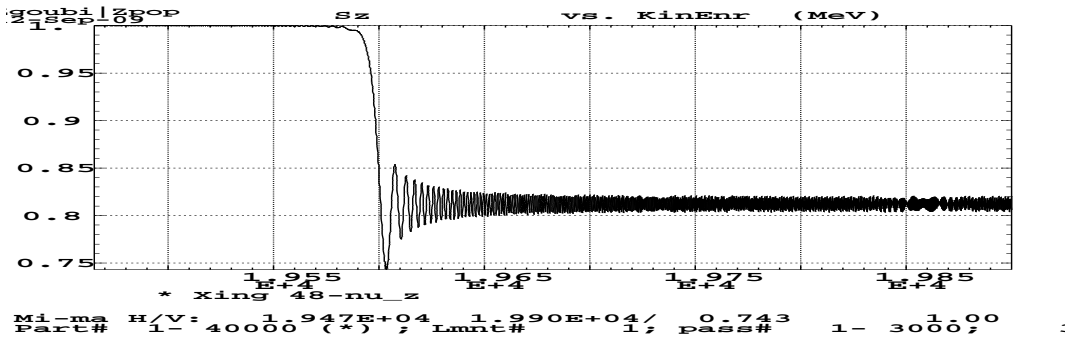


Figure 63:  $S_z$  versus kinetic energy.

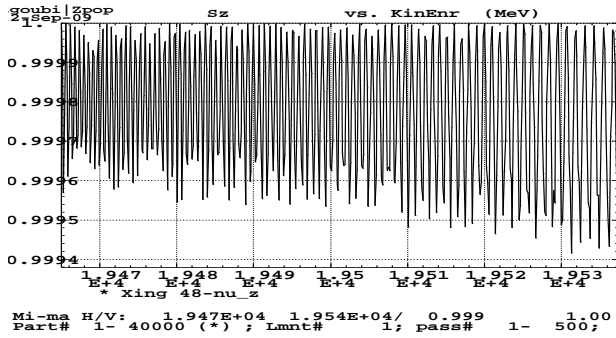


Figure 64: Zoom on initial  $S_z$ .

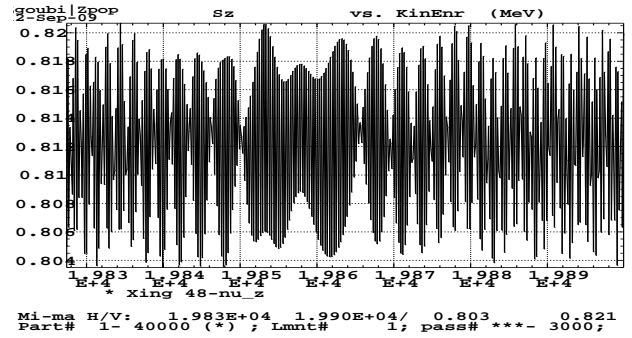


Figure 65: Zoom on final  $S_z$ .

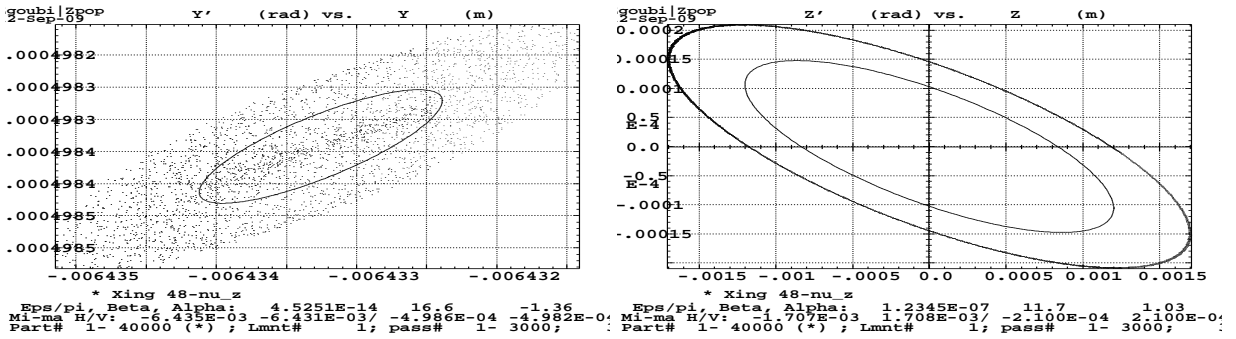


Figure 66:  $x-x'$  and  $z-z'$ .

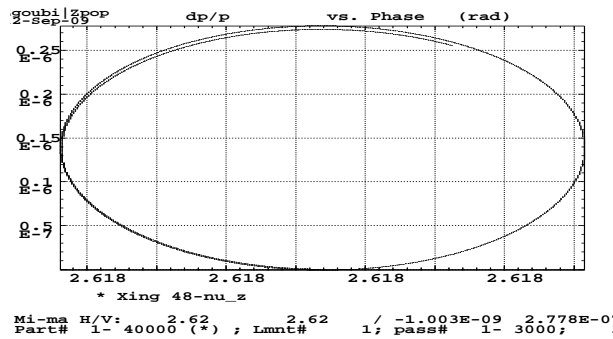


Figure 67:  $dp$ -phase.



$$\gamma G = 48 - \nu_z (19.59585 \text{ GeV}) - \epsilon_z/\pi = 0.5 \cdot 10^{-6}$$

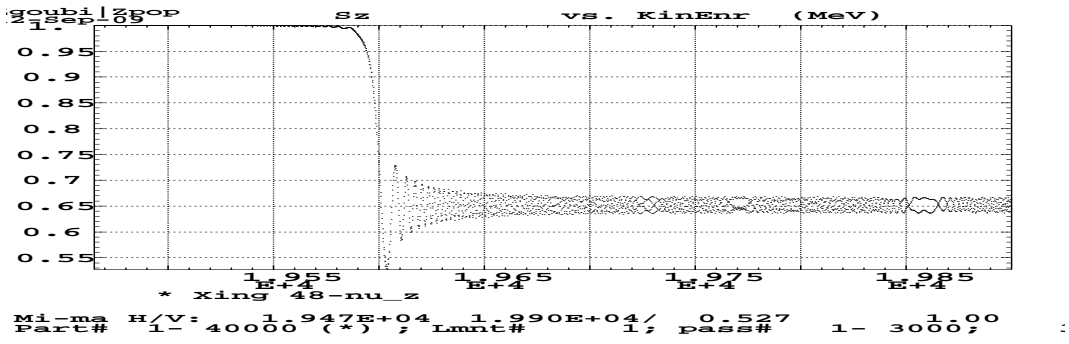


Figure 68:  $S_z$  versus kinetic energy.

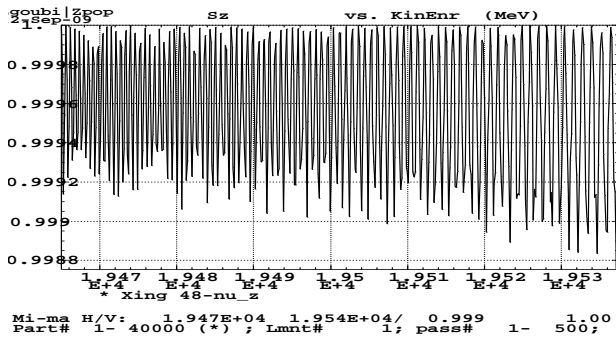


Figure 69: Zoom on initial  $S_z$ .

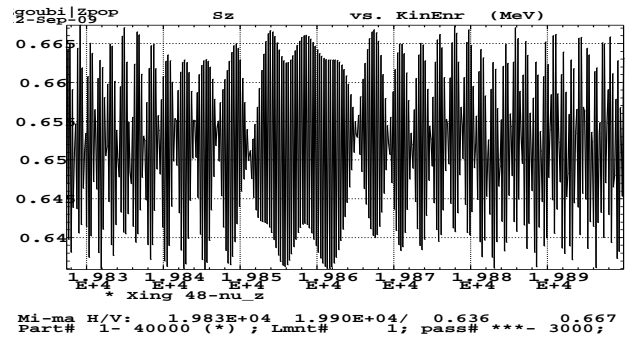


Figure 70: Zoom on final  $S_z$ .

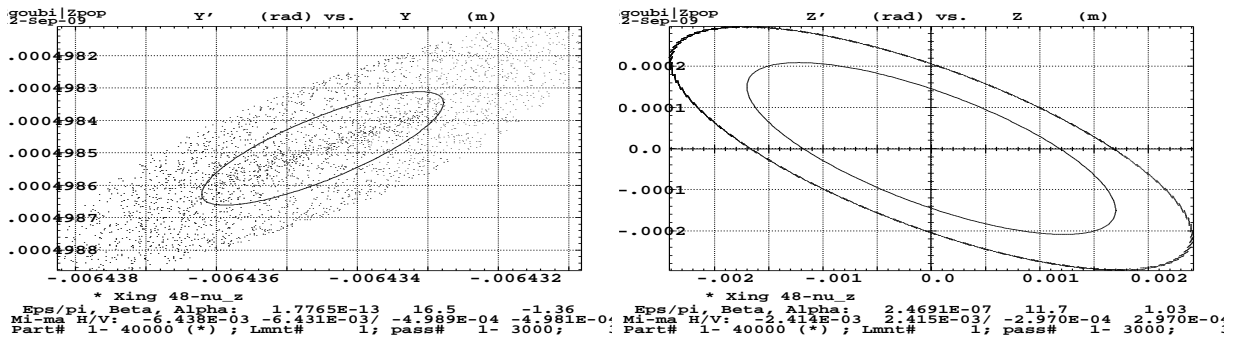


Figure 71:  $x-x'$  and  $z-z'$ .

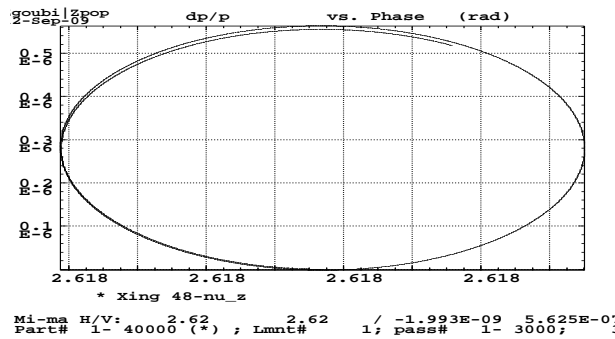


Figure 72:  $dp$ -phase.

$$\gamma G = 48 - \nu_z (19.59585 \text{ GeV}) - \epsilon_z/\pi = 10^{-6}$$

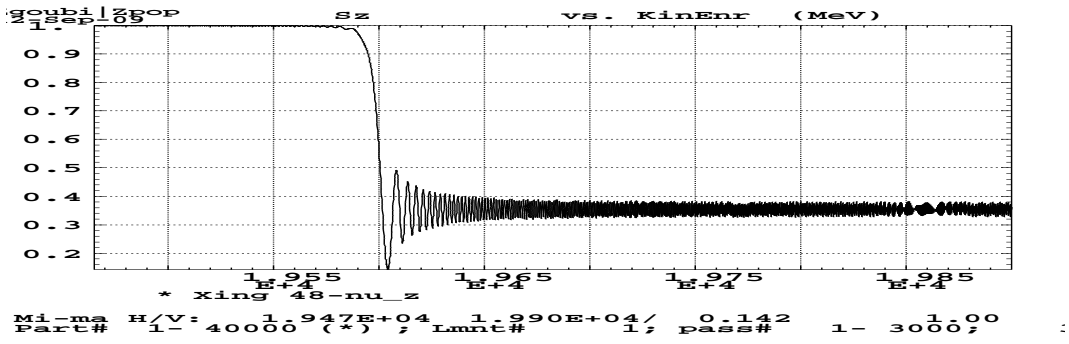


Figure 73:  $S_z$  versus kinetic energy.

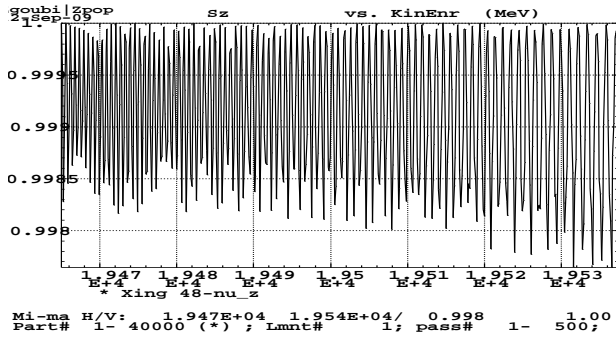


Figure 74: Zoom on initial  $S_z$ .

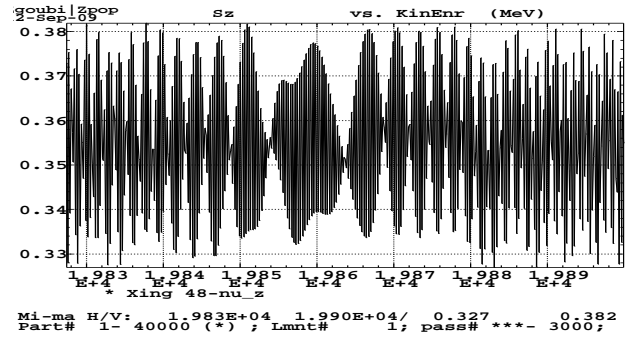


Figure 75: Zoom on final  $S_z$ .

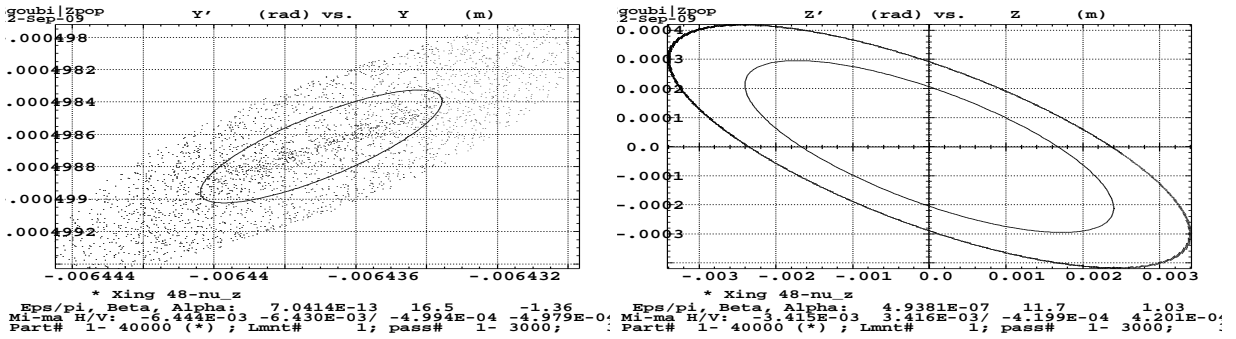


Figure 76:  $x-x'$  and  $z-z'$ .

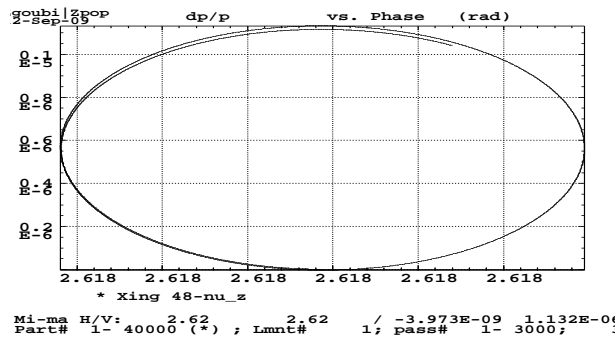


Figure 77:  $dp$ -phase.

$$\gamma G = 48 - \nu_z (19.59585 \text{ GeV}) - \epsilon_z/\pi = 2 \cdot 10^{-6}$$

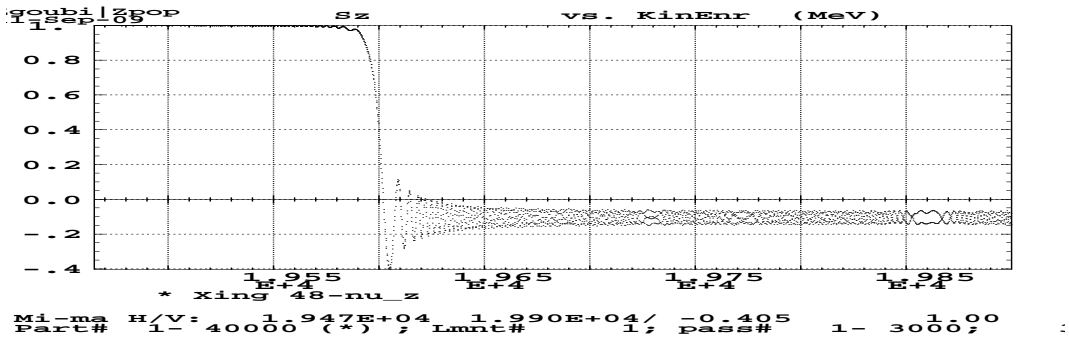


Figure 78:  $S_z$  versus kinetic energy.

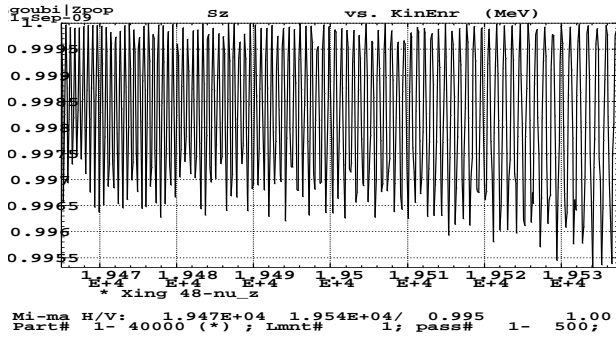


Figure 79: Zoom on initial  $S_z$ .

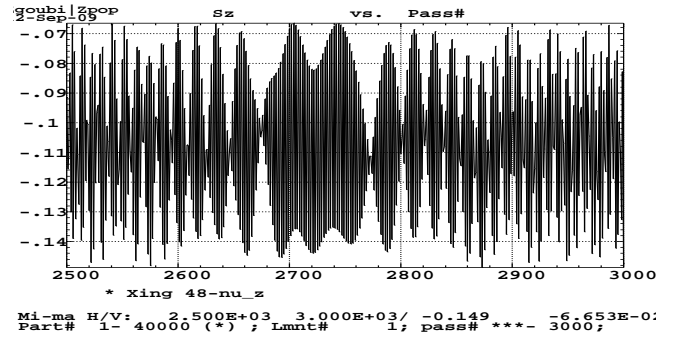


Figure 80: Zoom on final  $S_z$ .

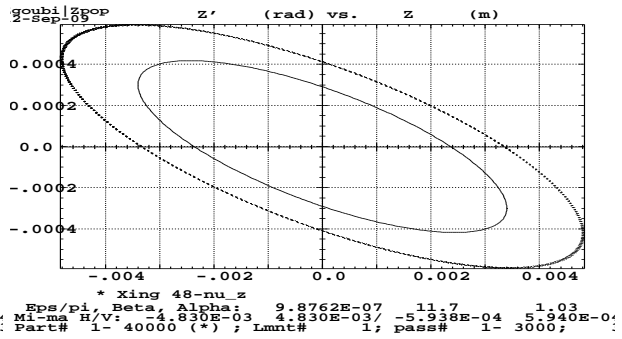
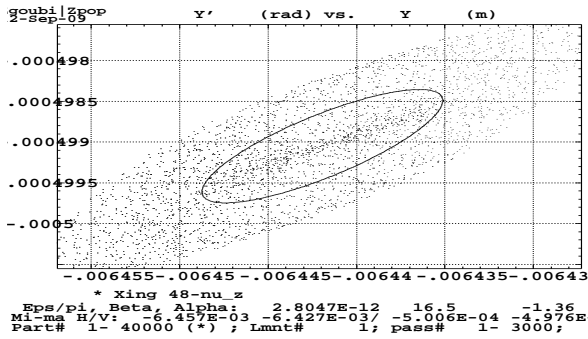


Figure 81:  $x-x'$  and  $z-z'$ .

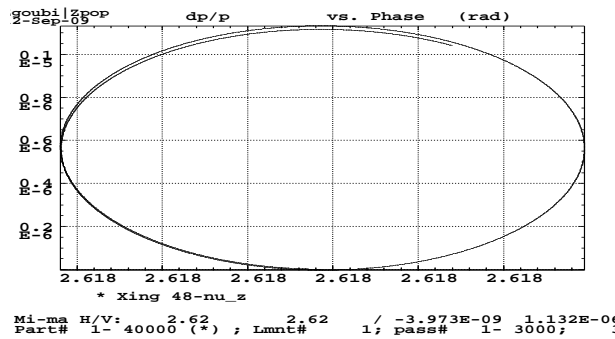


Figure 82:  $dp$ -phase.

**4.1.8  $\gamma G = 48 - \nu_z$ , bare lattice (all bends' sextu off, all quads off)**

Resonance strength computed from Zgoubi tracking differs from DEPOL's results in some cases of weak resonances, such as  $\gamma G = 48 - \nu_z$ . For that reason, in order to assess possible effect of sextupoles, we switch-off all sextupole components in all main bends. We also switch-off all tuning quadrupoles, the focusing is therefore due to the sole main bends' quadrupole component.

The following shows that the initial results are practically unchanged, the same resonance strength comes out of the ray-tracing.

Setting all sextupoles and quadrupoles off does not change much the ring parameters, 0-th and 1-st order machine parameters take the values given in Tab. 5. Earlier values are recalled for comparison.

A particle with vertical emittance  $\epsilon_y/\pi = 10^{-6}$  m.rad is launched through the resonance. Spin motion upon crossing does not change much either, this can be observed from Fig. 83, by comparison with Fig. 58, page 42.

Table 5: Bare lattice parameters. Old ones (copied from Tab. 1) are recalled in the right column for comparison.

		New parameters	Old parameters
Reference momentum	(relative)	1	1
Circumference <sup>4</sup>	(m)	807.0437	807.0438
Qx, Qy		0.71066, 0.76412	0.71195, 0.76346
<i>Periodic functions at "Begin AGS" :</i>			
$\beta_x, \beta_y$	(m)	19.7850, 11.7005	19.8432, 11.6751
$\alpha_x, \alpha_y$		-1.585, -1.037	-1.588, 1.033
$D_x, D'_x$	(m,-)	2.043, 0.144	2.034, 0.144
closed orbit, $x_{co}, x'_{co}$	mm, mrad	-0.645, -0.50	-6.43 -0.50 <sup>1,3</sup>
$\gamma G = 48 - \nu_z$		39.236	39.236
kinetic energy on resonance	(GeV)	19.6097	19.5958
$B\rho$ on resonance	(T.m)	68.4692	68.4229

**Tracking data**

Zgoubi.dat, excerpts :

```
Xing 48-nu_z. Bare lattice, bends' sextu off, quads off.
'OBJET'
68.032e3
8
1 1 1
-6.453198E-03 -5.003742E-04 0.0 0.0E+00 0.0E+00 1. 'p'
-1.588 19.843 0.
1.033 11.675 1e-6
0 1 0.
'SCALING'
1 2
MULTIPOL SBEN
-1
68.032
1
MULTIPOL QUAD
-1
0000000
1
'PARTICUL'
938.27203d0 1.602176487d-19 1.7928474d0 0. 0.
.....
'MULTIPOL' SBEN ALBF
0 .Dip
200.6554 10.00 0.11712499 0.04848519 -0.00050563e-20 0.0 0.0 0.0 0.0 0.0 0.0 0.0
0. 0. 10.00 4.0 0.800 0.00 0.00 0.00 0.00 0.0 0.0 0.0
4 .1455 2.2670 -.6395 1.1558 0. 0. 0.
0. 0. 10.00 4.0 0.800 0.00 0.00 0.00 0.00 0.0 0.0 0.0
4 .1455 2.2670 -.6395 1.1558 0. 0. 0.
0. 0. 0. 0. 0. 0. 0. 0. 0. 0. 0.
#20|200|20 Dip ALBF
3 0.0000000000000000 0.0000000000000000 -1.175115045000000E-002
.....
```

$$\gamma G = 48 - \nu_z (19.6097 \text{ GeV}) - \epsilon_z/\pi = 10^{-6}$$

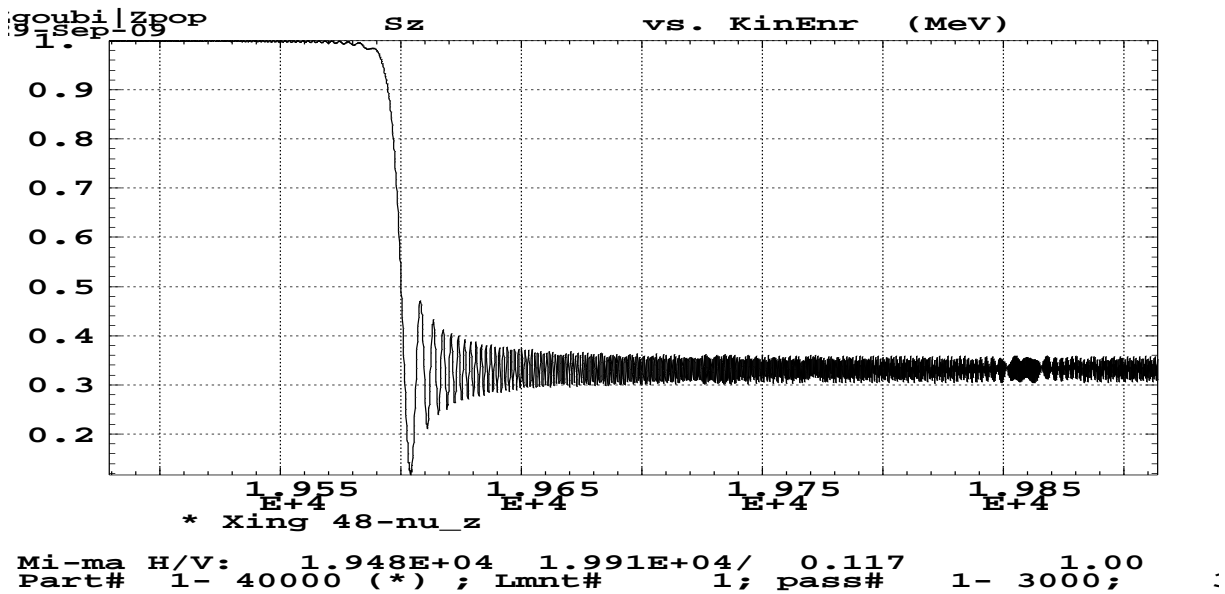


Figure 83:  $S_z$  versus kinetic energy. See Fig. 58, page 42 for comparison.

4.1.9  $\gamma G = 36 + \nu_z$  (22.48832 GeV)

## Tracking data

Zgoubi.dat, excerpts :

```

Xing 36+nu
'OBJET'
77.64321e3
8
  1  1  1
-0.64319816e-2 -0.49829722e-3  0.0 0.0E+00  0.0E+00  1.  'p'
-1.588  19.843  0.
1.033  11.675  .2e-7 =epsilon_z/pi
  0  1  0.
'SCALING'
1  2
MULTIPOL SBEN
-1
77.64321
1
MULTIPOL QUAD
-1
77.64321
1
'PARTICUL'
938.27203d0  1.602176487d-19  1.7928474d0  0.  0.
.....
'CAVITE'
2.1 .1 is to fill zgoubi.CAVITE.Out for plot using zpop/7/20
807.043778118095  12.
290.d3  2.617993877991494365  9cavitiesx32kV, phi_s=180-30deg
-----

```

From zgoubi.res :

```

Particle properties :
  Mass      = 938.272      MeV/c2
  Charge    = 1.602176E-19 C
  G factor  = 1.79285
Reference data :
  rigidity (kG.cm) : 77643.2
  mass (MeV/c2)    : 938.272
  momentum (MeV/c) : 23276.8
  energy, total (MeV) : 23295.8
  energy, kinetic (MeV) : 22357.5
  beta = v/c      : 0.9991885714
  gamma          : 24.82835560
  beta*gamma     : 24.80820916

```

## Strengths

From Figs. 20, 20 one gets

$\epsilon_z/\pi$ ( $10^{-6}$ )	$A^2$	$ J_n ^2$ ( $10^{-5}$ )	$A^2/\epsilon_z/\pi$	$ J_n ^2/\epsilon_z/\pi$	$p_{init}$	$p_{final}$
0.002	0.1329602	0.37325392	6.648009E+07	1866	1.	0.751
0.02	1.431838	4.0195435	7.1591912E+07	2009	1.	-0.522

$$\gamma G = 36 + \nu_z (22.48832 \text{ GeV}) - \epsilon_z/\pi = 0.002 \cdot 10^{-6}$$

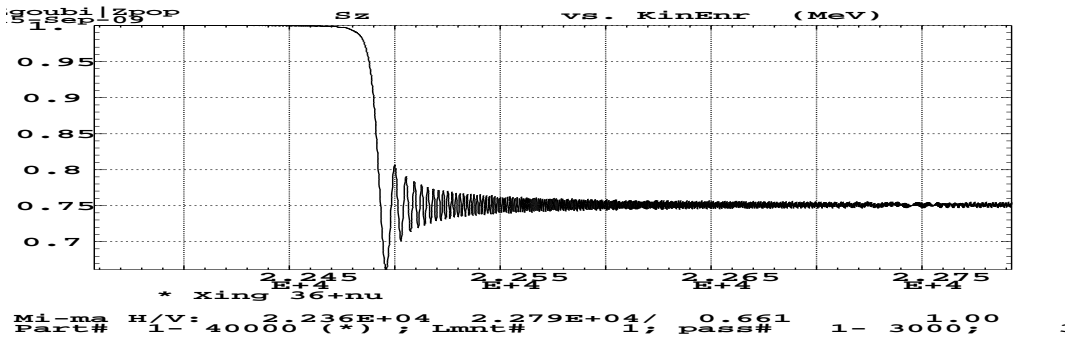


Figure 84:  $S_z$  versus kinetic energy.

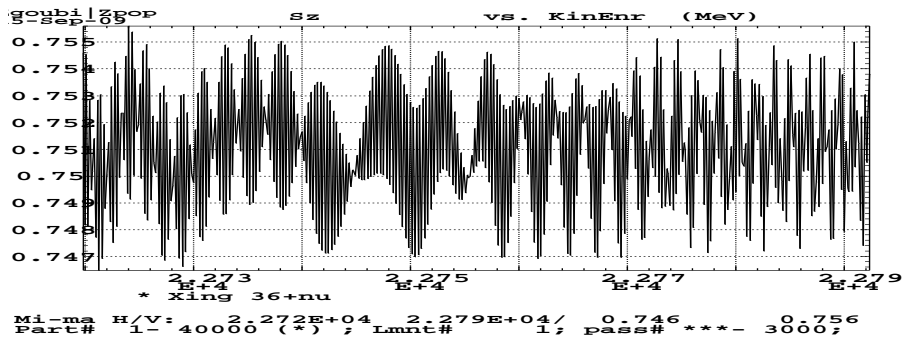


Figure 85: Zoom on final  $S_z$ .

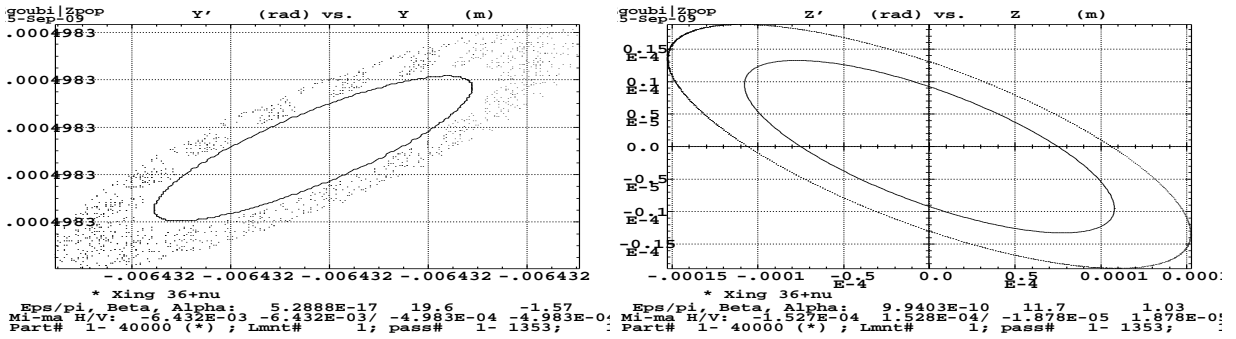


Figure 86:  $x-x'$  and  $z-z'$ .

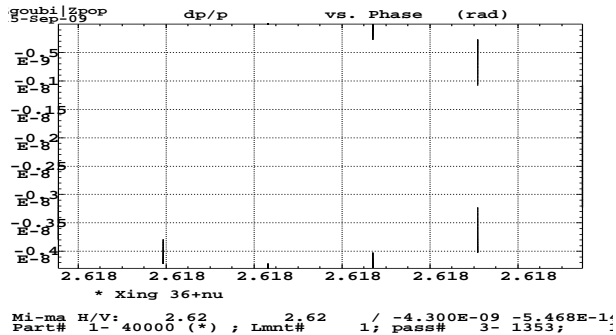


Figure 87:  $dp$ -phase.

$$\gamma G = 36 + \nu_z (22.48832 \text{ GeV}) - \epsilon_z / \pi = 0.02 \cdot 10^{-6}$$

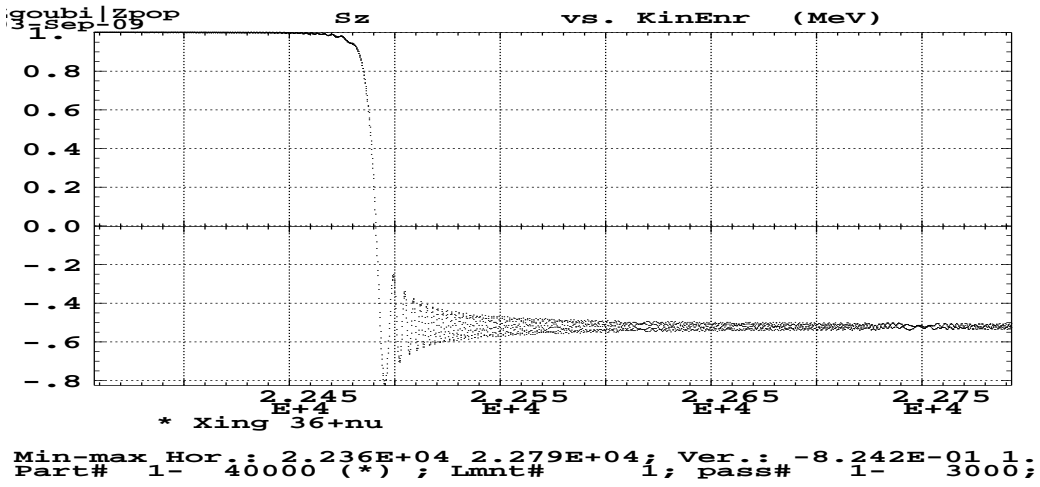


Figure 88:  $S_z$  versus kinetic energy.

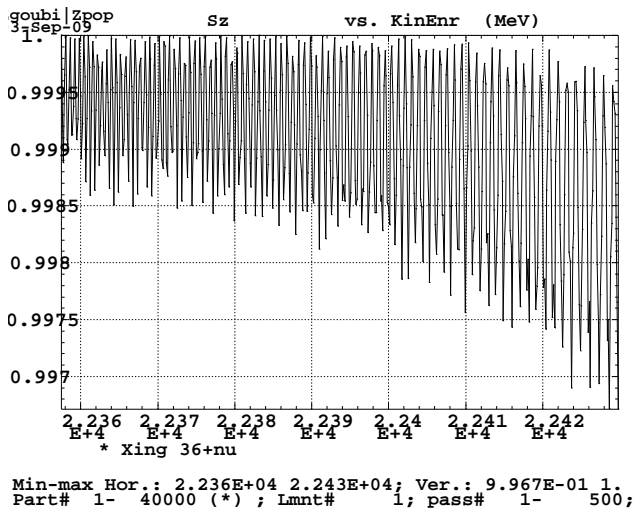


Figure 89: Zoom on initial  $S_z$ .

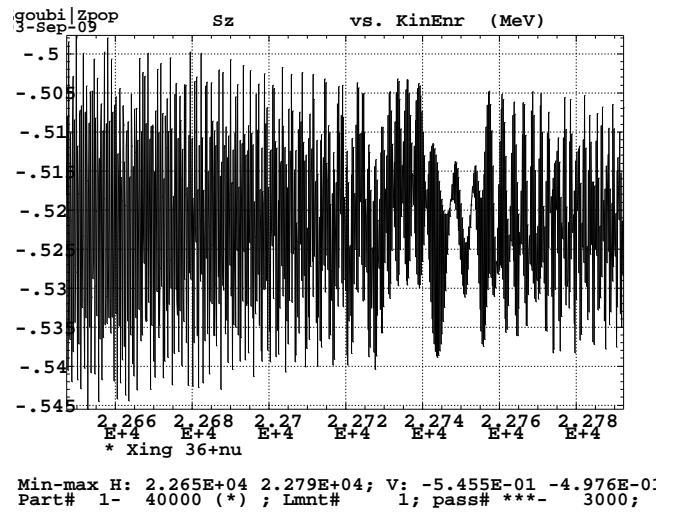


Figure 90: Zoom on final  $S_z$ .

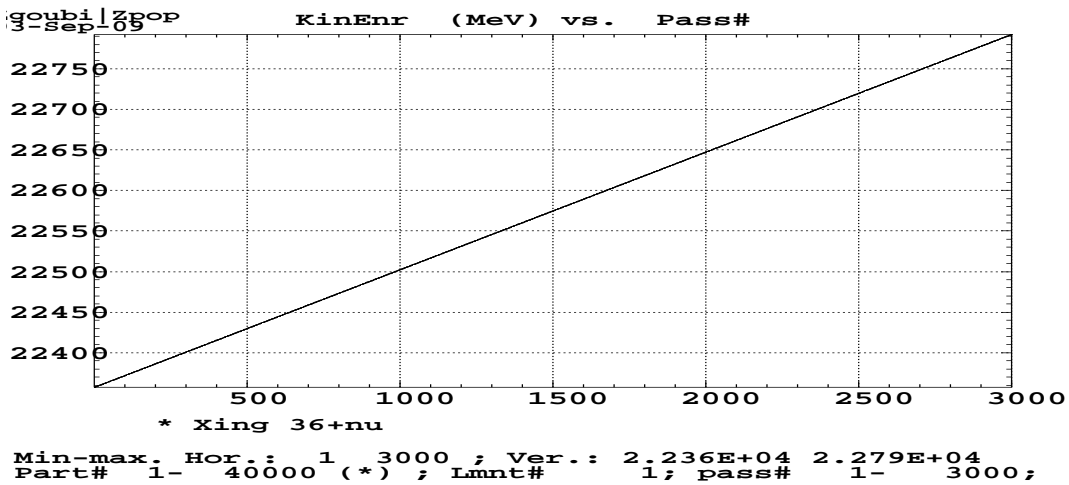


Figure 91: Kinetic E versus turn number.



$$\gamma G = 36 + \nu_z (22.48832 \text{ GeV}) - \epsilon_z/\pi = 0.02 \cdot 10^{-6}$$

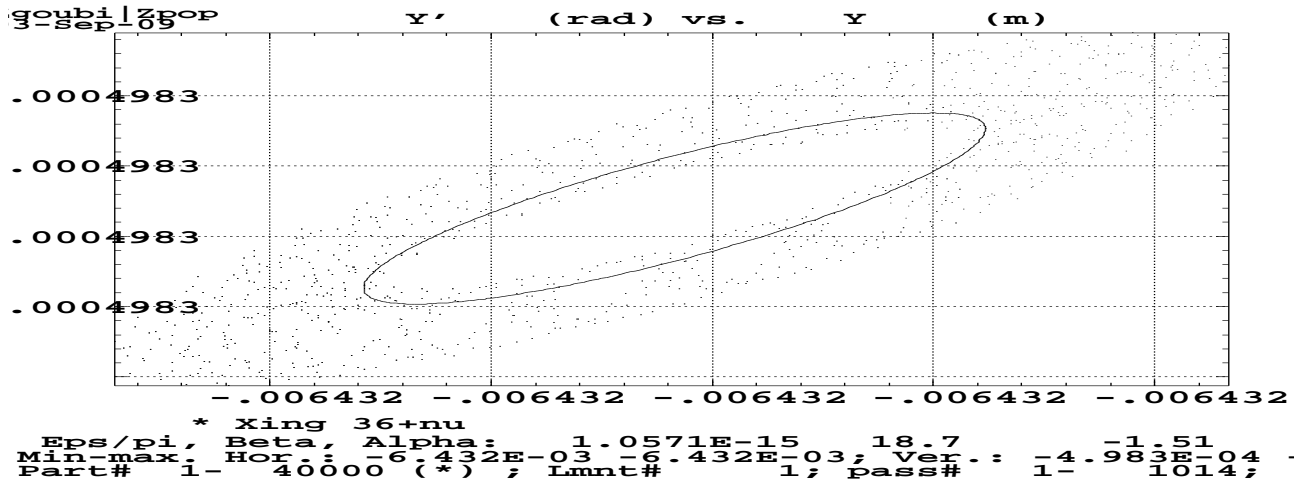


Figure 92: x-x'.

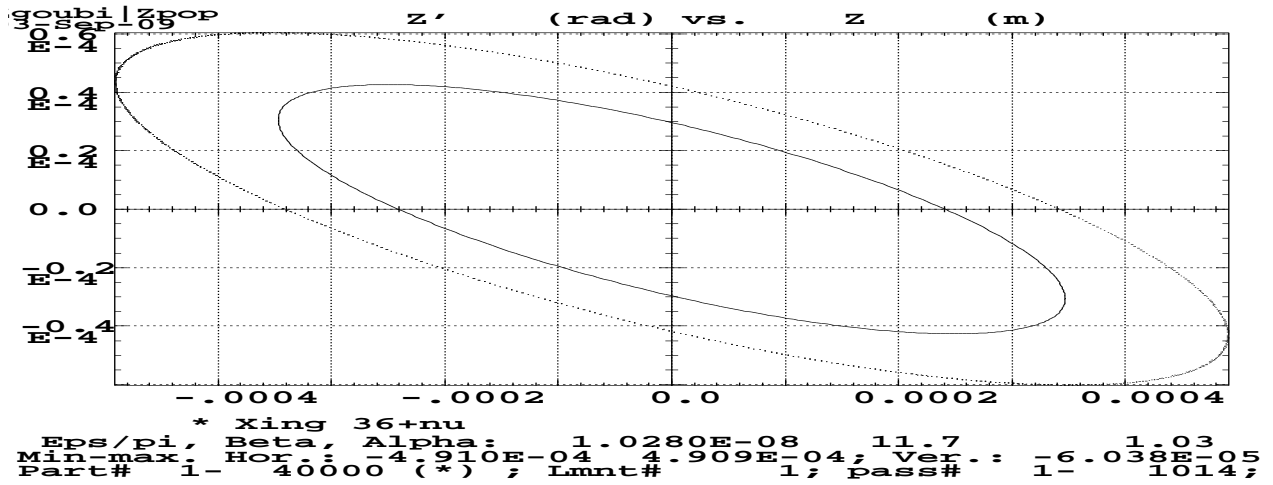


Figure 93: z-z'.

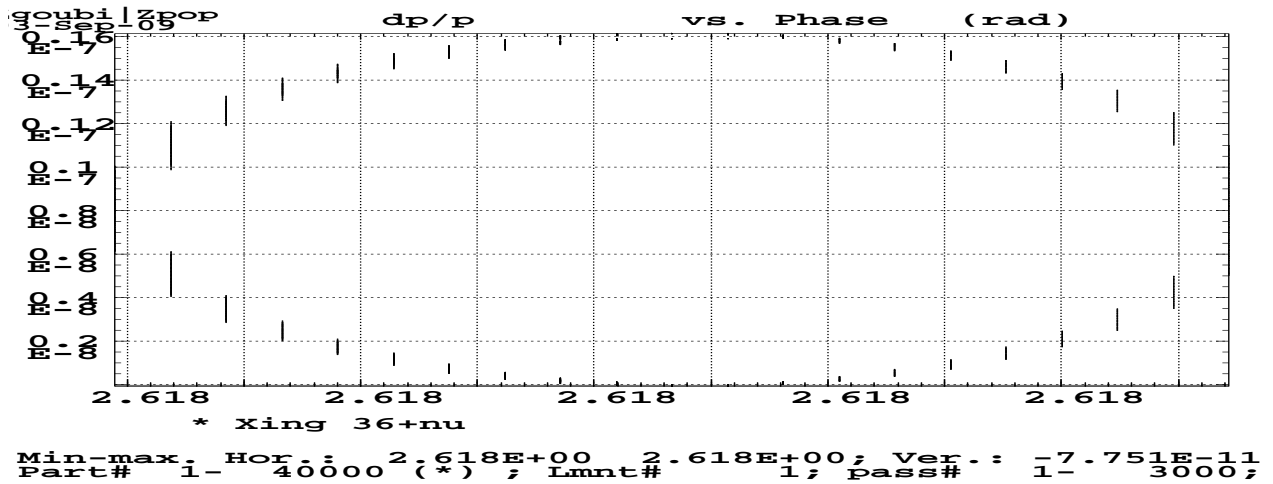


Figure 94: dp-phase.

## 4.2 Imperfection resonances

### 4.2.1 $\gamma G = 9$ (3.77180 GeV)

#### Tracking data

Zgoubi.dat, excerpts :

```
Xing gammaG = 9
'OBJET'
14.95063e3
2
1 1
-0.64333404 -0.49841318 7.55234854E-02 9.07085314E-02 0.0E+00 1. 'p'
1
'FAISCEAU'
'SCALING'
1 3
MULTIPOL VKIC
-1
14.95063 scales the vertical kick
1
MULTIPOL SBEN
-1
14.95063
1
MULTIPOL QUAD
-1
14.95063
1
'PARTICUL'
938.27203d0 1.602176487d-19 1.7928474d0 0. 0.
.....
'MULTIPOL' VKIC DVCA02
0 .kicker
0.1000E-03 10.00 2.e3 0.000000 0.0 0.0 0.0 0.0 0.0 0.0 0.0 0.0 0.0
.0 .0 1.00 0.00 0.00 0.00 0.00 0.0 0.0 0.0.
4 .1455 2.2670 -.6395 1.1558 0. 0. 0.
.0 .0 1.00 0.00 0.00 0.00 0.00 0.0 0.0 0.0.
4 .1455 2.2670 -.6395 1.1558 0. 0. 0.
1.570796327 0. 0. 0. 0. 0. 0. 0. 0. 0.
#20|20|20 Kick
1 0. 0. 0.
.....
'CAVITE'
2.1 .1 is to fill zgoubi.CAVITE.Out for plot using zpop/7/20
807.043778118095 12.
290.d3 0.5235987755982988731 9cavitiesx32kV, phi_s=30deg
'MARKER' #End
'REBELOTE'
1999 0.2 99
'END'
```

From zgoubi.res :

```
Particle properties :
Mass = 938.272 MeV/c2
Charge = 1.602176E-19 C
G factor = 1.79285
Reference data :
rigidity (kG.cm) : 14121.6
mass (MeV/c2) : 938.272
momentum (MeV/c) : 4233.56
energy, total (MeV) : 4336.29
energy, kinetic (MeV) : 3398.01
beta = v/c : 0.9763099040
gamma : 4.621565007
beta*gamma : 4.512079688
```

#### Strengths

From Figs. 96, 97, Eq. 2, one gets

kick (mrad)	$\hat{z}_{co}$ (mm)	$A^2$	$ J_n ^2$ ( $10^{-6}$ )	$A^2/\hat{z}_{co}$	$ J_n ^2/\hat{z}_{co}$	$P_{init}$	$P_{final}$
0.1	0.093				4.1295695		0.997457
1	0.93				4.1102805	1.	0.762110
	2.77	1.224737	34.381555			0.992	-0.412

$$\gamma G = 9 - \hat{z}_{co} = 2.77 \text{ mm}$$

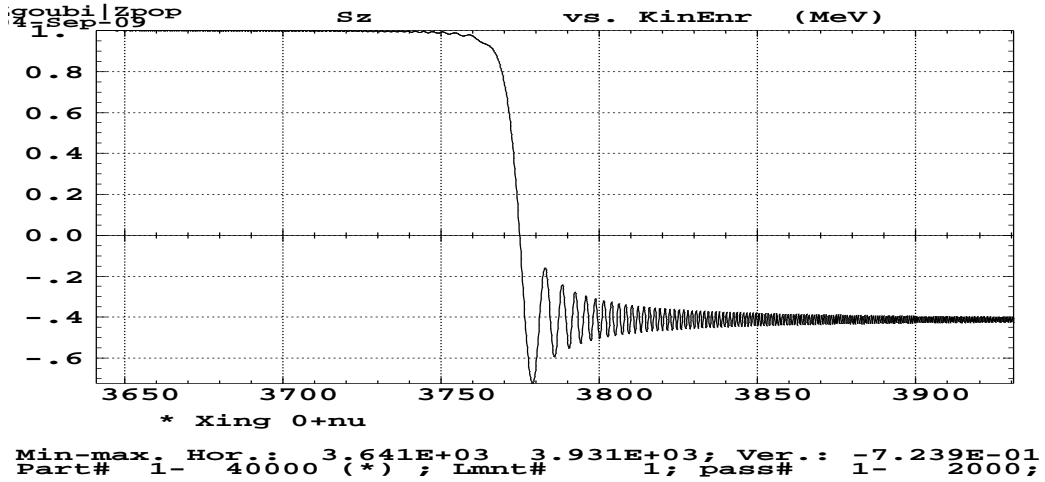


Figure 95:  $S_z$  versus kinetic energy.

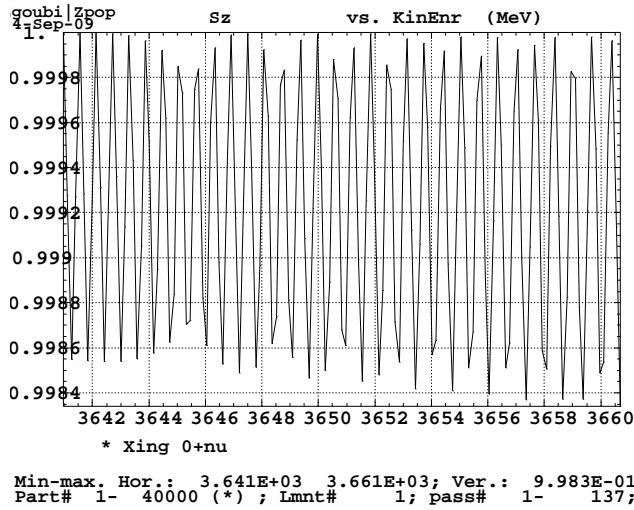


Figure 96: Zoom on initial  $S_z$ .

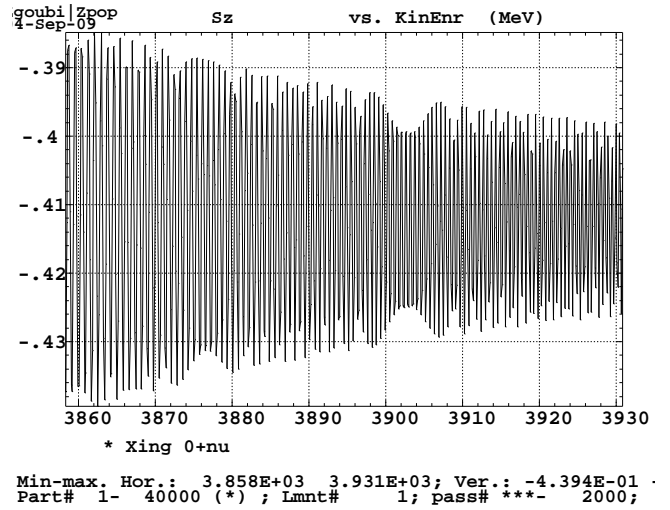


Figure 97: Zoom on final  $S_z$ .

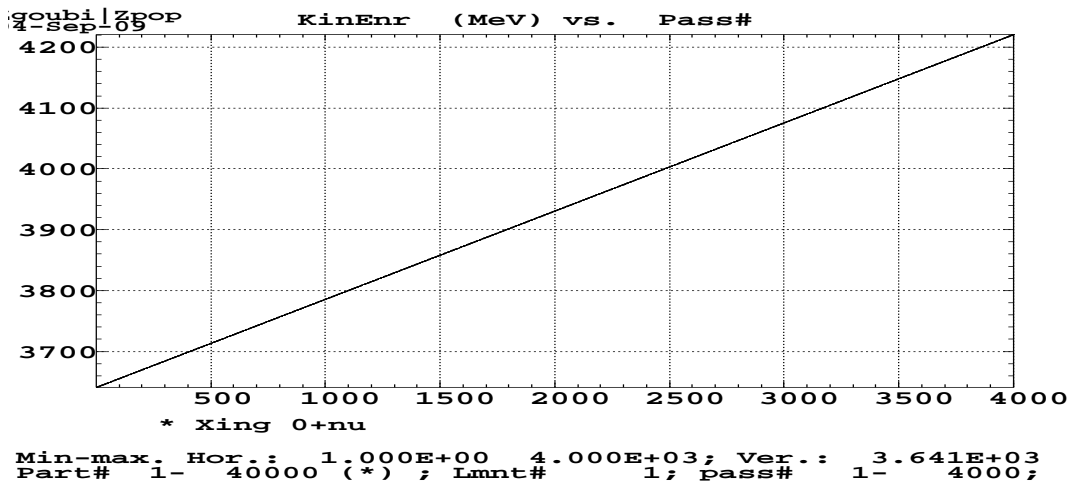


Figure 98: Kinetic E versus turn number.

$$\gamma G = 9 - \hat{z}_{co} = 2.77 \text{ mm}$$

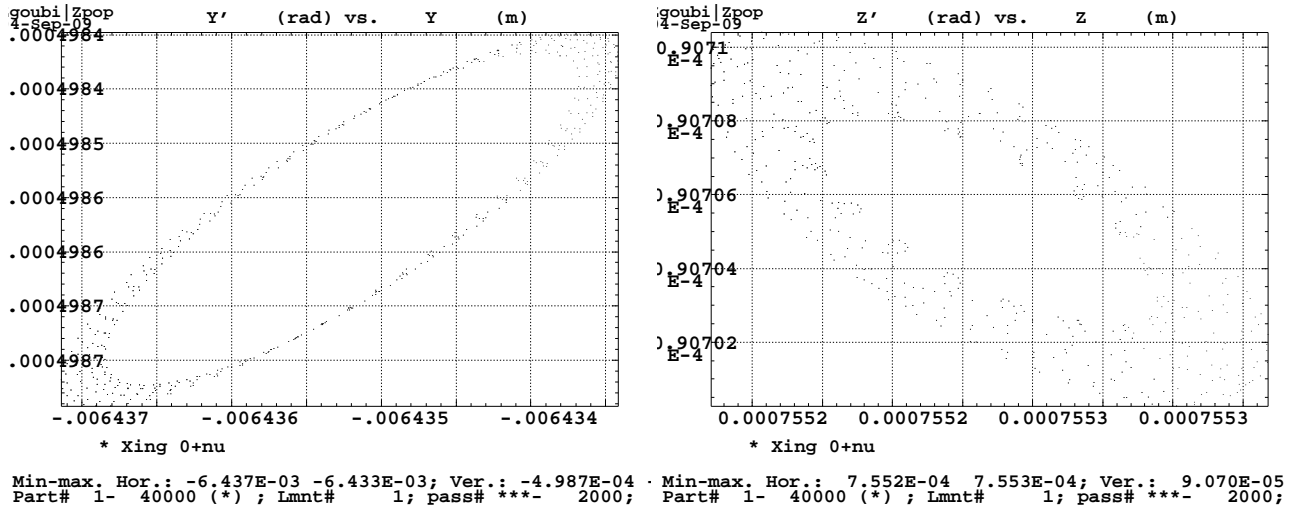


Figure 99: Left : x-x', right : z-z'.

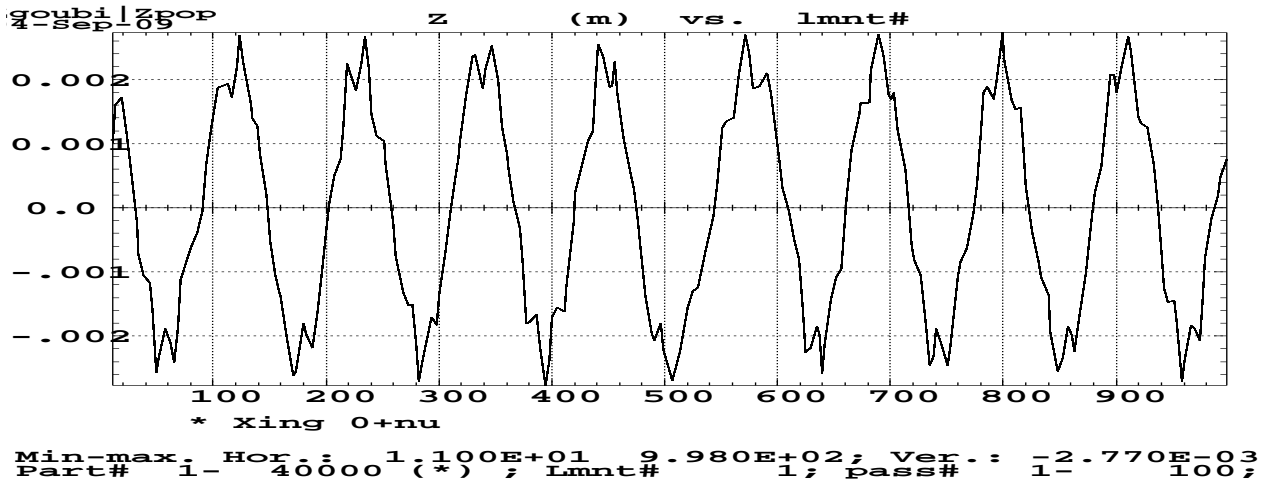


Figure 100: Vertical closed orbit along the ring circumference, versus pick-up number (about 990 P-Us over the 807 m circumference).

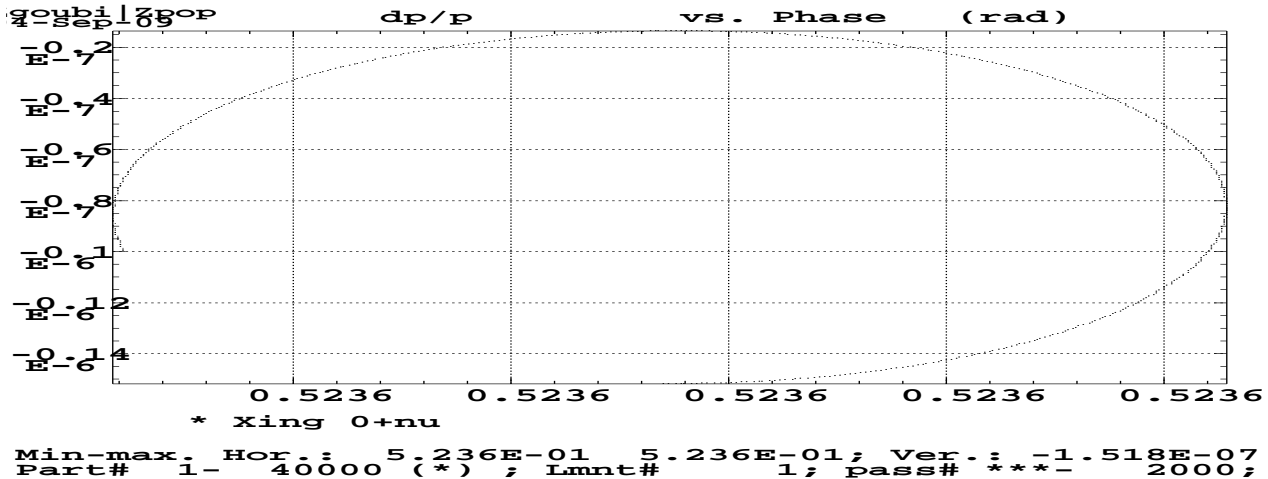


Figure 101: dp-phase.

4.2.2  $\gamma G = 12$  (5.341830 GeV)

## Tracking data

Zgoubi.dat, excerpts :

```

Xing gammaG = 12
'OBJET'
20.27157e3
2
1 1
-0.65068584 -0.50477891 0.37676032 0.45393654 0.0E+00 1. 'p'
1
'SCALING'
1 3
MULTIPOL VKIC
-1
20.27157 scales the vertical kick
1
MULTIPOL SBEN
-1
20.27157
1
MULTIPOL QUAD
-1
20.27157
1
.....
'MULTIPOL' VKIC DVCA02
0 .kicker
0.1000E-03 10.00 10.e3 0.000000 0.0 0.0 0.0 0.0 0.0 0.0 0.0 0.0
.0 .0 1.00 0.00 0.00 0.00 0.00 0. 0. 0. 0.
4 .1455 2.2670 -.6395 1.1558 0. 0. 0.
.0 .0 1.00 0.00 0.00 0.00 0.00 0. 0. 0. 0.
4 .1455 2.2670 -.6395 1.1558 0. 0. 0.
1.570796327 0. 0. 0. 0. 0. 0. 0. 0.
#20|20|20 Kick
1 0. 0. 0.
.....
'CAVITE'
2.1 .1 is to fill zgoubi.CAVITE.Out for plot using zpop/7/20
807.043778118095 12.
290.d3 0.5235987755982988731 9cavitiesx32kV, phi_s=30deg
-----
From zgoubi.res :

Particle properties :
      Mass      = 938.272      MeV/c2
      Charge    = 1.602176E-19 C
      G factor  = 1.79285

Reference data :
      rigidity (kG.cm) : 20271.6
      mass (MeV/c2) : 938.272
      momentum (MeV/c) : 6077.26
      energy, total (MeV) : 6149.27
      energy, kinetic (MeV) : 5211.00
      beta = v/c : 0.9882907009
      gamma : 6.553821507
      beta*gamma : 6.477080850

Accelerating cavity
OPTION 2
      Orbit length = 807.0 m
      RF harmonic = 12.00
      Peak voltage = 2.9000E+05 V
      RF frequency = 4.4054E+06 Hz
      Synchronous phase = 0.5236 rd
      Isochronous time = 2.7239E-06 s
      qV.SIN(Phi_s) = 0.1450 MeV
      cos(Phi_s) = 0.8660
      Nu_s/sqrt(alpha) = 8.8318E-03
      qp-acc*sqrt(alpha) = 9.2558E-04

Spin stuff :
      alpha = G*dgamma/dtta = 4.4096356E-05
      B-dot *rho(m) = 179.7 T/s

```

## Strength

From Figs. 103, 104 one gets

$$p_{init} \approx 0.9999, \quad p_{final} \approx 5.674E - 2$$

Eq. 2 yields

$$A^2 = 0.6379532$$

$$|J_n|^2 = 9.9891440E - 06$$

$$\gamma G = 12 \text{ (5.341830 GeV)}$$

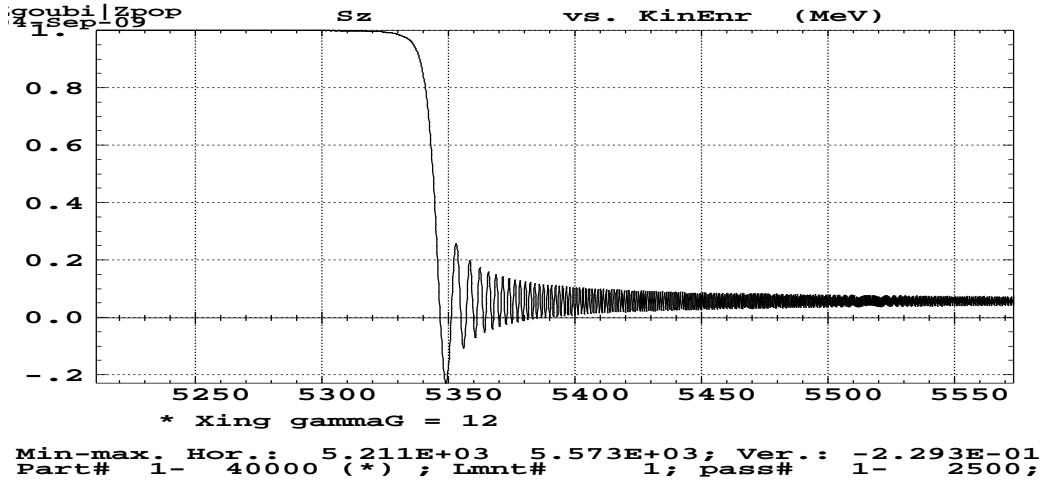


Figure 102:  $S_z$  versus kinetic energy.

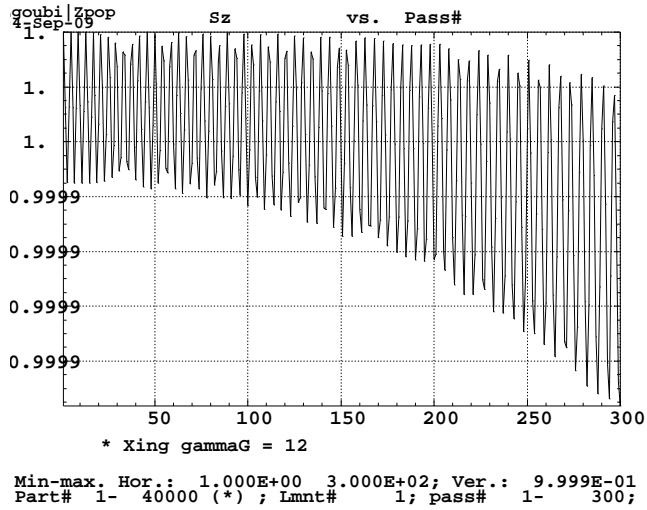


Figure 103: Zoom on initial  $S_z$ .

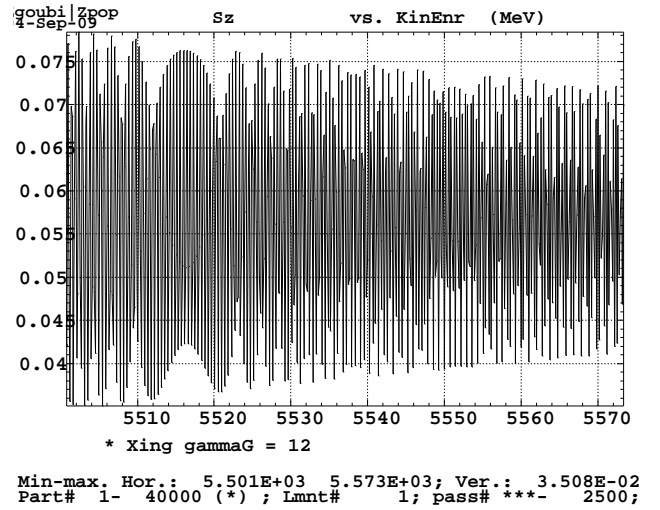


Figure 104: Zoom on final  $S_z$ .

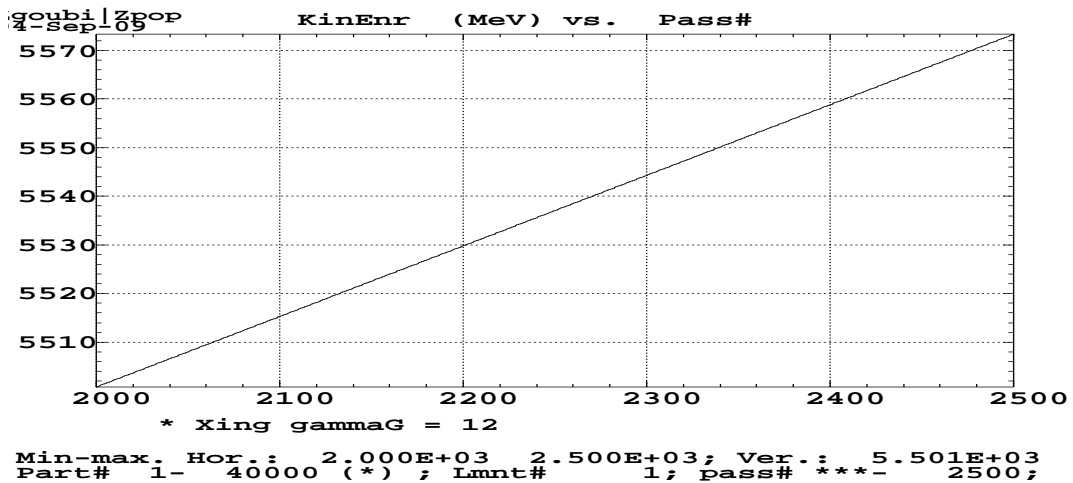


Figure 105: Kinetic E versus turn number.

$$\gamma G = 12 \text{ (5.341830 GeV)}$$

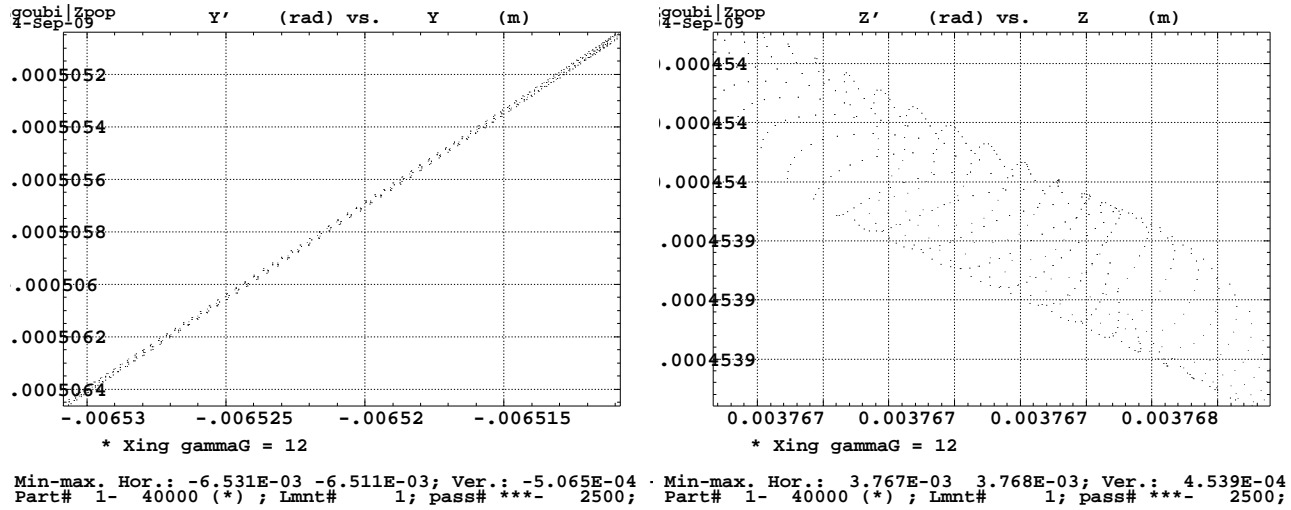


Figure 106: Left : x-x', right : z-z'.

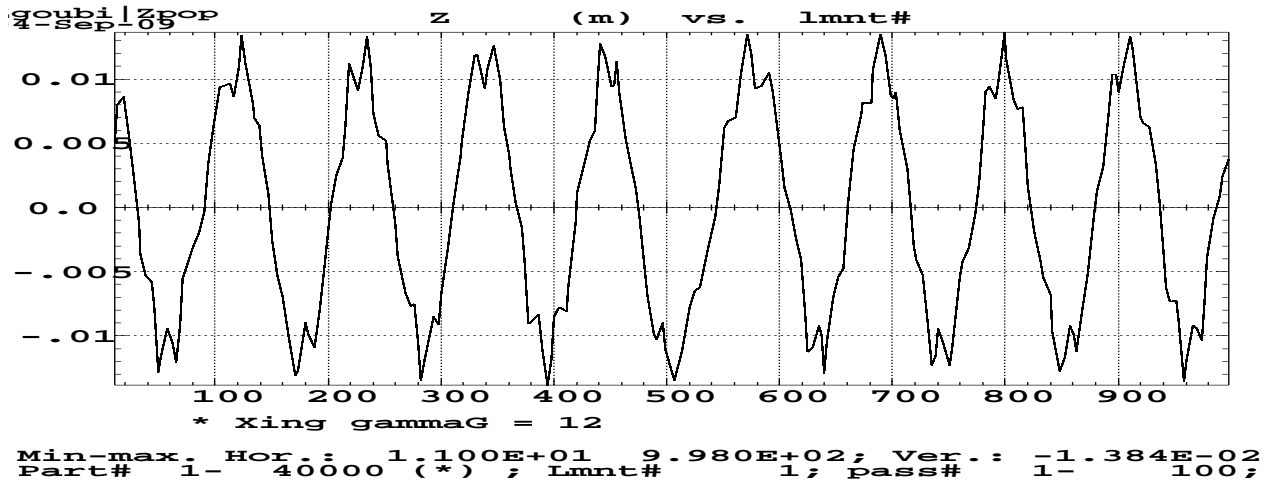


Figure 107: z closed orbit along the ring circumference versus pick-up number (about 990 P-Us over the 807 m circumference).

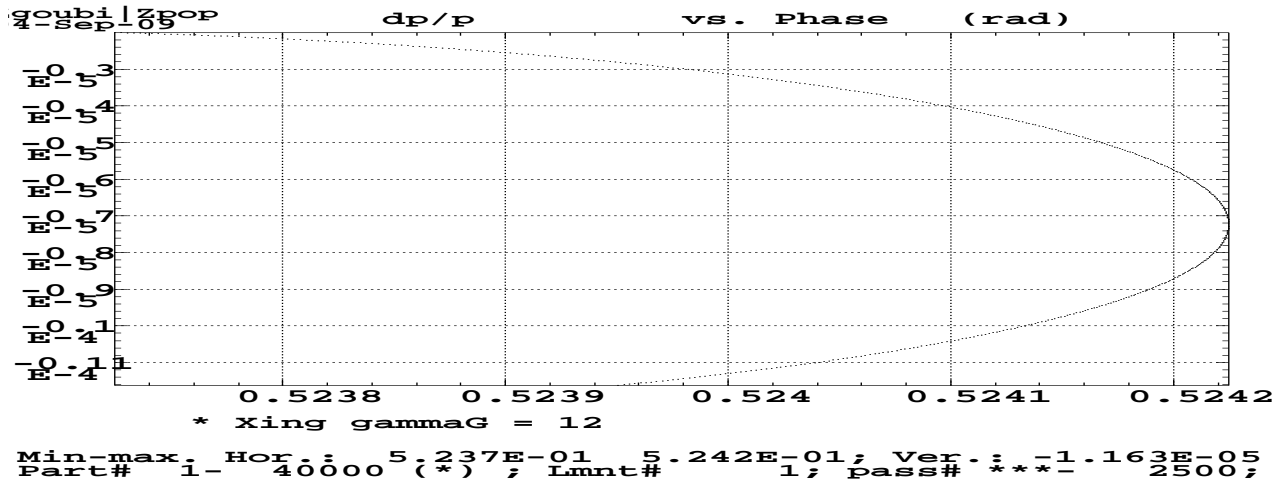


Figure 108: dp-phase.

### 4.2.3 $\gamma G = 13$ (5.865171 GeV)

#### Tracking data

Zgoubi.dat, excerpts :

```

Xing gammaG = 13
'OBJET'
22.03628e3
2
1 1
-0.65068584 -0.50477891 0.37676032 0.45393654 0.0E+00 1. 'p'
1
'FAISCEAU'
'SCALING'
1 3
MULTIPOL VKIC
-1
22.036287 scales the vertical kick
1
MULTIPOL SBEN
-1
22.03628
1
MULTIPOL QUAD
-1
22.03628
1
'PARTICUL'
938.27203d0 1.602176487d-19 1.7928474d0 0. 0.
.....
'MULTIPOL' VKIC DVCA02
0 .kicker
0.1000E-03 10.00 10.e3 0.000000 0.0 0.0 0.0 0.0 0.0 0.0 0.0 0.0
.0 .0 1.00 0.00 0.00 0.00 0.00 0. 0. 0. 0.
4 .1455 2.2670 -.6395 1.1558 0. 0. 0.
.0 .0 1.00 0.00 0.00 0.00 0.00 0. 0. 0. 0.
4 .1455 2.2670 -.6395 1.1558 0. 0. 0.
1.570796327 0. 0. 0. 0. 0. 0. 0. 0. 0.
#20|20|20 Kick
1 0. 0. 0.
.....
'CAVITE'
2.1 .1 is to fill zgoubi.CAVITE.Out for plot using zpop/7/20
807.043778118095 12.
290.d3 0.5235987755982988731 9cavitiesx32kV, phi_s=30deg
-----
From zgoubi.res :

```

Particle properties :

```

Mass = 938.272 MeV/c2
Charge = 1.602176E-19 C
G factor = 1.79285

```

Reference data :

```

rigidity (kG.cm) : 22036.3
mass (MeV/c2) : 938.272
momentum (MeV/c) : 6606.31
energy, total (MeV) : 6672.61
energy, kinetic (MeV) : 5734.34
beta = v/c : 0.9900642821
gamma : 7.111591821
beta*gamma : 7.040933050

```

## Strength

From Figs. 110, 111 one gets

$$p_{init} \approx 1., \quad p_{final} \approx 0.1574500$$

Eq. 2 yields

$$A^2 = 0.5469143$$

$$|J_n|^2 = 1.5353313E - 05$$



$$\gamma G = 13 \text{ (5.865171 GeV)}$$

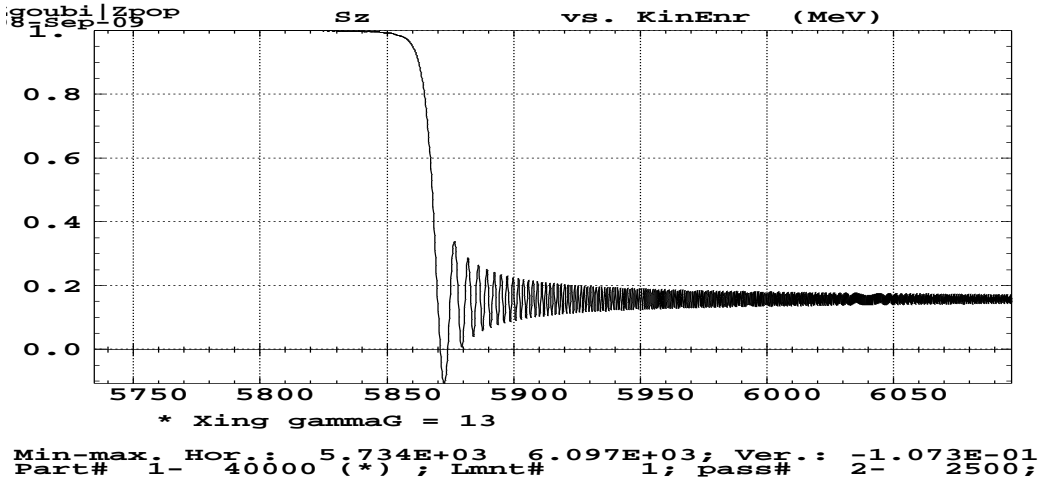


Figure 109:  $S_z$  versus kinetic energy.

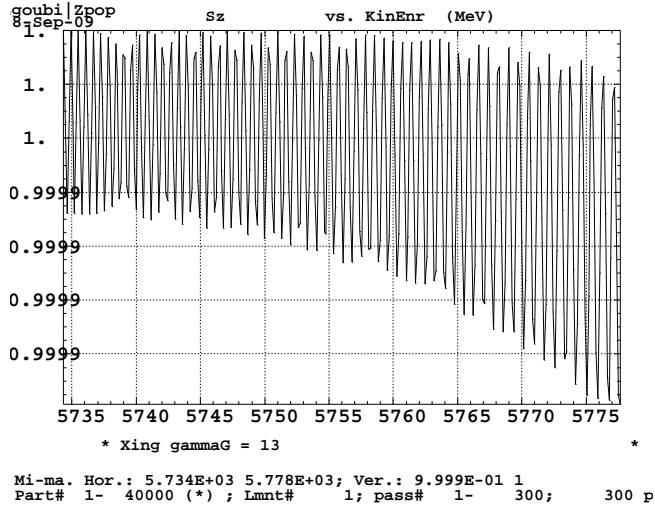


Figure 110: Zoom on initial  $S_z$ .

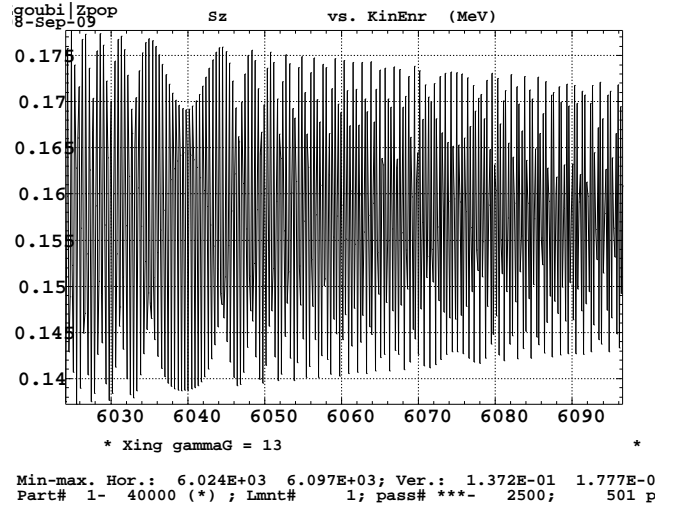


Figure 111: Zoom on final  $S_z$ .

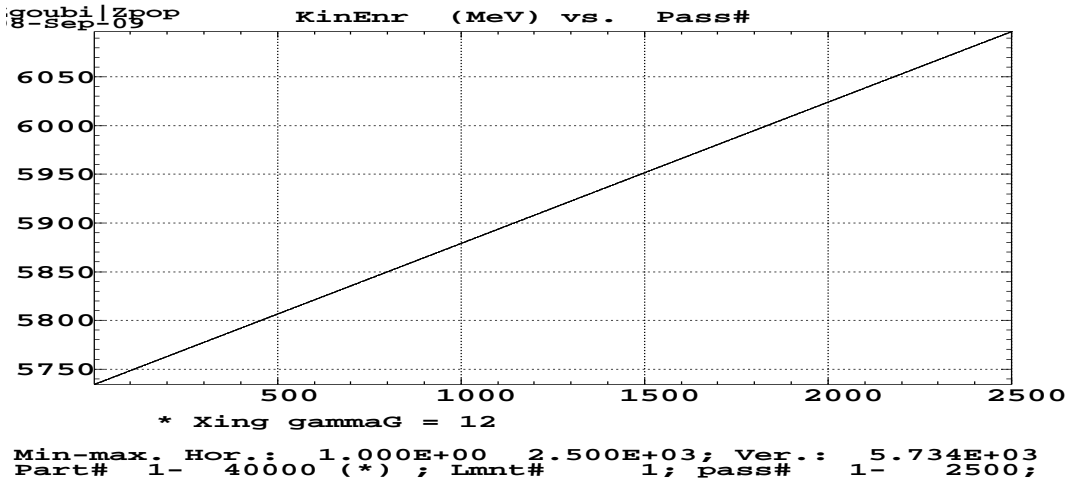


Figure 112: Kinetic E versus turn number.

$\gamma G = 13$  (5.865171 GeV)

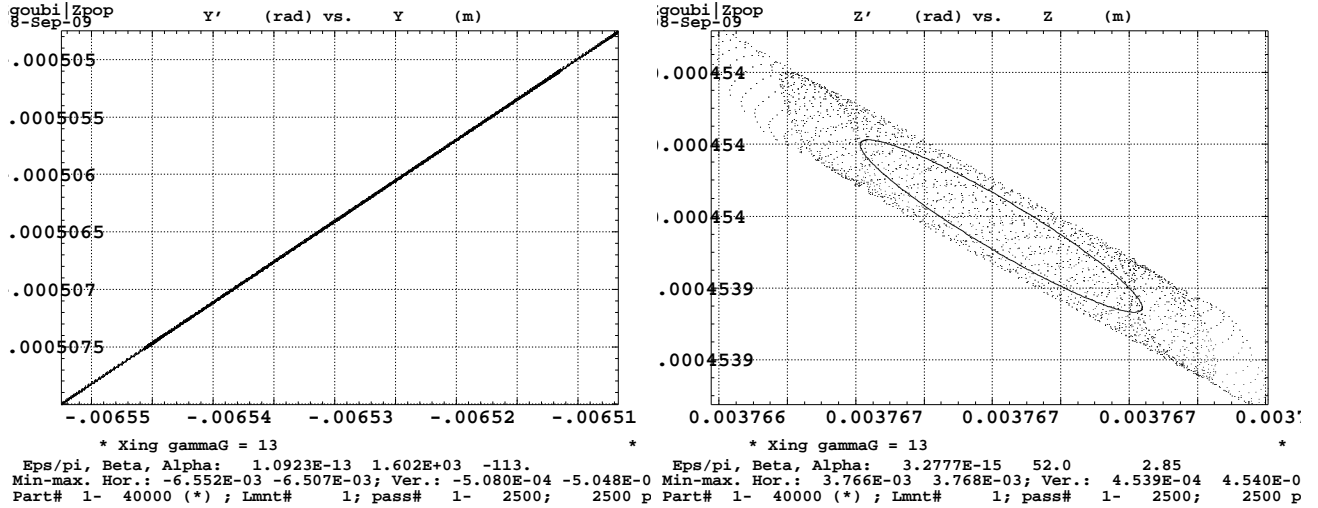


Figure 113: Left : x-x', right : z-z'.

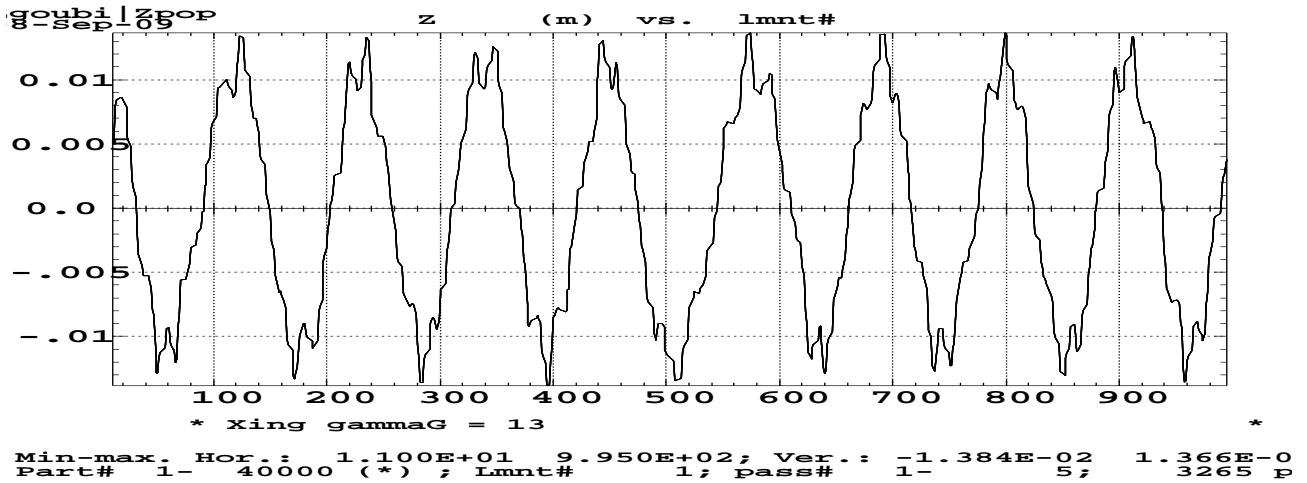


Figure 114: z closed orbit along the ring circumference (horizontal axis is pick-up number).

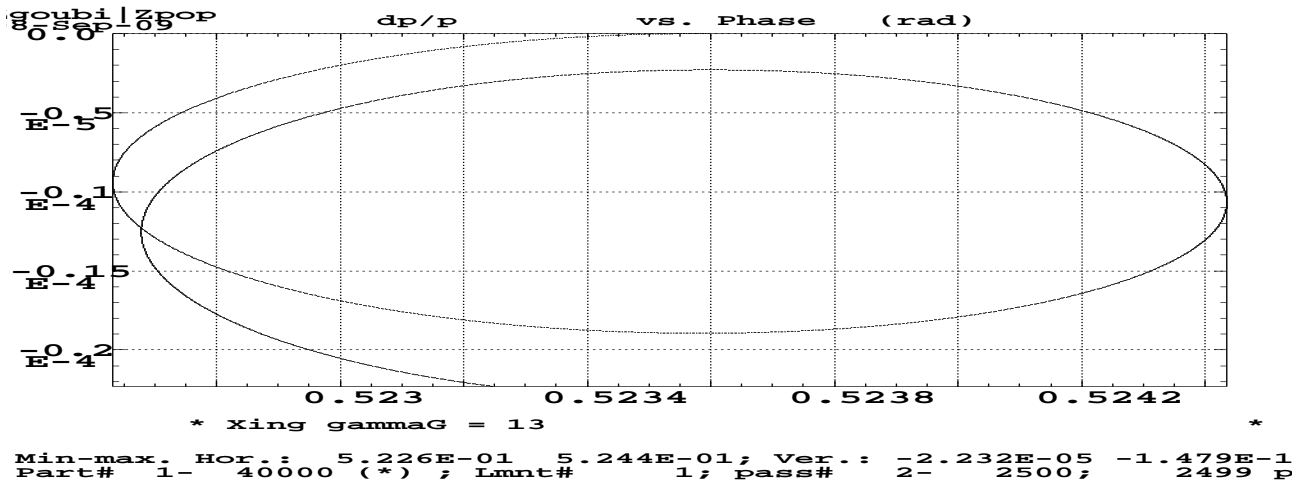


Figure 115: dp-phase.

4.2.4  $\gamma G = 23$  (11.09859 GeV)

## Tracking data

Zgoubi.dat, excerpts :

```

Xing gammaG = 23
'OBJET'
39.59072e3
2
1 1
-0.65068584 -0.50477891 0.37676032 0.45393654 0.0E+00 1. 'p'
1
'FAISCEAU'
'SCALING' 3
1 3
MULTIPOL VKIC
-1
39.59072 scales the vertical kick
1
MULTIPOL SBEN
-1
39.59072
1
MULTIPOL QUAD
-1
39.59072
1
'PARTICUL' 4
938.27203d0 1.602176487d-19 1.7928474d0 0. 0.
.....
'MULTIPOL' VKIC DVCA02
0 .kicker
0.1000E-03 10.00 10.e3 0.000000 0.0 0.0 0.0 0.0 0.0 0.0 0.0 0.0
.0 .0 1.00 0.00 0.00 0.00 0.00 0. 0. 0. 0.
4 .1455 2.2670 -.6395 1.1558 0. 0. 0.
.0 .0 1.00 0.00 0.00 0.00 0.00 0. 0. 0. 0.
4 .1455 2.2670 -.6395 1.1558 0. 0. 0.
1.570796327 0. 0. 0. 0. 0. 0. 0. 0.
#20|20|20 Kick
1 0. 0. 0.
.....
'CAVITE' 85 86
2.1 .1 is to fill zgoubi.CAVITE.Out for plot using zpop/7/20
807.043778118095 12.
290.d3 2.617993877991494365 9cavitiesx32kV, phi_s=180-30deg

```

## Strength

From Figs. 117, 118 one gets

$$p_{init} \approx 0.9975, \quad p_{final} \approx -0.647$$

Eq. 2 yields

$$A^2 = 1.734326$$

$$|J_n|^2 = 4.8687059E - 05$$

$$\gamma G = 23 \text{ (11.09859 GeV)}$$

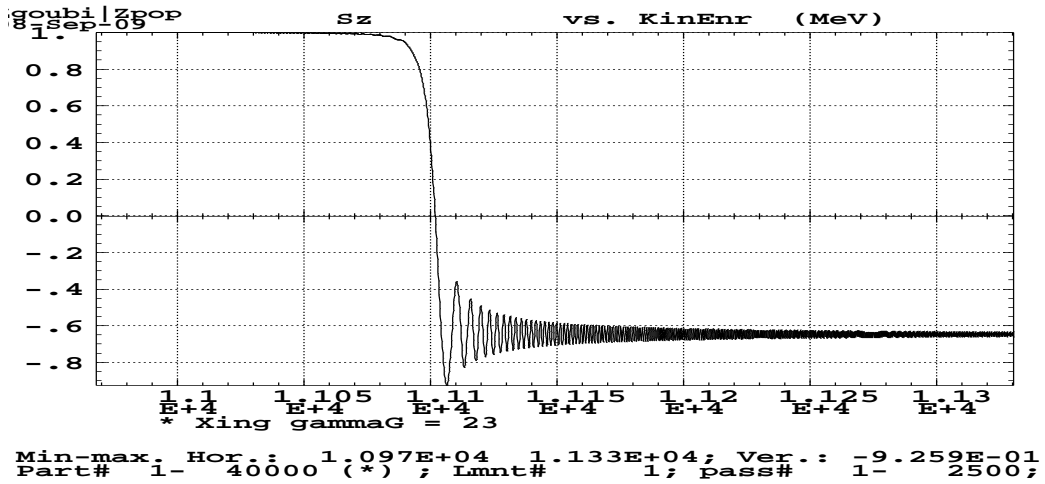


Figure 116:  $S_z$  versus kinetic energy.

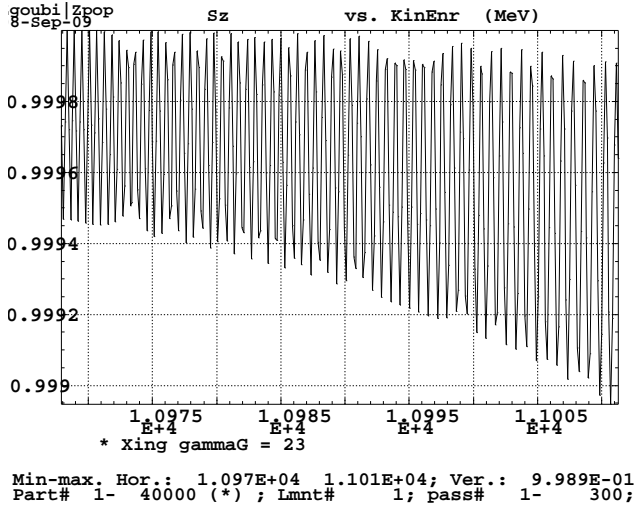


Figure 117: Zoom on initial  $S_z$ .

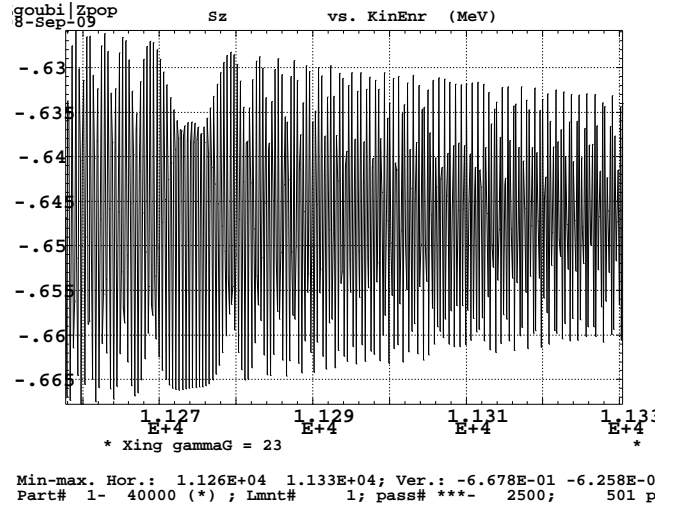


Figure 118: Zoom on final  $S_z$ .

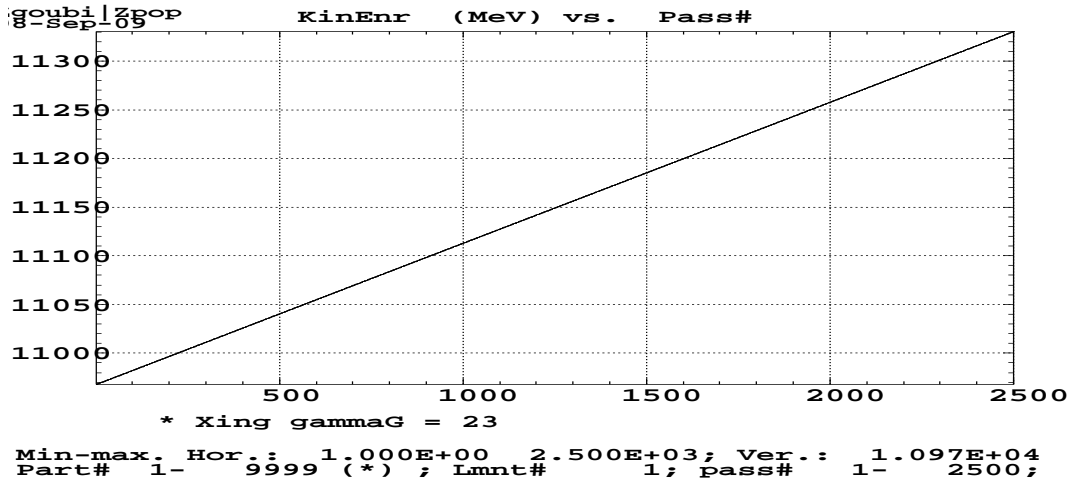


Figure 119: Kinetic E versus turn number.

$\gamma G = 23$  (11.09859 GeV)

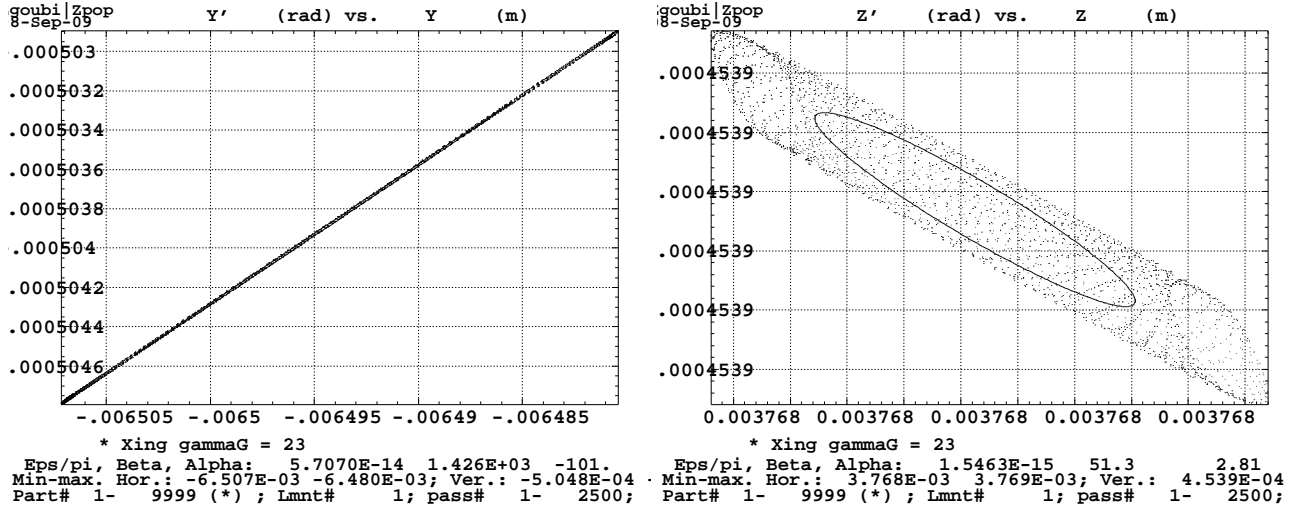


Figure 120: Left : x-x', right : z-z'.

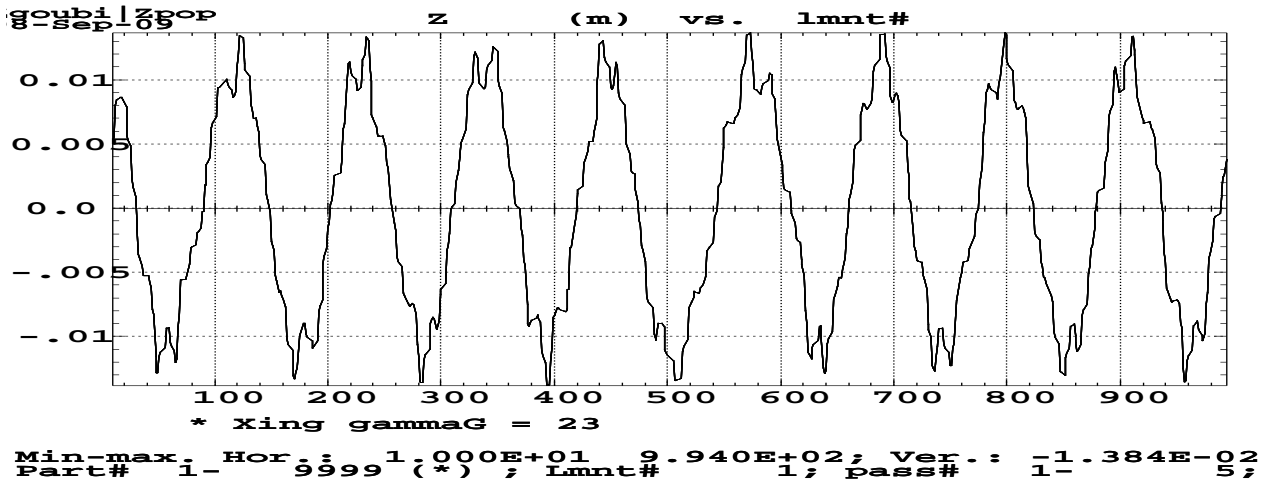


Figure 121: z closed orbit along the ring circumference (horizontal axis is pick-up number).

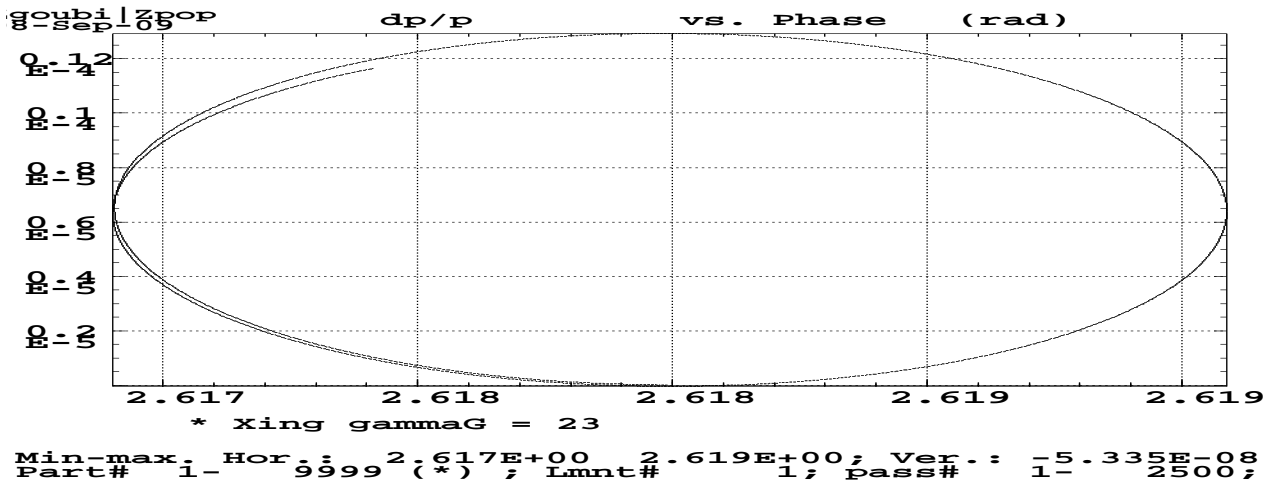


Figure 122: dp-phase.

4.2.5  $\gamma G = 27$  (13.19196 GeV)

## Tracking data

Zgoubi.dat, excerpts :

```

'OBJET'
46.59195e3
2
1 1
-0.65068584 -0.50477891 0.037676032 0.045393654 0.0E+00 1. 'p'
1
'FAISCEAU'
'SCALING'
1 3
MULTIPOL VKIC
-1
46.59195 scales the vertical kick
1
MULTIPOL SBEN
-1
46.59195
1
MULTIPOL QUAD
-1
46.59195
1
.....
'MULTIPOL' VKIC DVCA02
0 .kicker
0.1000E-03 10.00 1.e3 0.000000 0.0 0.0 0.0 0.0 0.0 0.0 0.0 0.0 0.0
.0 .0 1.00 0.00 0.00 0.00 0.00 0. 0. 0. 0.
4 .1455 2.2670 -.6395 1.1558 0. 0. 0.
.0 .0 1.00 0.00 0.00 0.00 0.00 0. 0. 0. 0.
4 .1455 2.2670 -.6395 1.1558 0. 0. 0.
1.570796327 0. 0. 0. 0. 0. 0. 0. 0.
#20|20|20 Kick
1 0. 0. 0.
.....
'CAVITE'
2.1 .1 is to fill zgoubi.CAVITE.Out for plot using zpop/7/20
807.043778118095 12.
290.d3 2.617993877991494365 9cavitiesx32kV, phi_s=180-30deg

```

From zgoubi.res :

Particle properties :

```

      Mass      = 938.272      MeV/c2
      Charge    = 1.602176E-19 C
      G factor  = 1.79285
Reference data :
rigidity (kG.cm) : 46591.9
mass (MeV/c2)   : 938.272
momentum (MeV/c) : 13967.9
energy, total (MeV) : 13999.4
energy, kinetic (MeV) : 13061.1
beta = v/c      : 0.9977514753
gamma           : 14.92039915
beta*gamma      : 14.88685026

```

## Strength

From Figs. 124, 125 one gets

$$p_{init} \approx 0.9998, \quad p_{final} \approx -0.167355$$

Eq. 2 yields

$$A^2 = 0.8763353$$

$$|J_n|^2 = 2.4601020E - 05$$

$$\gamma G = 27 \text{ (13.19196 GeV)}$$

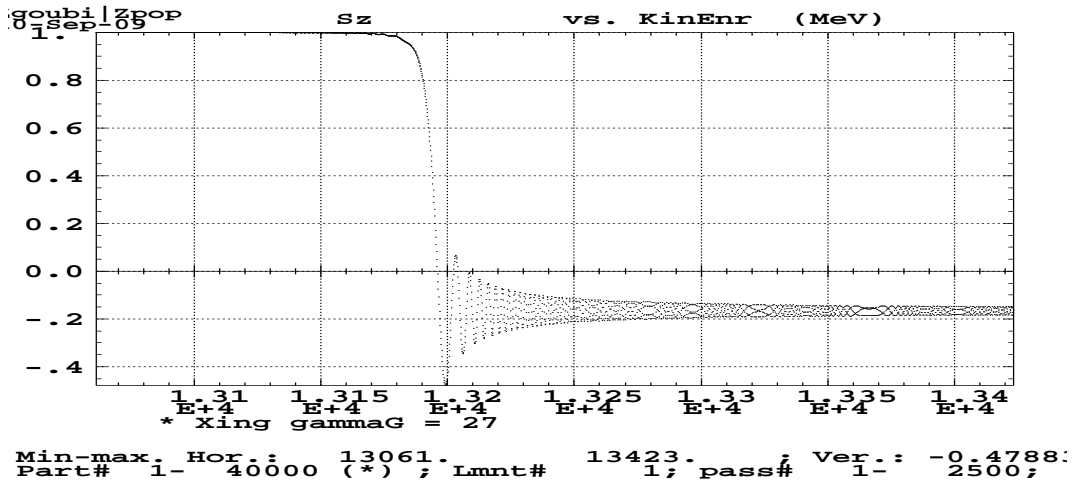


Figure 123:  $S_z$  versus kinetic energy. Check : 36-Qy next to  $gG=27$  is on the path at  $E=13.31575$  GeV, yet not visible as expected since  $\epsilon_z \approx 0$ .

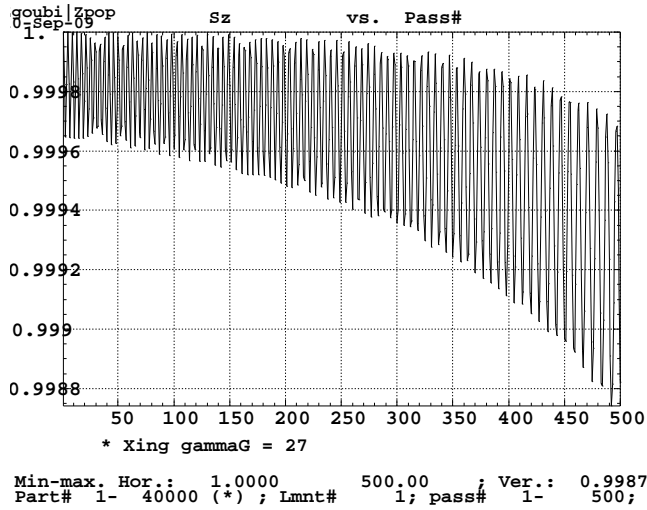


Figure 124: Zoom on initial  $S_z$ .

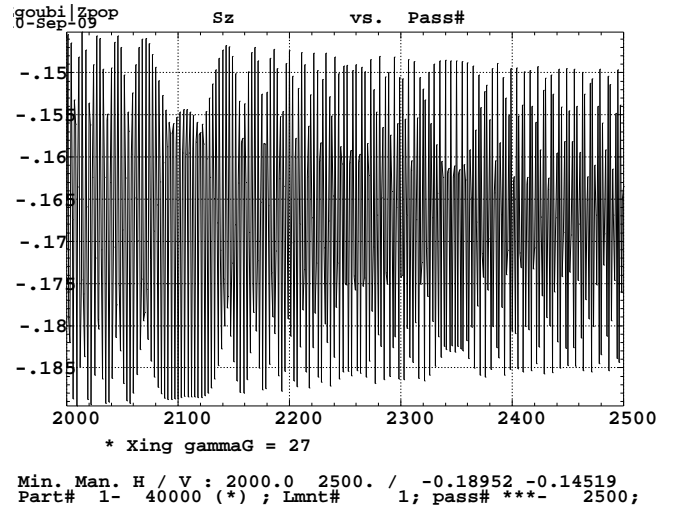


Figure 125: Zoom on final  $S_z$ .

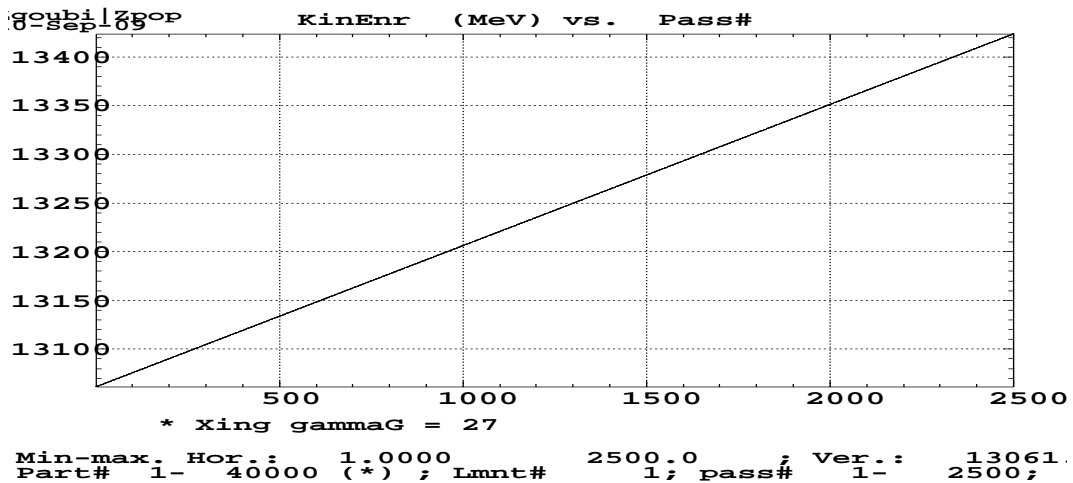


Figure 126: Kinetic E versus turn number.

$\gamma G = 27$  (13.19196 GeV)

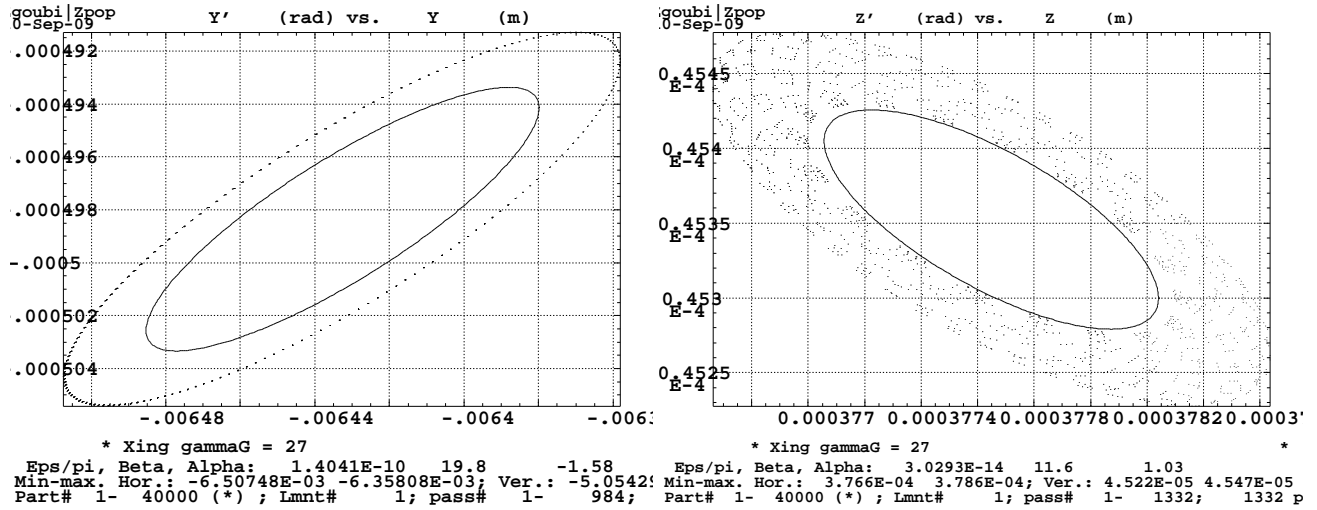


Figure 127: Left : x-x', right : z-z'.

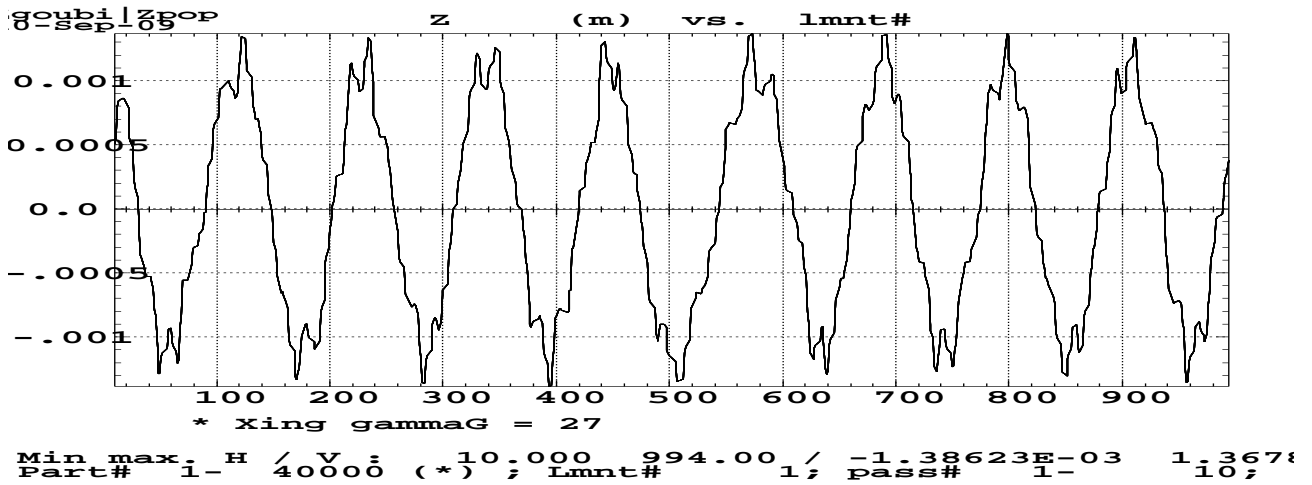


Figure 128: z closed orbit along the ring circumference (horizontal axis is pick-up number), 9 turns over the ring are superimposed.

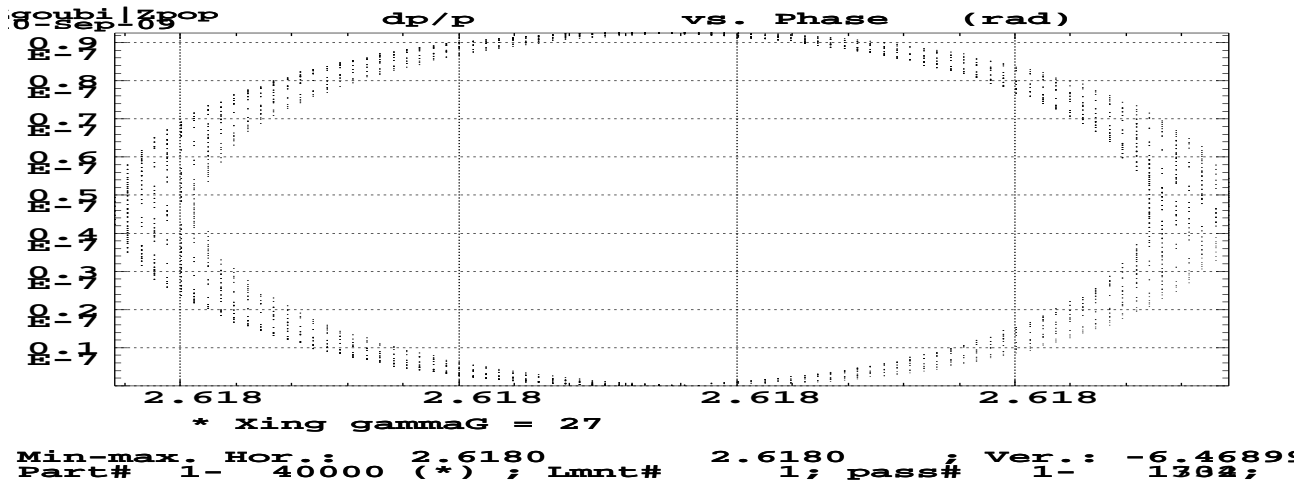


Figure 129: dp-phase.



## 4.2.6 $\gamma G = 45$ (22.61211 GeV)

### Tracking data

Zgoubi.dat, excerpts :

```
Xing gammaG = 45
'OBJET'
78.05648e3
2
1 1
-0.65068584 -0.50477891 0.0075352064 0.0090787308 0.0E+00 1. 'p'
1
'FAISCEAU'
'SCALING'
1 3
MULTIPOL VKIC
-1
78.05648 scales the vertical kick
1
MULTIPOL SBEN
-1
78.05648
1
MULTIPOL QUAD
-1
78.05648
1
.....
'MULTIPOL' VKIC DVCA02
0 .kicker
0.1000E-03 10.00 0.2e3 0.000000 0.0 0.0 0.0 0.0 0.0 0.0 0.0 0.0
0.0 1.00 0.00 0.00 0.00 0.00 0.0 0.0 0.0 0.0
4 .1455 2.2670 -.6395 1.1558 0.0 0.0
0.0 1.00 0.00 0.00 0.00 0.00 0.0 0.0 0.0 0.0
4 .1455 2.2670 -.6395 1.1558 0.0 0.0
1.570796327 0.0 0.0 0.0 0.0 0.0 0.0
#20|20|20 Kick
1 0.0 0.0
.....
'CAVITE'
2.1 .1 is to fill zgoubi.CAVITE.Out for plot using zpop/7/20
807.043778118095 12.
290.d3 2.617993877991494365 9cavitiesx32kV, phi_s=180-30deg
```

from zgoubi.res :

Particle properties :

Mass	=	938.272	MeV/c2
Charge	=	1.602176E-19	C
G factor	=	1.79285	

Reference data :

rigidity (kG.cm)	:	78056.5
mass (MeV/c2)	:	938.272
momentum (MeV/c)	:	23400.7
energy, total (MeV)	:	23419.5
energy, kinetic (MeV)	:	22481.3
beta = v/c	:	0.9991971305
gamma	:	24.96029519
beta*gamma	:	24.94025534

### Strength

From Figs. 131, 132 one gets

$$p_{init} \approx 0.999755, \quad p_{final} \approx 0.62962$$

Eq. 2 yields

$$A^2 = 0.2047056,$$

$$|J_n|^2 = 5.7466214E - 06$$

$$\hat{z}_{c.o.} = 0.275 \text{ mm}$$

$$\gamma G = 45 \text{ (22.61211 GeV)}$$

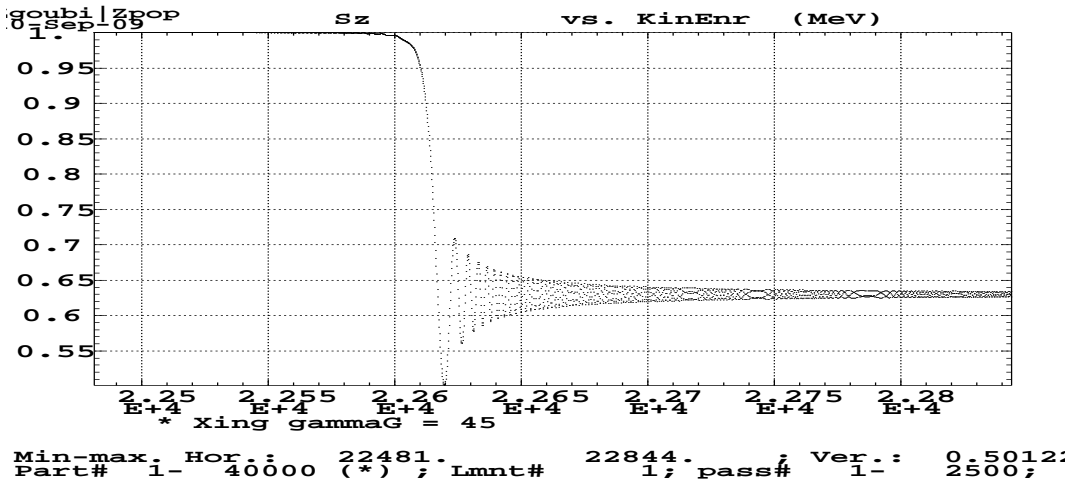


Figure 130:  $S_z$  versus kinetic energy.

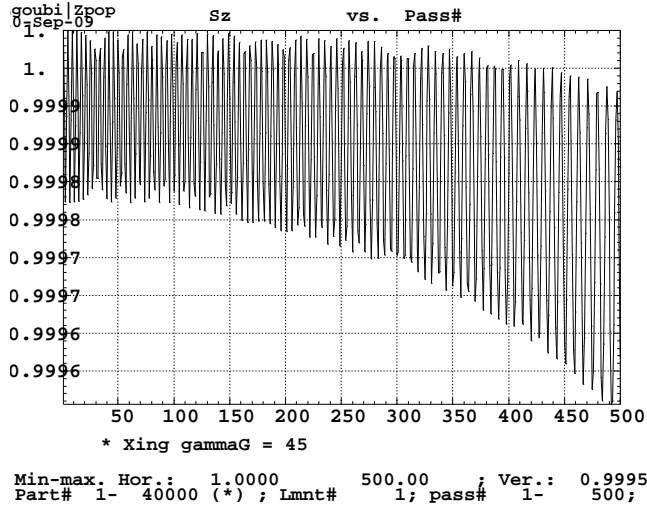


Figure 131: Zoom on initial  $S_z$ .

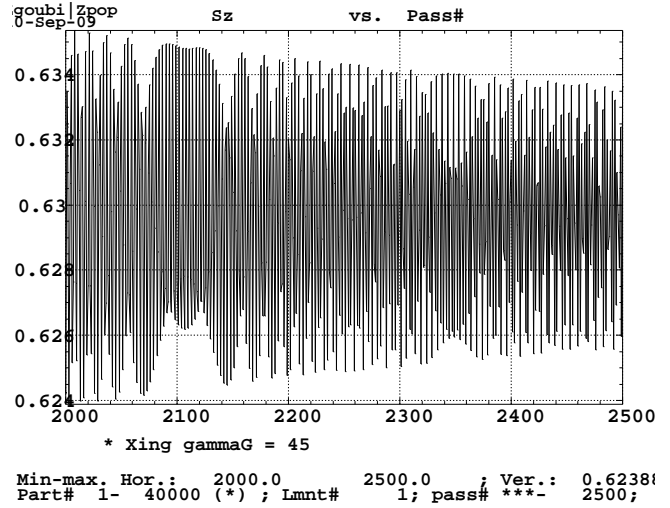


Figure 132: Zoom on final  $S_z$ .

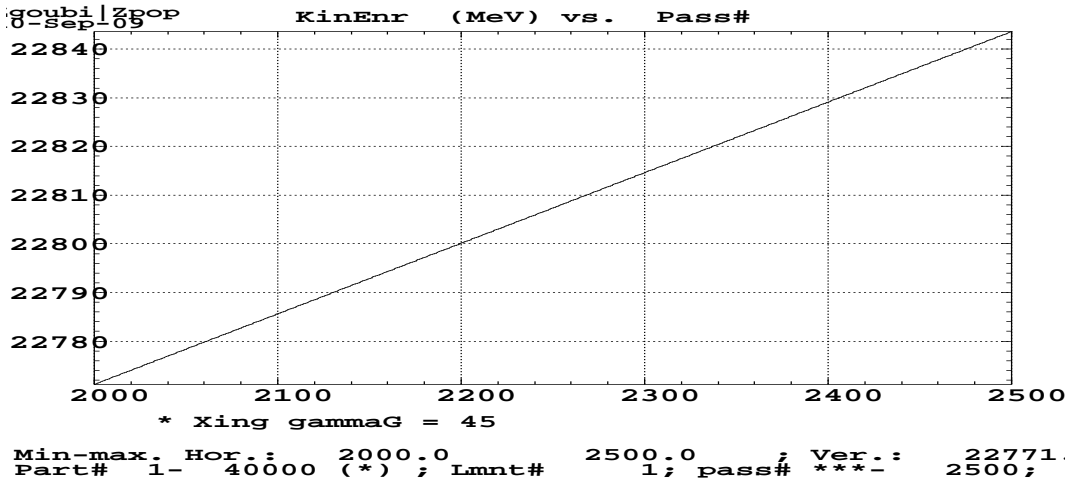


Figure 133: Kinetic E versus turn number.

$\gamma G = 45$  (22.61211 GeV)

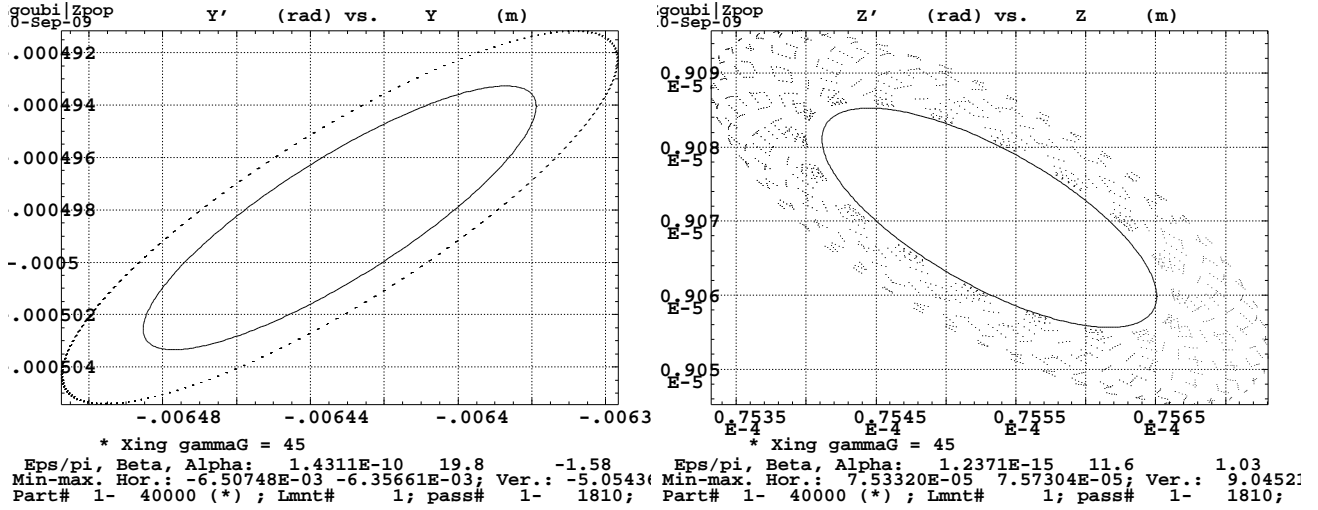


Figure 134: Left : x-x', right : z-z'.

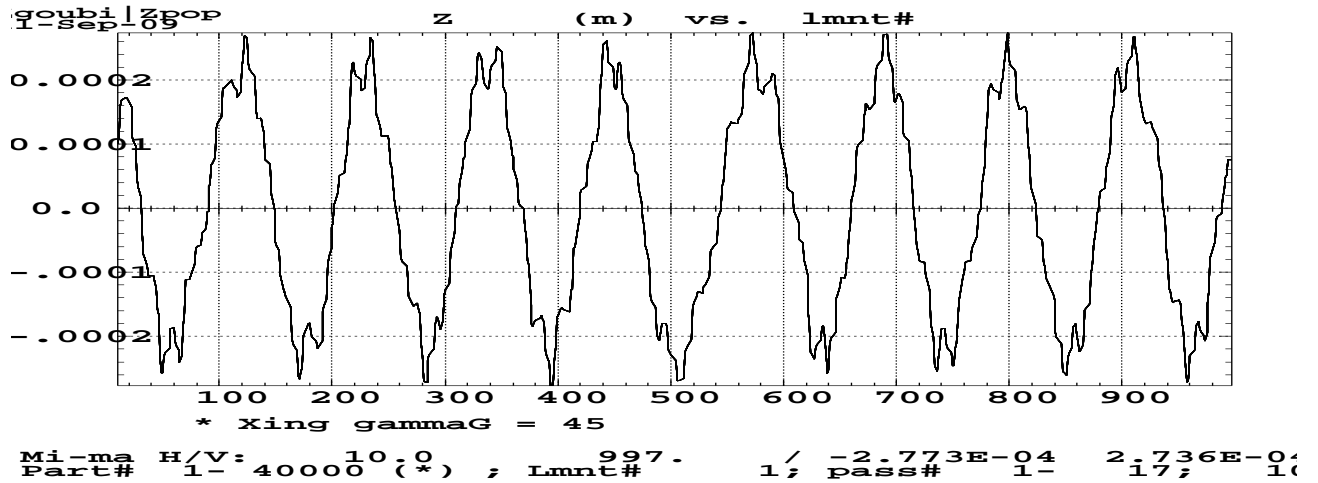


Figure 135: z closed orbit along the ring circumference (horizontal axis is pick-up number).

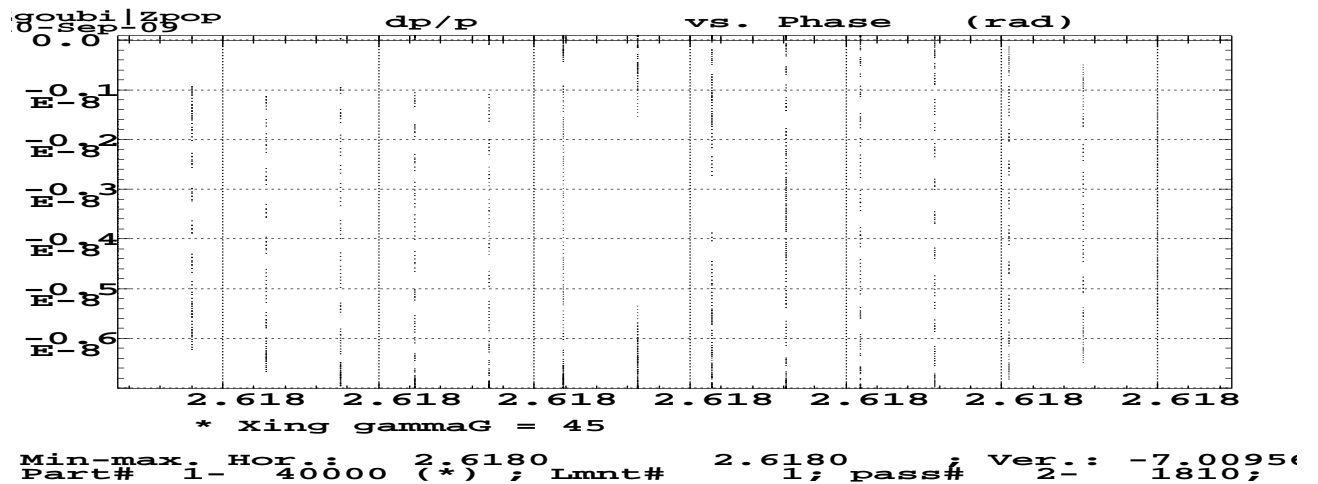


Figure 136: dp-phase.

## 5 Static neighboring of resonances

### 5.1 Intrinsic resonances

In static mode, at distance

$$\Delta = \text{distance to the resonance} = \gamma G - (n \times M - \nu_z)$$

from an isolated spin resonance, the average value of the vertical component of an initially vertical  $\vec{S}$  satisfies

$$\bar{S}_z^2 = \frac{1}{1 + |J_n|^2/\Delta^2}, \quad \text{hence} \quad |J_n|^2 = \Delta^2 / \left( \frac{1}{1 - \bar{S}_z^2} - 1 \right)$$

which yields  $|J_n|$  from a measurement of  $S_z(\Delta)$ .

In order to perform a simulation of stable precession of  $\vec{S}$  around a fixed axis, test particles are launched at various, fixed, energies  $\gamma = (\Delta + (n \times M - \nu_z))/G$  (hence various  $\Delta$ ), on non-zero vertical invariant  $\epsilon_z$ , on chromatic horizontal closed orbit corresponding to that energy and with initial  $\vec{S} \equiv \vec{S}_z$  polarization.

The matching of the  $z$ -projection of the ray-traced  $S_z$  component with  $\bar{S}_z$ , Eq. above, delivers best  $\nu_z$  and  $\epsilon$  values, these are displayed in Tab. 7 page 70.

#### 5.1.1 $\gamma G = \nu_z$ (3.648013 GeV)

#### Strengths

Resonance strengths and vertical tunes are derived from the numerical simulation results by matching of numerical  $\bar{S}_z(\gamma G)$  using Eq. 4, page 10.

This yields the results in Tab. 6.

Table 6: Dependence of resonance strength squared ( $|J_n|^2$ ) on vertical invariant ( $\epsilon_z$ ).  $\nu_z$  compares fairly well with Fourier analysis of particle motion on  $\epsilon_z$  invariant.

$\epsilon_z/\pi$ ( $10^{-6}$ m.rad)	$\nu_z$ (Fourier)	$\nu_z$ (fit)	$ J_n ^2$ ( $10^{-5}$ )	$ J_n ^2/\epsilon_z/\pi$
0.00188		8.7634	0.07406	390
0.0164		8.7630	0.7458	455



$$\gamma G = \nu_z (3.648013 \text{ GeV}) - \epsilon_z / \pi = 0.0019 \cdot 10^{-6}$$

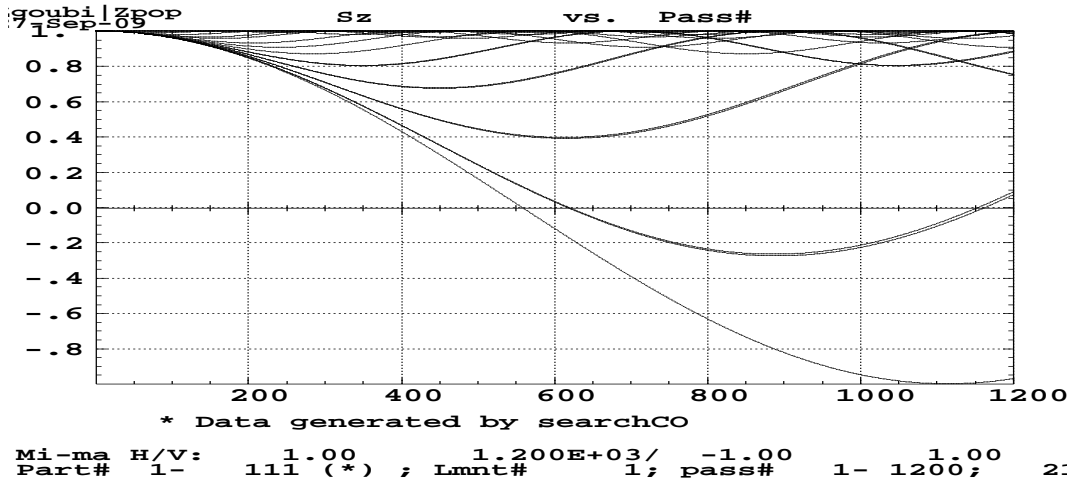


Figure 137:  $S_z$  versus turn number for various distances to the resonance.

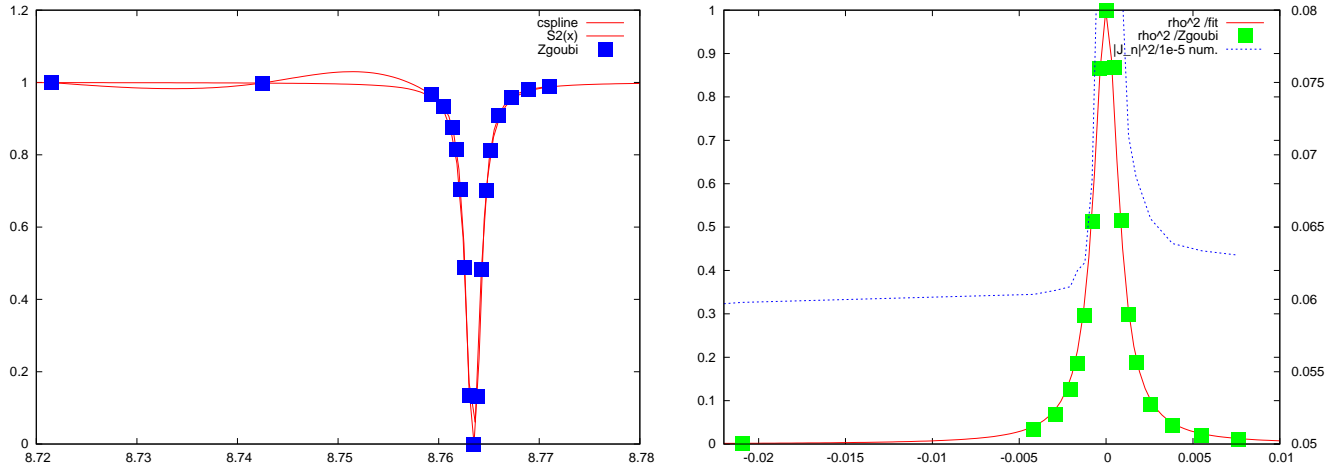


Figure 138: Matching  $S_z^2(\Delta)$  (left, Eq. 4) and  $\rho^2(\Delta)$  (right, Eq. 5) The right plot also shows  $|J_n|^2$  from numerical data (with expectable lack of accuracy in the region  $\Delta \rightarrow 0$ ).

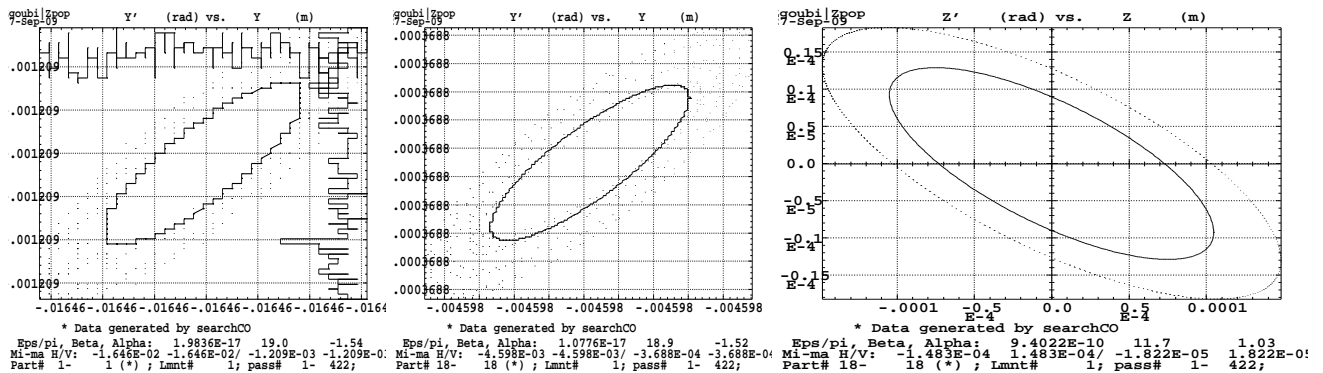


Figure 139: Left :  $x-x'$  of particles at min. and max.  $p/p_0$ . Right :  $z-z'$  (all particles superimposed).



$$\gamma G = \nu_z (3.648013 \text{ GeV}) - \epsilon_z / \pi = 0.017 10^{-6}$$

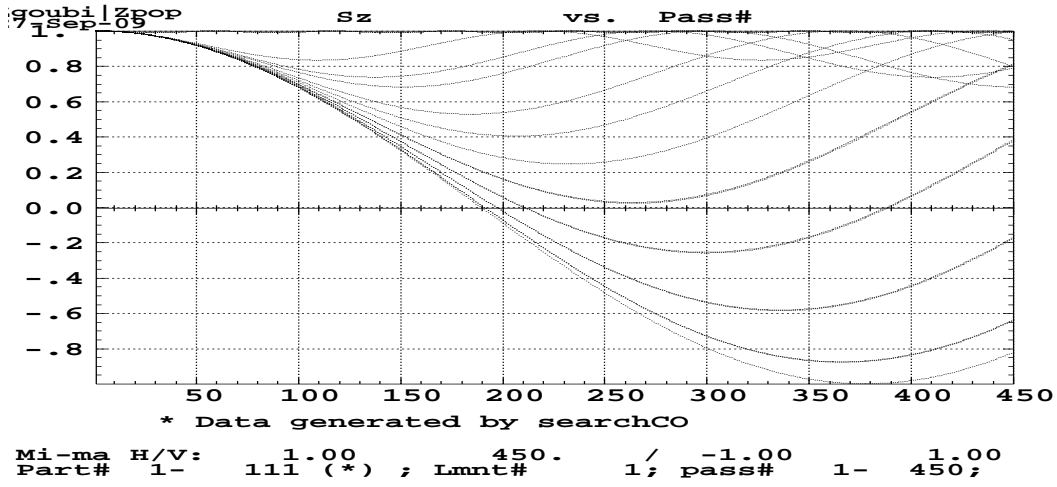


Figure 140:  $S_z$  versus turn number for various distances to the resonance.

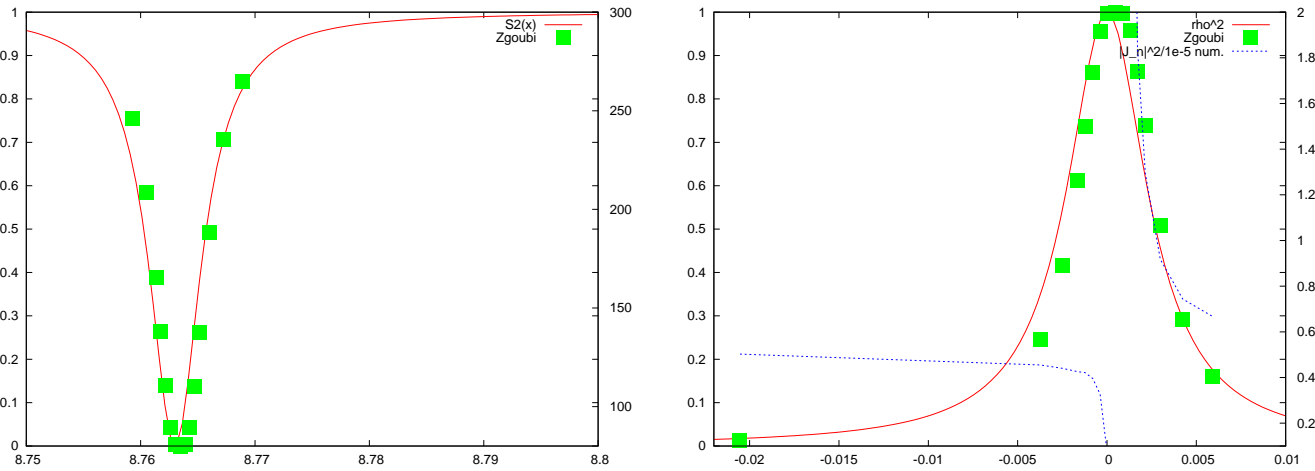


Figure 141: Matching  $S_z^2(\Delta)$  (left, Eq. 4) and  $\rho^2(\Delta)$  (right, Eq. 5) The right plot also shows  $|J_n|^2$  from numerical data (with expectable lack of accuracy in the region  $\Delta \rightarrow 0$ ).

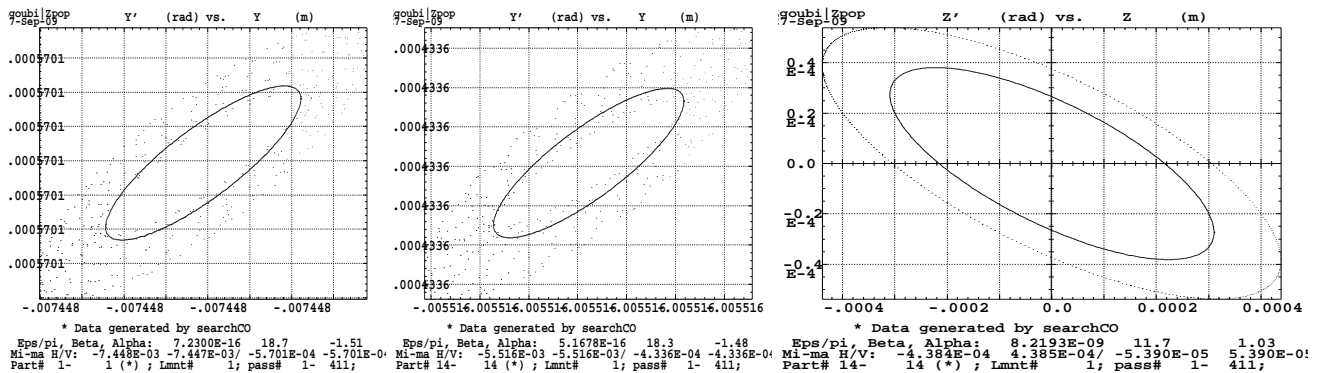


Figure 142: Left :  $x-x'$  of particles at min. and max.  $p/p_0$ . Right :  $z-z'$  (all particles superimposed).



**5.1.2  $\gamma G = 48 - \nu_z$  (19.59585 GeV)****Strengths**

Resonance strengths and vertical tunes are derived from the numerical simulation results by matching of numerical  $\bar{S}_z(\gamma G)$  using Eq. 4, page 10.

This yields the results in Tab. 7.  $\nu_z$  compares fairly well with Fourier analysis of particle motion on  $\epsilon_z$  invariant.  $|J_n|^2/\epsilon_z/\pi$  appears to be but weakly dependent on  $\epsilon_z$  in agreement with the results of resonance crossing, Sec. 4.1.7 (Tab. 4 page 35), and with Eq. 10.

Table 7: Dependence of resonance strength squared,  $|J_n|^2$ , on vertical invariant ( $\epsilon_z$ ).

$\epsilon_z/\pi$ ( $10^{-6}$ m.rad)	$\nu_z$ (Fourier)	$\nu_z$ (fit)	$ J_n ^2$ ( $10^{-5}$ )	$ J_n ^2/\epsilon_z/\pi$
0.125	.774	8.7740	0.354	27
2	.774	8.77	6.249	31



$$\gamma G = 48 - \nu_z (19.59585 \text{ GeV}) - \epsilon_z/\pi = 0.125 \cdot 10^{-6}$$

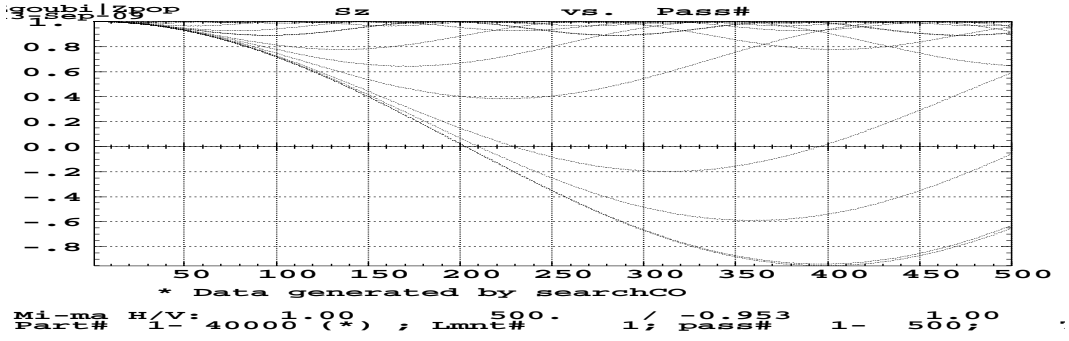


Figure 143:  $S_z$  versus turn number for various distances to the resonance.

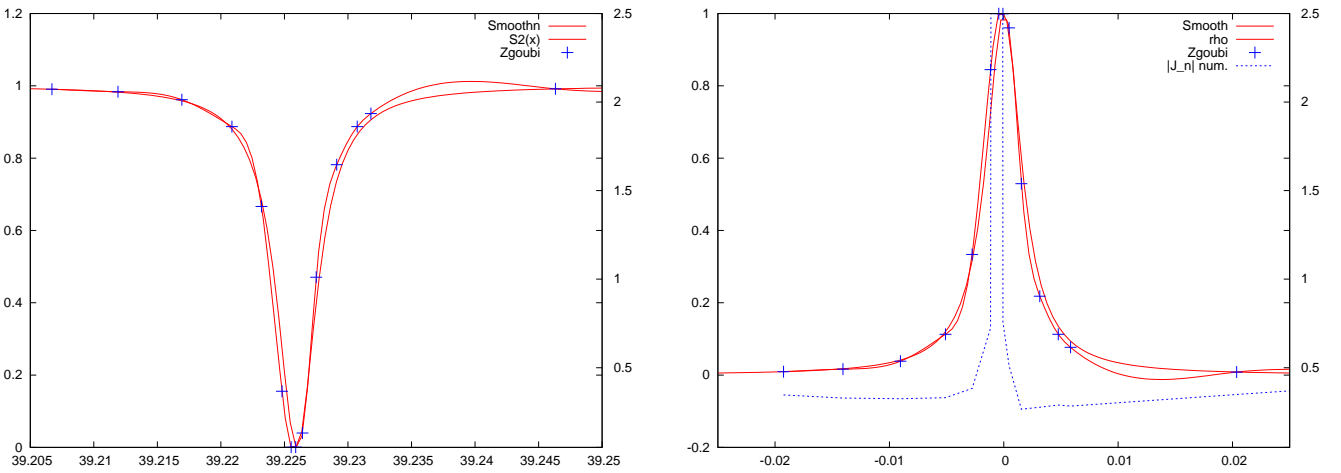


Figure 144: Matching  $S_z^2(\Delta)$  (left, Eq. 4) and  $\rho^2(\Delta)$  (right, Eq. 5) The right plot also shows  $|J_n|^2$  from numerical data (with expectable lack of accuracy in the region  $\Delta \rightarrow 0$ ).

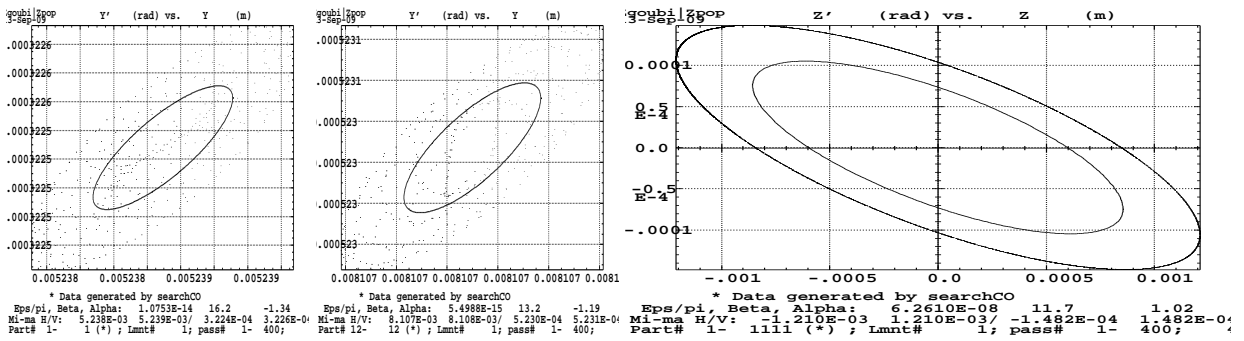


Figure 145: Left :  $x-x'$  of particles at min. and max.  $p/p_0$ . Right :  $z-z'$  (all particles superimposed).



$$\gamma G = 48 - \nu_z (19.59585 \text{ GeV}) - \epsilon_z/\pi = 2 \cdot 10^{-6}$$

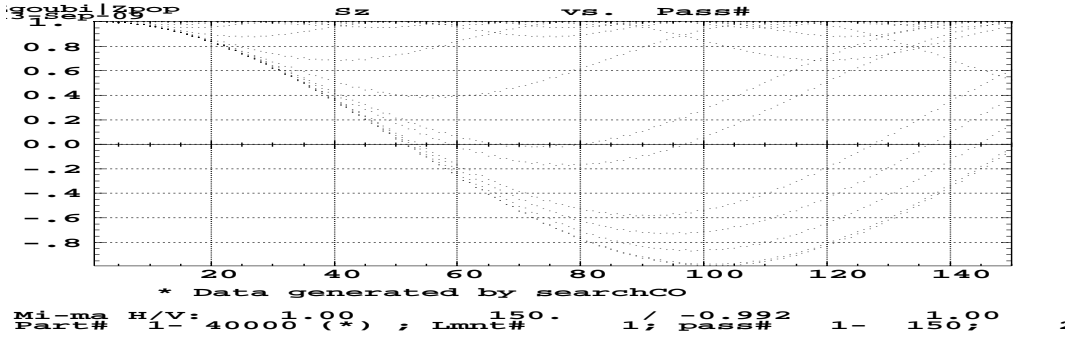


Figure 146:  $S_z$  versus turn number for various distances to the resonance.

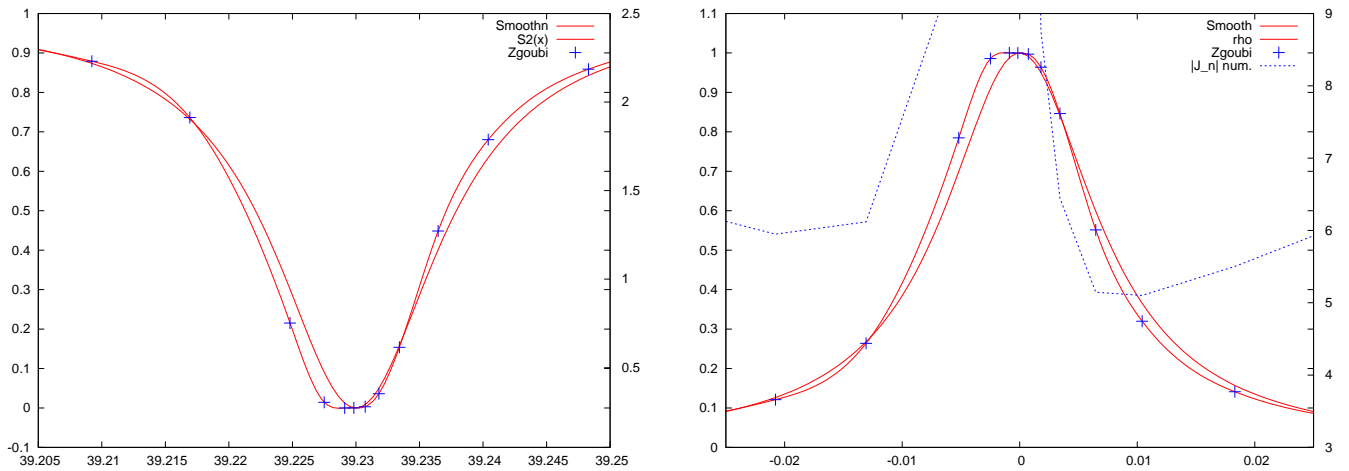


Figure 147: Matching  $S_z^2(\Delta)$  (left, Eq. 4) and  $\rho^2(\Delta)$  (right, Eq. 5) The right plot also shows  $|J_n|^2$  from numerical data (with expectable lack of accuracy in the region  $\Delta \rightarrow 0$ ).

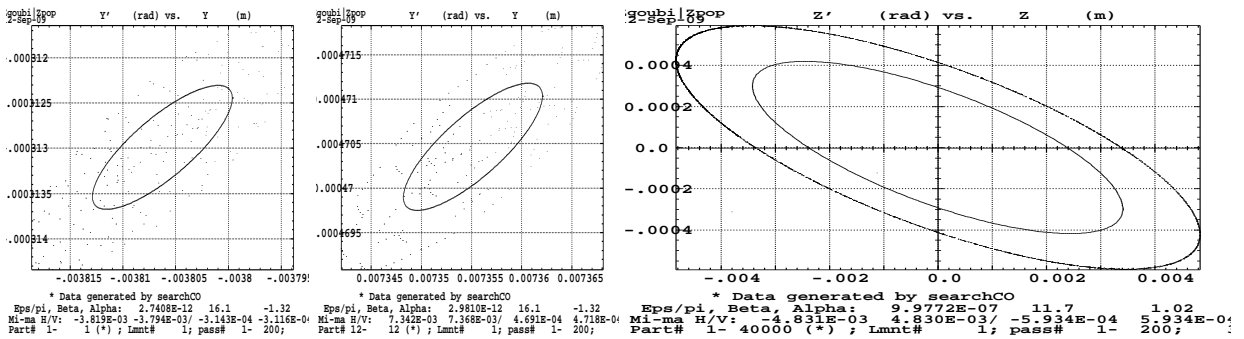


Figure 148: Left :  $x-x'$  of particles at min. and max.  $p/p_0$ .

**5.1.3  $\gamma G = 36 + \nu_z$  (22.48832 GeV)****Strengths**

Resonance strengths and vertical tunes are derived from the numerical simulation results by matching of numerical  $\bar{S}_z(\gamma G)$  using Eq. 4, page 10.

This yields the results in Tab. 8.

Table 8: Dependence of resonance strength squared ( $|J_n|^2$ ) on vertical invariant ( $\epsilon_z$ ).  $\nu_z$  compares fairly well with Fourier analysis of particle motion on  $\epsilon_z$  invariant.

$\epsilon_z/\pi$ ( $10^{-6}$ m.rad)	$\nu_z$ (Fourier)	$\nu_z$ (fit)	$ J_n ^2$ ( $10^{-5}$ )	$ J_n ^2/\epsilon_z/\pi$
0.0017	.763	8.7631	0.80592	4700
0.17		8.7639	94.5166	5559



$$\gamma G = 36 + \nu_z (22.48832 \text{ GeV}) - \epsilon_z/\pi = 0.0017 \cdot 10^{-6}$$

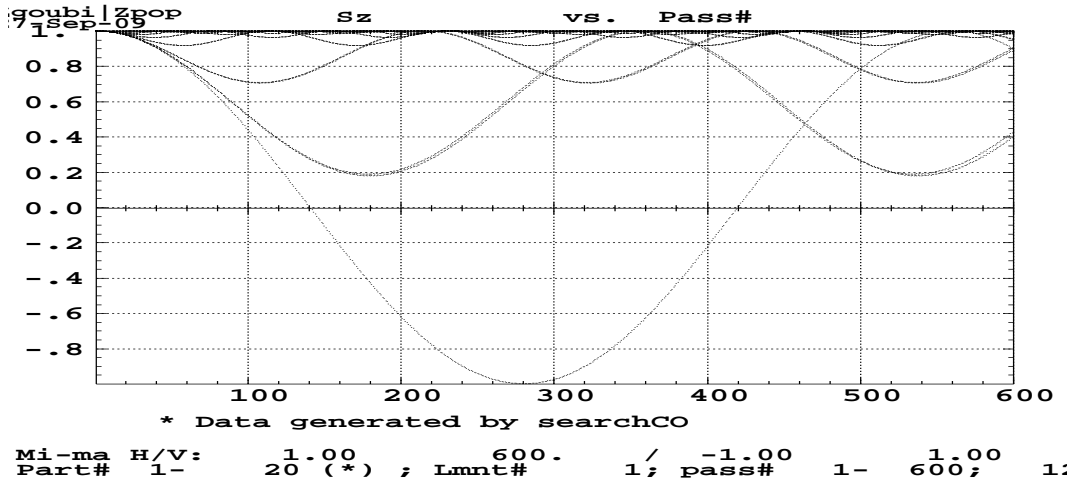


Figure 149:  $S_z$  versus turn number for various distances to the resonance.

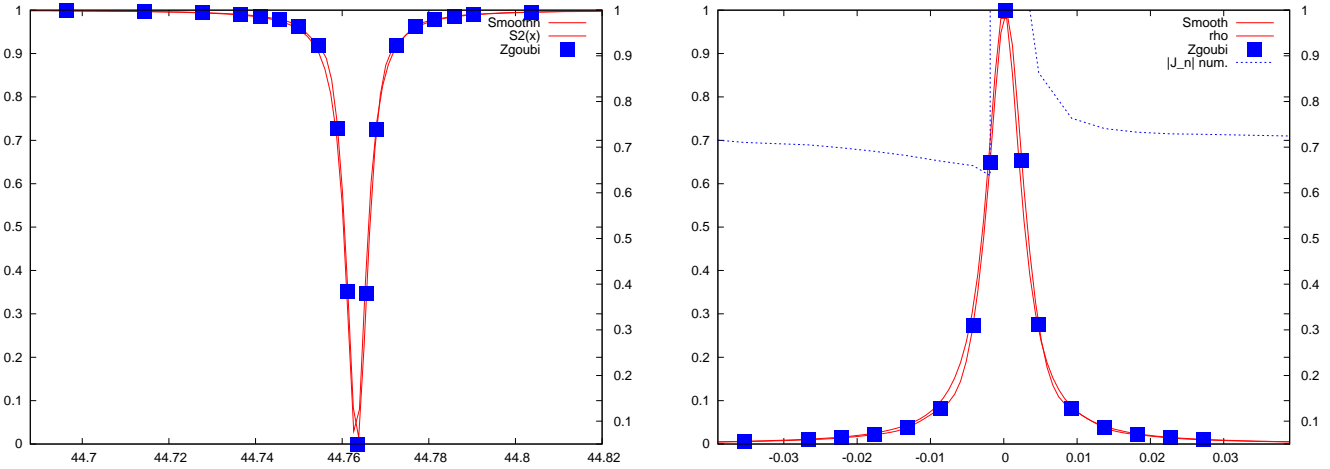


Figure 150: Matching  $S_z^2(\Delta)$  (left, Eq. 4) and  $\rho^2(\Delta)$  (right, Eq. 5) The right plot also shows  $|J_n|^2$  from numerical data (with expectable lack of accuracy in the region  $\Delta \rightarrow 0$ ).

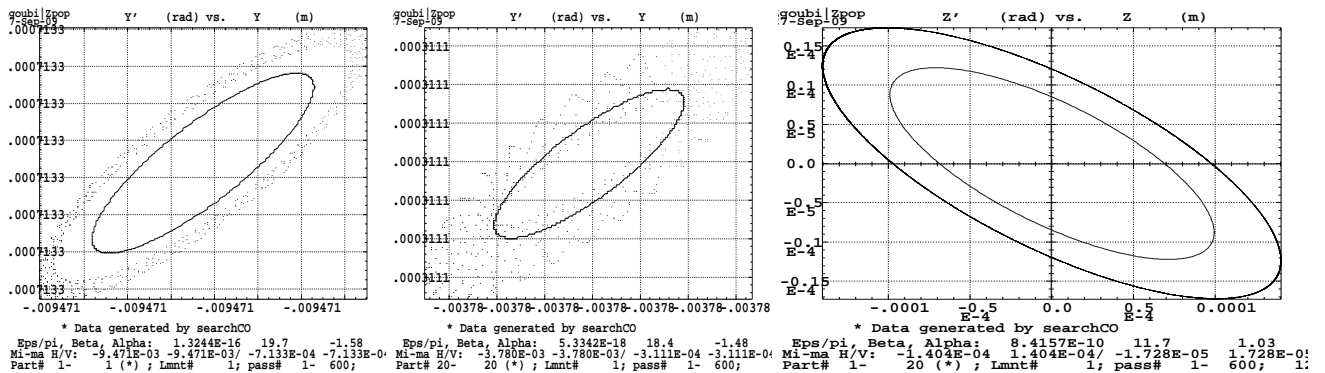


Figure 151: Left :  $x-x'$  of particles at min. and max.  $p/p_0$ . Right :  $z-z'$  (all particles superimposed).



$$\gamma G = 36 + \nu_z (22.48832 \text{ GeV}) - \epsilon_z / \pi = 0.17 \cdot 10^{-6}$$

## Tracking data

Zgoubi.dat, excerpts :

36+nu, static

'OBJET'

78.07999e3

2

```

20 1 V invariant=0.17e-6
-9.470844E-01 -7.132618E-01 -0.0643 -0.0498 0.0E+00 9.98500000E-01 'p' 22453.23 MeV
-8.662617E-01 -6.560475E-01 -0.0643 -0.0498 0.0E+00 9.98900000E-01 'p' 22462.59 MeV
-8.055577E-01 -6.130895E-01 -0.0643 -0.0498 0.0E+00 9.99200000E-01 'p' 22469.61 MeV
-7.650340E-01 -5.844263E-01 -0.0643 -0.0498 0.0E+00 9.99400000E-01 'p' 22474.28 MeV
-7.447550E-01 -5.700858E-01 -0.0643 -0.0498 0.0E+00 9.99500000E-01 'p' 22476.62 MeV
-7.244648E-01 -5.557393E-01 -0.0643 -0.0498 0.0E+00 9.99600000E-01 'p' 22478.96 MeV
-7.041638E-01 -5.413870E-01 -0.0643 -0.0498 0.0E+00 9.99700000E-01 'p' 22481.30 MeV
-6.838522E-01 -5.270291E-01 -0.0643 -0.0498 0.0E+00 9.99800000E-01 'p' 22483.64 MeV
-6.635304E-01 -5.126658E-01 -0.0643 -0.0498 0.0E+00 9.99900000E-01 'p' 22485.98 MeV
-6.533656E-01 -5.054822E-01 -0.0643 -0.0498 0.0E+00 9.99950000E-01 'p' 22487.15 MeV
-6.431983E-01 -4.982973E-01 -0.0643 -0.0498 0.0E+00 1.00000000E+00 'p' 22488.32 MeV
-6.330285E-01 -4.911112E-01 -0.0643 -0.0498 0.0E+00 1.00005000E+00 'p' 22489.49 MeV
-6.228561E-01 -4.839238E-01 -0.0643 -0.0498 0.0E+00 1.00010000E+00 'p' 22490.66 MeV
-6.025037E-01 -4.695452E-01 -0.0643 -0.0498 0.0E+00 1.00020000E+00 'p' 22493.00 MeV
-5.821413E-01 -4.551616E-01 -0.0643 -0.0498 0.0E+00 1.00030000E+00 'p' 22495.33 MeV
-5.617687E-01 -4.407730E-01 -0.0643 -0.0498 0.0E+00 1.00040000E+00 'p' 22497.67 MeV
-5.413860E-01 -4.263795E-01 -0.0643 -0.0498 0.0E+00 1.00050000E+00 'p' 22500.01 MeV
-5.209933E-01 -4.119812E-01 -0.0643 -0.0498 0.0E+00 1.00060000E+00 'p' 22502.35 MeV
-4.597547E-01 -3.687569E-01 -0.0643 -0.0498 0.0E+00 1.00090000E+00 'p' 22509.37 MeV
-3.779636E-01 -3.110579E-01 -0.0643 -0.0498 0.0E+00 1.00130000E+00 'p' 22518.72 MeV

```

1 1

'SCALING'

1 2

MULTIPOL SBEN

-1

78.07999

1

MULTIPOL QUAD

-1

78.07999

1

'PARTICUL'

938.27203d0 1.602176487d-19 1.7928474d0 0.0.

3

4

Checking computation results : for the 20 particles above, from 200 turns analysis, their H closed orbits, fractional tunes (Fourier analysis) and complements to 1, H and V invariant values, energy :

%	XCO	X'CO	XNU	ZNU	1-XNU	1-ZNU	epsilon/pi_X,Z,1	time(mus)	E(MeV)
-9.471191E-03	-7.132492E-04	0.256831	0.238846	0.743169	0.761154	5.925320E-14	8.428749E-08	1.697588E-09	2.69412 22453.2
-8.665436E-03	-6.562084E-04	0.265155	0.238248	0.734845	0.761752	7.102949E-14	8.424973E-08	1.188318E-08	2.69413 22462.6
-8.056784E-03	-6.132896E-04	0.271387	0.237779	0.728613	0.762221	5.860524E-14	8.422212E-08	7.922146E-09	2.69414 22469.6
-7.649985E-03	-5.843489E-04	0.275548	0.237463	0.724452	0.762537	5.496437E-14	8.420384E-08	1.075151E-08	2.69415 22474.3
-7.449236E-03	-5.701867E-04	0.277640	0.237307	0.722360	0.762693	5.424775E-14	8.419471E-08	6.790436E-09	2.69415 22476.6
-7.246618E-03	-5.559006E-04	0.279730	0.237154	0.720270	0.762846	5.443044E-14	8.418559E-08	1.641024E-08	2.69416 22479.0
-7.041855E-03	-5.414722E-04	0.281801	0.236998	0.718199	0.763002	5.458121E-14	8.417649E-08	6.790453E-09	2.69416 22481.3
-6.838782E-03	-5.269547E-04	0.283885	0.236844	0.716115	0.763156	5.488327E-14	8.416743E-08	9.619820E-09	2.69416 22483.6
-6.638039E-03	-5.128970E-04	0.285944	0.236693	0.714056	0.763307	5.496553E-14	8.415843E-08	4.526980E-09	2.69417 22486.0
-6.534031E-03	-5.055584E-04	0.287019	0.236616	0.712981	0.763384	5.491074E-14	8.415396E-08	1.923968E-08	2.69417 22487.1
-6.432217E-03	-4.982846E-04	0.288055	0.236539	0.711945	0.763461	5.505559E-14	8.414952E-08	3.961112E-09	2.69417 22488.3
-6.332021E-03	-4.911956E-04	0.289102	0.236460	0.710898	0.763540	5.518761E-14	8.414509E-08	5.658735E-09	2.69417 22489.5
-6.230466E-03	-4.841332E-04	0.290139	0.236382	0.709861	0.763618	5.511605E-14	8.414069E-08	1.697622E-09	2.69417 22490.7
-6.024385E-03	-4.694925E-04	0.292236	0.236227	0.707764	0.763773	5.515216E-14	8.413197E-08	1.188337E-08	2.69418 22493.0
-5.823444E-03	-4.552429E-04	0.294313	0.236069	0.705687	0.763931	5.520688E-14	8.412332E-08	2.829376E-09	2.69418 22495.3
-5.619226E-03	-4.409711E-04	0.296394	0.235905	0.703606	0.764095	5.503099E-14	8.411473E-08	4.527008E-09	2.69418 22497.7
-5.413718E-03	-4.263393E-04	0.298460	0.235742	0.701540	0.764258	5.531948E-14	8.410615E-08	5.092890E-09	2.69419 22500.0
-5.211530E-03	-4.120730E-04	0.300571	0.235577	0.699429	0.764423	5.505439E-14	8.409755E-08	7.922284E-09	2.69419 22502.4
-4.598617E-03	-3.688727E-04	0.306842	0.235073	0.693158	0.764927	5.526524E-14	8.407108E-08	3.395277E-09	2.69420 22509.4
-3.780573E-03	-3.110925E-04	0.315188	0.234408	0.684812	0.765592	5.530870E-14	8.403336E-08	1.697647E-08	2.69421 22518.7

$$\gamma G = 36 + \nu_z (22.48832 \text{ GeV}) - \epsilon_z/\pi = 0.17 \cdot 10^{-6}$$

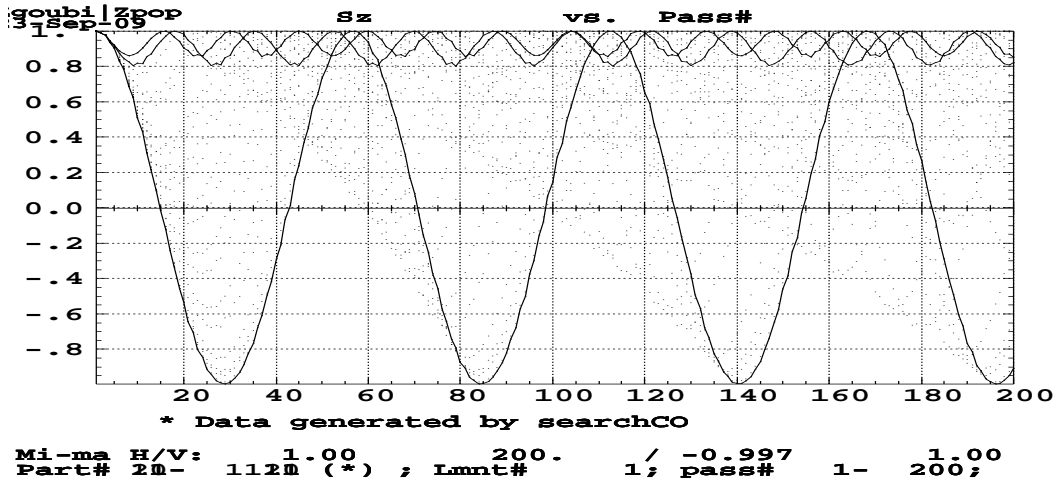


Figure 152:  $S_z$  versus turn number for various distances to the resonance.

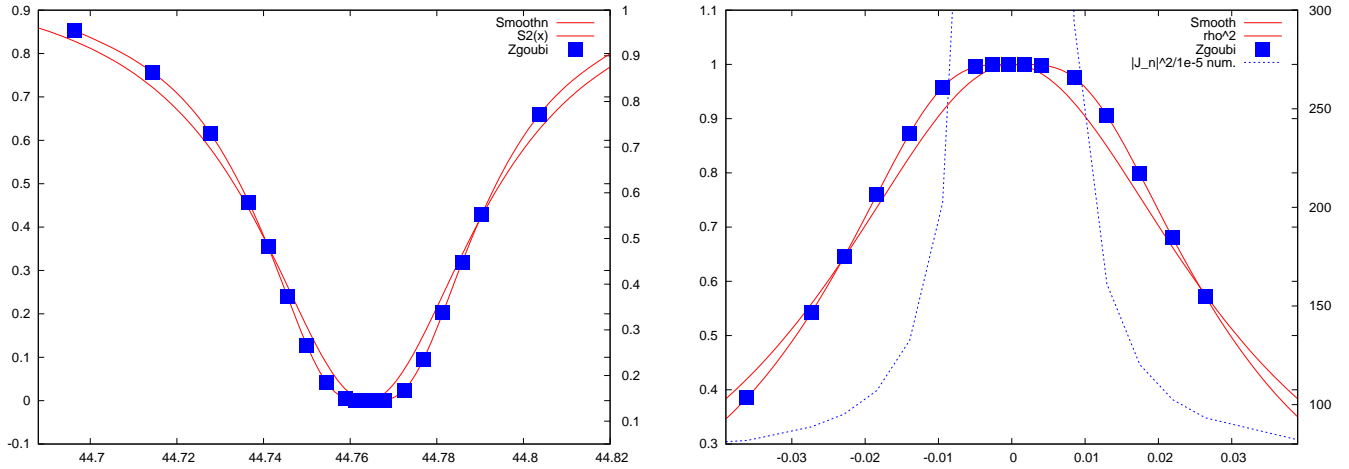


Figure 153: Matching  $S_z^2(\Delta)$  (left, Eq. 4) and  $\rho^2(\Delta)$  (right, Eq. 5) The right plot also shows  $|J_n|^2$  from numerical data (with expectable lack of accuracy in the region  $\Delta \rightarrow 0$ ).

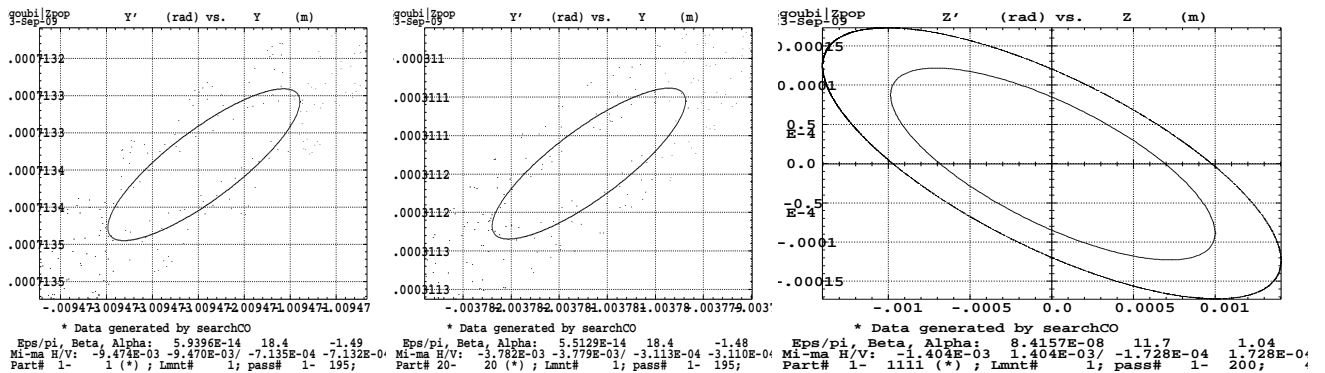


Figure 154: Left :  $x-x'$  of particles at min. and max.  $p/p_0$ . Right :  $z-z'$  (all particles superimposed).

## 6 Fresnel integrals approximation of weak resonances

The goal of this section is to check zgoubi against the weak resonance approximation of resonance crossing dynamics, see Sec. 2.3.4.

Matching the tracking results by the Fresnel integral approximation would yield the crossing speed  $\alpha$  and the resonance strength  $|J_n|$ . In the figures below crossing velocity is taken to be the same as used earlier,  $\alpha = 4.4096356 \cdot 10^{-5}$ , and resonance strength is taken from Tabs. 2, 3, Froissard-Stora crossing conditions, whereas  $\nu_z = 8.76346$  from Zgoubi, as earlier.

- $\gamma G = \nu_z (3.648013 \text{ GeV}) - \epsilon_z/\pi = 0.002 \cdot 10^{-6}$

$\pi|J_n|^2/\alpha \approx 0.014$ , higher order terms have negligible effect.

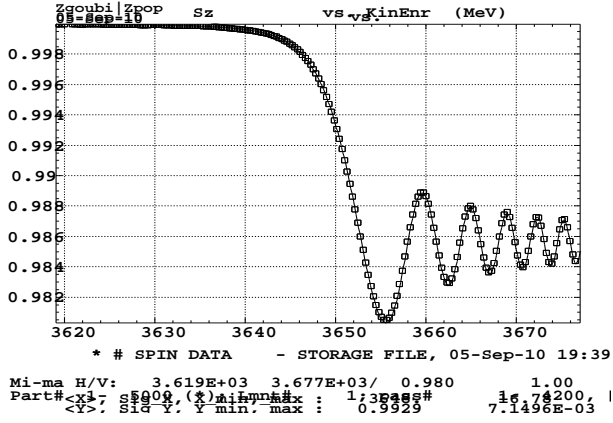


Figure 155: Superimposition of Fresnel integral model (squares) and zgoubi tracking (solid line),  $\epsilon_z/\pi = 0.002 \cdot 10^{-6}$ .

- $\gamma G = \nu_z (3.648013 \text{ GeV}) - \epsilon_z/\pi = 0.01 \cdot 10^{-6}$

$\pi|J_n|^2/\alpha \approx 0.071$ , higher order terms have sensible effect.

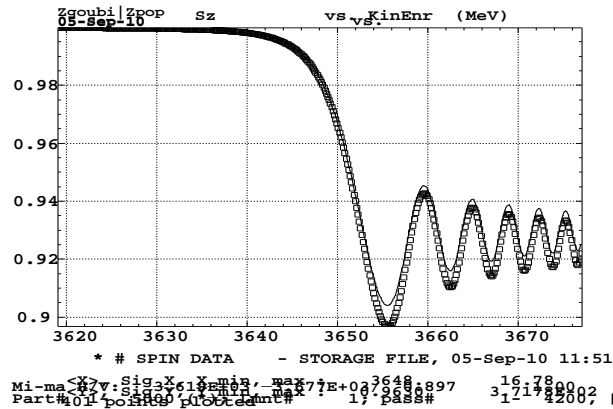


Figure 156: Superimposition of Fresnel integral model (squares) and zgoubi tracking (solid line) in a case of greater effect compared to the previous Fig. 155 :  $\epsilon_z/\pi = 0.01 \cdot 10^{-6}$ . The truncation of Froissard-Stora formula leads to an overestimate of  $p_f/p_i$  (Eq. 7).

$$\begin{aligned} & \bullet \theta < 0 : \\ \left(\frac{p(\theta)}{p_i}\right)^2 &= 1 - \frac{\pi}{\alpha} |J_n|^2 \left[ (0.5 - C(-\theta \sqrt{\frac{a}{\pi}}))^2 + (0.5 - S(-\theta \sqrt{\frac{a}{\pi}}))^2 \right] \\ & \bullet \theta > 0 : \\ \left(\frac{p(\theta)}{p_i}\right)^2 &= 1 - \frac{\pi}{\alpha} |J_n|^2 \left[ (0.5 + C(\theta \sqrt{\frac{a}{\pi}}))^2 + (0.5 + S(\theta \sqrt{\frac{a}{\pi}}))^2 \right] \end{aligned}$$

$$C(x) = \int_0^x \cos\left(\frac{\pi}{2} t^2\right) dt, \quad S(x) = \int_0^x \sin\left(\frac{\pi}{2} t^2\right) dt$$

$$2 \exp(-A^2) - 1 \approx 1 - A^2 \text{ no longer holds}$$

- $\gamma G = 36 + \nu_z (22.4883 \text{ GeV}) - \epsilon_z/\pi = 0.0001 \cdot 10^{-6}$

$\pi|J_n|^2/\alpha \approx 0.013$ , higher order terms have negligible effect.

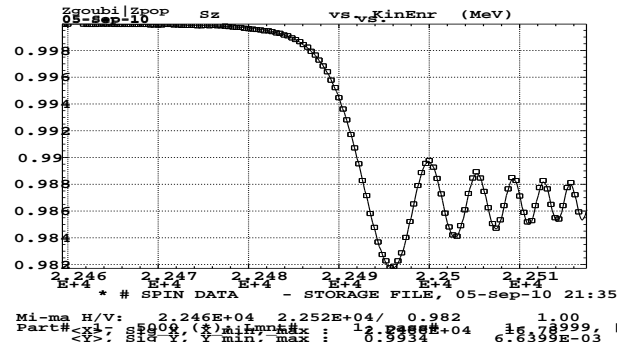


Figure 157: Superimposition of Fresnel integral model (squares) and zgoubi tracking (solid line)  $\epsilon_z/\pi = 0.0001 \cdot 10^{-6}$ .

- $\gamma G = 9 (3.7718 \text{ GeV}) - z_{CO} = 1.3 \text{ mm}$

$\pi|J_n|^2/\alpha \approx 0.0059$ , higher order terms have negligible effect.

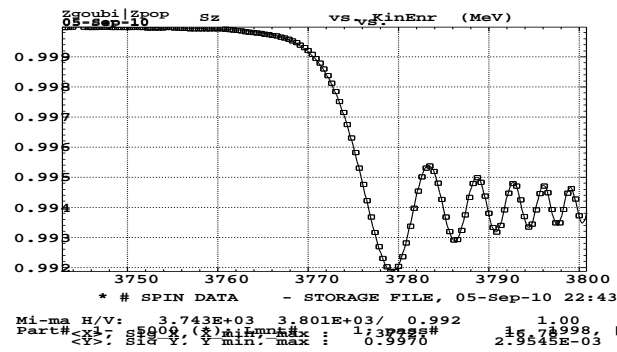


Figure 158: Superimposition of Fresnel integral model (squares) and zgoubi tracking (solid line).

- $\gamma G = 45 (22.61211 \text{ GeV}) - z_{CO} = 0.028 \text{ mm}$

$\pi|J_n|^2/\alpha \approx 0.004$ , higher order terms have negligible effect.

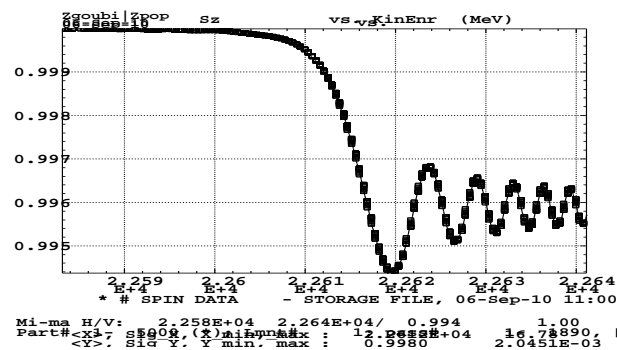


Figure 159: Superimposition of Fresnel integral model (squares) and zgoubi tracking (solid line).

## 7 $\vec{n}_0$ spin vector, AGS bare lattice

To perform this experiment, we consider a single particle at fixed energy, we sit at  $T = 3775.00$  GeV within the span of  $\gamma G = 9$  ( $T = 3.7716$  GeV). The resonance is excited by a  $\hat{z} \approx 2.8$  mm vertical closed orbit defect (same as earlier, Fig. 100 page 49).

The particle is launched on closed H and V orbit ( $\epsilon_x = \epsilon_z = 0$ , Fig. 160) with first  $S_z = 1$ , the polarization vector then oscillates around the  $\vec{n}_0$  vector, Fig. 161.

The FIT procedure allows finding  $\vec{n}_0$ , typical zgoubi.dat input in App. B.2.

Given the FIT results, the particle is then launched, again on closed H and V orbit, with now  $\vec{S} = \text{closed orbit } \vec{S}$ . Fig. 162 shows that the polarization vector, as observed turn after turn at 'Begin SUPERA' (entrance to A1BF main dipole), is now stationary.

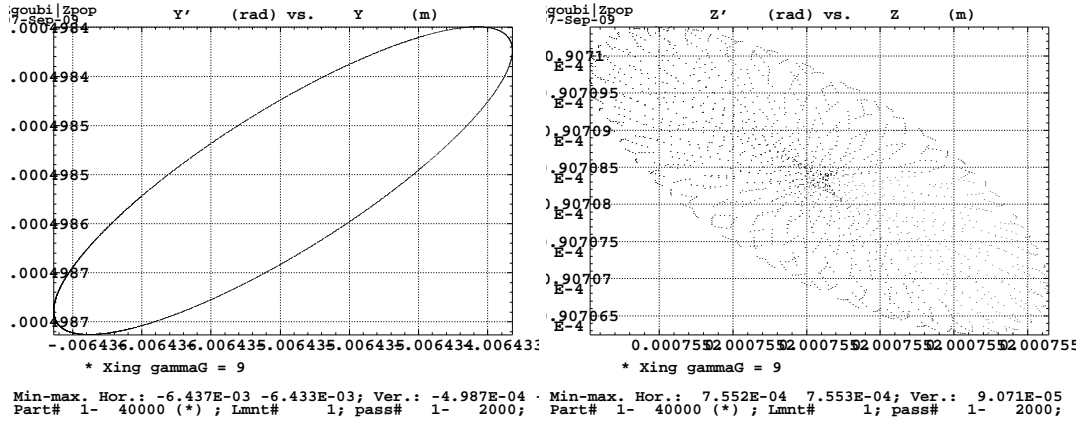


Figure 160: The particle sits on H and V closed orbits - observed at 'Begin SUPERA' (entrance to A1BF main dipole). Namely, the particle describes quasi zero  $\epsilon_x$  and  $\epsilon_y$  invariants, as shown here.

$$\vec{S}_{initial} = \vec{S}_z$$

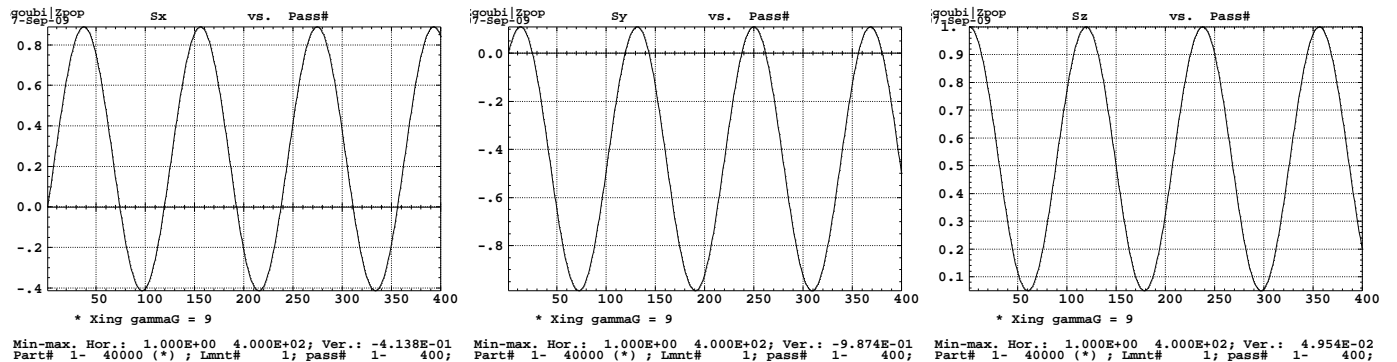
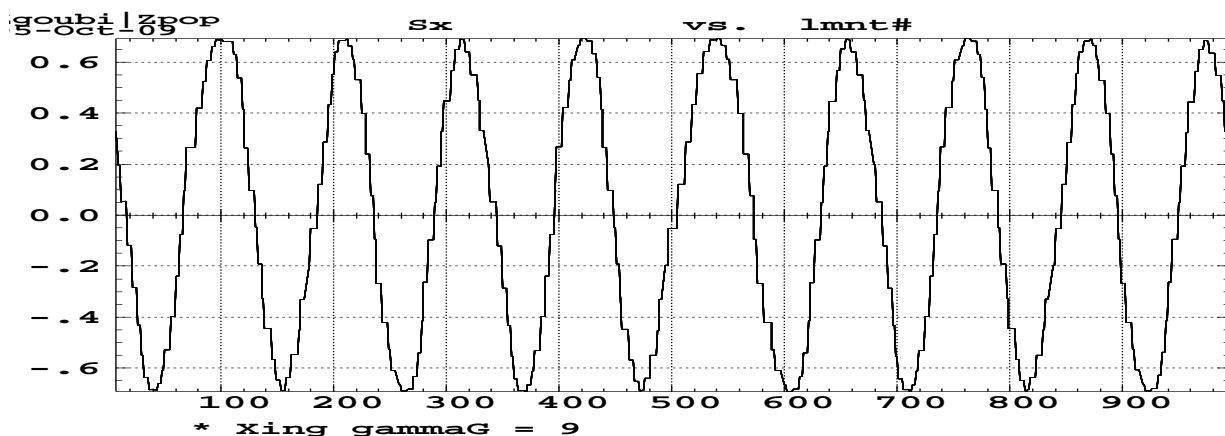
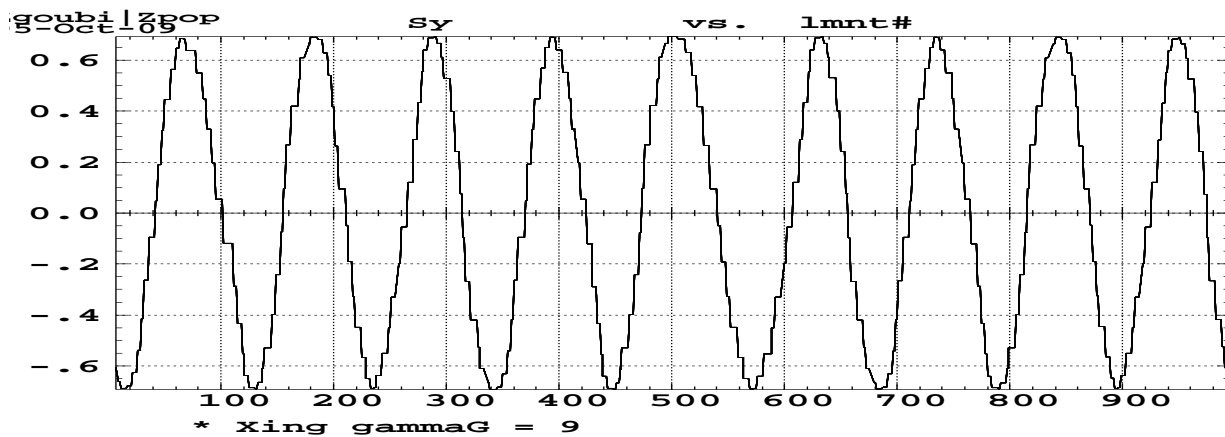


Figure 161: From top to bottom,  $S_x$   $S_y$   $S_z$  versus turn number observed at 'Begin SUPERA'. Static case ( $T = 3775.00$  GeV), given  $\vec{S}_{initial} = \vec{S}_z$ .

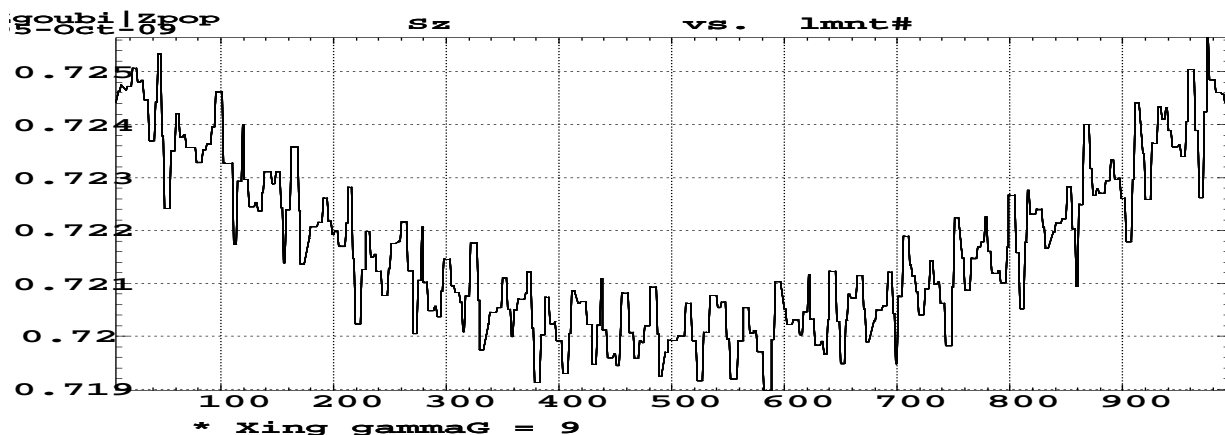
$\vec{n}_0$  vector over a turn,  $\vec{S}_{initial} = \vec{S}_{final} \equiv \text{closed-orbit } \vec{S}$



Mi-ma H/V: 7.00 995. / -0.692 0.692  
Part# 1- 40000 (\*) ; Lmnt# 1; pass# 1- 10;



Mi-ma H/V: 7.00 995. / -0.693 0.692  
Part# 1- 40000 (\*) ; Lmnt# 1; pass# 1- 10;



Mi-ma H/V: 7.00 995. / 0.719 0.726  
Part# 1- 40000 (\*) ; Lmnt# 1; pass# 1- 10;

Figure 162: From top to bottom,  $S_x$   $S_y$   $S_z$  along machine circumference versus pick-up number (about 990 P-Us over the 807 m circumference). Static case ( $T = 3775.00$  GeV), given  $\vec{S}_{initial} \equiv \text{closed-orbit } \vec{S}$ .

# APPENDIX

## A MAD files

Excerpts of MAD files are reproduced, for reference.

### A.1 Command file

```
option,-echo
gam=4.5/1.7928474
mass = 0.93827231
MOM := sqrt(gam*gam-1)*mass

call file = "f.constants"
call file = "f.conversions"

call "nosnake.sub"
title "G*gam=4.5 A20snk 2.5T, E20snk 1.5T, A19cor = B1cor"

call file = "f.snkinsert.lat"
call file = "f.lat"
XXX:=0

!TITLE, "AGS SEB MAD, initiated 2/6/98, KAB"
USE, AGS
beam, particle=proton, gamma=gam, size=0.001, sigt=1

use, ags
print,#E
twiss, tape, deltap=-0.01,0.0,0.01 save

stop
```

### A.2 "print" file

```
I G*gam=4.5 A20snk 2.5T, E20snk 1.5T, A19cor = B1cor "MAD" Version: 8.23/08 Run: 24/08/09 06.33.46
Linear lattice functions. TWISS line: AGS range: #S/#E
Delta(p)/p: -0.010000 symm: F super: 1 page 1
```

ELEMENT SEQUENCE			H O R I Z O N T A L										V E R T I C A L					
pos.	element	occ.	dist I	betax	alfax	mux	x(co)	px(co)	Dx	Dpx	I	betay	alfay	muy	y(co)	py(co)	Dy	Dpy
no.	name	no.	[m]	[m]	[1]	[2pi]	[mm]	[.001]	[m]	[1]	I	[m]	[1]	[2pi]	[mm]	[.001]	[m]	[1]
begin	AGS	1	0.000	19.403	-1.574	0.000	-19.5858	-1.363	1.974	0.131	I	11.696	1.050	0.000	0.0000	0.000	0.000	0.000
end	AGS	1	807.076	19.403	-1.574	8.918	-19.5858	-1.363	1.974	0.131	I	11.696	1.050	8.750	0.0000	0.000	0.000	0.000
total length =			807.075641		Qx	=	8.917998		Qy	=	8.750382							
delta(s) =			-120.036170	mm	Qx'	=	-22.144970		Qy'	=	1.106873							
alfa =			0.131374E-01		betax(max)	=	22.522370		betay(max)	=	22.897941							
gamma(tr) =			8.724595		Dx(max)	=	2.416062		Dy(max)	=	0.000000							
					Dx(r.m.s.)	=	1.886261		Dy(r.m.s.)	=	0.000000							
					xco(max)	=	21.526346		yco(max)	=	0.000000							
					xco(r.m.s.)	=	17.795141		yco(r.m.s.)	=	0.000000							

```
I G*gam=4.5 A20snk 2.5T, E20snk 1.5T, A19cor = B1cor "MAD" Version: 8.23/08 Run: 24/08/09 06.33.46
Linear lattice functions. TWISS line: AGS range: #S/#E
Delta(p)/p: 0.000000 symm: F super: 1 page 1
```

ELEMENT SEQUENCE			H O R I Z O N T A L										V E R T I C A L					
pos.	element	occ.	dist I	betax	alfax	mux	x(co)	px(co)	Dx	Dpx	I	betay	alfay	muy	y(co)	py(co)	Dy	Dpy
no.	name	no.	[m]	[m]	[1]	[2pi]	[mm]	[.001]	[m]	[1]	I	[m]	[1]	[2pi]	[mm]	[.001]	[m]	[1]
begin	AGS	1	0.000	19.785	-1.585	0.000	0.0000	0.000	2.211	0.154	I	11.701	1.037	0.000	0.0000	0.000	0.000	0.000
end	AGS	1	807.076	19.785	-1.585	8.711	0.0000	0.000	2.211	0.154	I	11.701	1.037	8.764	0.0000	0.000	0.000	0.000
total length =			807.075641		Qx	=	8.710595		Qy	=	8.764380							
delta(s) =			0.000000	mm	Qx'	=	-22.734051		Qy'	=	1.734352							
alfa =			0.140063E-01		betax(max)	=	22.917409		betay(max)	=	22.743834							
gamma(tr) =			8.449647		Dx(max)	=	2.356352		Dy(max)	=	0.000000							
					Dx(r.m.s.)	=	1.984102		Dy(r.m.s.)	=	0.000000							
					xco(max)	=	0.000000		yco(max)	=	0.000000							
					xco(r.m.s.)	=	0.000000		yco(r.m.s.)	=	0.000000							

```
I G*gam=4.5 A20snk 2.5T, E20snk 1.5T, A19cor = B1cor "MAD" Version: 8.23/08 Run: 24/08/09 06.33.46
Linear lattice functions. TWISS line: AGS range: #S/#E
Delta(p)/p: 0.010000 symm: F super: 1 page 1
```

ELEMENT SEQUENCE			H O R I Z O N T A L										V E R T I C A L					
pos.	element	occ.	dist I	betax	alfax	mux	x(co)	px(co)	Dx	Dpx	I	betay	alfay	muy	y(co)	py(co)	Dy	Dpy
no.	name	no.	[m]	[m]	[1]	[2pi]	[mm]	[.001]	[m]	[1]	I	[m]	[1]	[2pi]	[mm]	[.001]	[m]	[1]
begin	AGS	1	0.000	18.727	-1.324	0.000	20.7717	1.436	2.337	0.162	I	11.695	1.023	0.000	0.0000	0.000	0.000	0.000
end	AGS	1	807.076	18.727	-1.324	8.499	20.7717	1.436	2.337	0.162	I	11.695	1.023	8.784	0.0000	0.000	0.000	0.000
total length =			807.075641		Qx	=	8.498805		Qy	=	8.784146							
delta(s) =			126.662810	mm	Qx'	=	-21.581260		Qy'	=	2.394821							
alfa =			0.149658E-01		betax(max)	=	27.834540		betay(max)	=	22.586341							
gamma(tr) =			8.174277		Dx(max)	=	2.472667		Dy(max)	=	0.000000							
					Dx(r.m.s.)	=	2.097844		Dy(r.m.s.)	=	0.000000							
					xco(max)	=	22.031544		yco(max)	=	0.000000							
					xco(r.m.s.)	=	18.634115		yco(r.m.s.)	=	0.000000							

# B Zgoubi data file specimen

## B.1 1-turn first order mapping calculation

Typical zgoubi.dat file including appropriate commands for MATRIX calculation.

Data generated by searchCO

```

'OBJET' 1000.0 1
5
.001 .001 .001 .001 0. .0001
-6.431975E-01 -4.982951E-01 0.0E+00 0.0 0.0 1.000E+00 'o'
'PARTICUL' 2
938.27203d0 1.602176487d-19 1.7928474d0 0. 0.
'SCALING' 3
0 3
MULTIPOL SBEN
2
7.50690875556628 7.50690875556628
1 99999
MULTIPOL QUAD
2
7.50690875556628 7.50690875556628
1 99999
'PICKUPS' 4
1
#S
'FAISTORE' 5
b_zgoubi.fai #S
1
'MARKER' #S
'MARKER' MARK BSUPERA
'MULTIPOL' SBEN ALBF
0 .Dip
200.6554 10. 0.11712499 0.04848519 -0.00050563 0 0 0 0 0 0 0
0. 0. 10. 4.0 0.800 0.00 0.00 0.00 0.00 0. 0. 0. 0.
4 .1455 2.2670 -.6395 1.1558 0. 0. 0.
0. 0. 10. 4.0 0.800 0.00 0.00 0.00 0.00 0. 0. 0. 0.
4 .1455 2.2670 -.6395 1.1558 0. 0. 0.
0. 0. 0. 0. 0. 0. 0. 0. 0. 0. 0. 0.
#20|20|20 Dip ALBF
3 0.0000 0.0000 -1.1751150450E-002
'DRIFT' DRIF D2S 9
60.9515
'MULTIPOL' SBEN A2BF 10
0 .Dip
200.6554 10. 0.11712499 0.04848519 -0.00050563 0 0 0 0 0 0 0
0. 0. 10. 4.0 0.800 0.00 0.00 0.00 0.00 0. 0. 0. 0.
4 .1455 2.2670 -.6395 1.1558 0. 0. 0.
0. 0. 10. 4.0 0.800 0.00 0.00 0.00 0.00 0. 0. 0. 0.
4 .1455 2.2670 -.6395 1.1558 0. 0. 0.
0. 0. 0. 0. 0. 0. 0. 0. 0. 0. 0. 0.
#20|20|20 Dip A2BF
3 0.0000 0.0000 -1.1751150450E-002
'DRIFT' DRIF DPUE 11
28.7000
'MARKER' MARK PUE_A02 12
'MULTIPOL' HKIC DHCA02 13
0 .kicker
0.1000E-03 10. 0.0E+00 0 0 0 0 0 0 0 0 0 0 0 0
.0 .0 1.00 0.00 0.00 0.00 0.00 0. 0. 0. 0.
4 .1455 2.2670 -.6395 1.1558 0. 0. 0.
.0 .0 1.00 0.00 0.00 0.00 0.00 0. 0. 0. 0.
4 .1455 2.2670 -.6395 1.1558 0. 0. 0.
0.0000 0. 0. 0. 0. 0. 0. 0. 0. 0. 0. 0.
#20|20|20 Kick
1 0. 0. 0.
'MULTIPOL' VKIC DVCA02 14
0 .kicker
0.1000E-03 10. 0.0E+00 0 0 0 0 0 0 0 0 0 0 0 0
.0 .0 1.00 0.00 0.00 0.00 0.00 0. 0. 0. 0.
4 .1455 2.2670 -.6395 1.1558 0. 0. 0.
.0 .0 1.00 0.00 0.00 0.00 0.00 0. 0. 0. 0.
4 .1455 2.2670 -.6395 1.1558 0. 0. 0.
1.570796327 0. 0. 0. 0. 0. 0. 0. 0. 0. 0. 0.
#20|20|20 Kick
1 0. 0. 0.
'DRIFT' DRIF D2TX 15
32.2485
'MULTIPOL' SBEN A3CD 16
0 .Dip
238.7522 10. 0.11712611 -0.04865238 -0.00043783 0 0 0 0 0 0 0
0. 0. 10. 4.0 0.800 0.00 0.00 0.00 0.00 0. 0. 0. 0.
4 .1455 2.2670 -.6395 1.1558 0. 0. 0.
0. 0. 10. 4.0 0.800 0.00 0.00 0.00 0.00 0. 0. 0. 0.
4 .1455 2.2670 -.6395 1.1558 0. 0. 0.
0. 0. 0. 0. 0. 0. 0. 0. 0. 0. 0. 0.
#20|24|20 Dip A3CD
3 0.0000 0.0000 -1.3982515350E-002
'DRIFT' DRIF DSQ 17
37.1047
'MULTIPOL' QUAD QHFV 18
0 .Quad
39.0880 10. 0.00000 0.00000 0 0 0 0 0 0 0 0 0 0
0. 0. 6.00 3.00 1.00 0.00 0.00 0.00 0.00 0. 0. 0. 0.
6 .1122 6.2671 -1.4982 3.5882 -2.1209 1.723
0. 0. 0. 0. 0. 0. 0. 0. 0. 0. 0. 0.
#30|39|30 Quad QHFV
1 0. 0. 0.
'MULTIPOL' QUAD QPOL 19
0 .Quad
39.0880 10. 0.00000 0.00000 0 0 0 0 0 0 0 0 0 0
0. 0. 6.00 3.00 1.00 0.00 0.00 0.00 0.00 0. 0. 0. 0.
6 .1122 6.2671 -1.4982 3.5882 -2.1209 1.723
0. 0. 6.00 3.00 1.00 0.00 0.00 0.00 0.00 0.00 0. 0. 0. 0.
6 .1122 6.2671 -1.4982 3.5882 -2.1209 1.723
0. 0. 0. 0. 0. 0. 0. 0. 0. 0. 0. 0.
#30|39|30 Quad QPOL
1 0. 0. 0.
'DRIFT' DRIF DSQ 20
37.1047
'DRIFT' DRIF DPUE 982
28.7000
'MARKER' MARK PUE_L18 983
'MULTIPOL' HKIC DHCL18 984
0 .kicker
0.1000E-03 10. 0.0E+00 0 0 0 0 0 0 0 0 0 0 0 0
.0 .0 1.00 0.00 0.00 0.00 0.00 0. 0. 0. 0.
4 .1455 2.2670 -.6395 1.1558 0. 0. 0.
.0 .0 1.00 0.00 0.00 0.00 0.00 0. 0. 0. 0.
4 .1455 2.2670 -.6395 1.1558 0. 0. 0.
0.0000 0. 0. 0. 0. 0. 0. 0. 0. 0. 0. 0.
#20|20|20 Kick
1 0. 0. 0.
'MULTIPOL' VKIC DVCL18 985
0 .kicker
0.1000E-03 10. 0.0E+00 0 0 0 0 0 0 0 0 0 0 0 0
.0 .0 1.00 0.00 0.00 0.00 0.00 0. 0. 0. 0.
4 .1455 2.2670 -.6395 1.1558 0. 0. 0.
1.570796327 0. 0. 0. 0. 0. 0. 0. 0. 0. 0. 0.
#20|20|20 Kick
1 0. 0. 0.
'DRIFT' DRIF D2TX 986
32.2485
'MULTIPOL' SBEN L19BD 987
0 .Dip
200.6554 10. 0.11712499 -0.04843927 -0.00050017 0 0 0 0 0 0 0 0
0. 0. 10. 4.0 0.800 0.00 0.00 0.00 0.00 0. 0. 0. 0.
4 .1455 2.2670 -.6395 1.1558 0. 0. 0.
0. 0. 10. 4.0 0.800 0.00 0.00 0.00 0.00 0. 0. 0. 0.
4 .1455 2.2670 -.6395 1.1558 0. 0. 0.
0. 0. 0. 0. 0. 0. 0. 0. 0. 0. 0. 0.
#20|20|20 Dip L19BD
3 0.0000 0.0000 -1.1751150450E-002
'DRIFT' DRIF D2S 988
60.9515
'MULTIPOL' SBEN L20BD 989
0 .Dip
200.6554 10. 0.11712499 -0.04843927 -0.00050017 0. 0. 0. 0. 0. 0. 0 0
0. 0. 10. 4.0 0.800 0.00 0.00 0.00 0.00 0.00 0. 0. 0. 0.
4 .1455 2.2670 -.6395 1.1558 0. 0. 0.
0. 0. 10. 4.0 0.800 0.00 0.00 0.00 0.00 0.00 0. 0. 0. 0.
4 .1455 2.2670 -.6395 1.1558 0. 0. 0.
0.0000 0. 0. 0. 0. 0. 0. 0. 0. 0. 0. 0.
#20|20|20 Dip L20BD
3 0.0000 0.0000 -1.1751150450E-002
'DRIFT' DRIF DSG10 990
31.7339
'MULTIPOL' HKIC SML20 991
0 .kicker
0.2413E+03 10. 0.0E+00 0 0 0 0 0 0 0 0 0 0 0 0
.0 .0 1.00 0.00 0.00 0.00 0.00 0. 0. 0. 0.
4 .1455 2.2670 -.6395 1.1558 0. 0. 0.
.0 .0 1.00 0.00 0.00 0.00 0.00 0. 0. 0. 0.
4 .1455 2.2670 -.6395 1.1558 0. 0. 0.
0.0000 0. 0. 0. 0. 0. 0. 0. 0. 0. 0. 0.
#20|20|20 Kick
1 0. 0. 0.
'DRIFT' DRIF DSG10 992
31.7339
'MARKER' MARK ESUPERL 993
'MATRIX' 994
1 11
'FAISCEAU' 995
'END' 996

```

```

0. 0. 6.00 3.00 1.00 0.00 0.00 0.00 0.00 0. 0. 0. 0.
6 .1122 6.2671 -1.4982 3.5882 -2.1209 1.723
0. 0. 0. 0. 0. 0. 0. 0. 0. 0. 0. 0.
#30|39|30 Quad QHFV
1 0. 0. 0.
'MULTIPOL' QUAD QPOL 19
0 .Quad
39.0880 10. 0.00000 0.00000 0 0 0 0 0 0 0 0 0 0
0. 0. 6.00 3.00 1.00 0.00 0.00 0.00 0.00 0. 0. 0. 0.
6 .1122 6.2671 -1.4982 3.5882 -2.1209 1.723
0. 0. 6.00 3.00 1.00 0.00 0.00 0.00 0.00 0.00 0. 0. 0. 0.
6 .1122 6.2671 -1.4982 3.5882 -2.1209 1.723
0. 0. 0. 0. 0. 0. 0. 0. 0. 0. 0. 0.
#30|39|30 Quad QPOL
1 0. 0. 0.
'DRIFT' DRIF DSQ 20
37.1047
'DRIFT' DRIF DPUE 982
28.7000
'MARKER' MARK PUE_L18 983
'MULTIPOL' HKIC DHCL18 984
0 .kicker
0.1000E-03 10. 0.0E+00 0 0 0 0 0 0 0 0 0 0 0 0
.0 .0 1.00 0.00 0.00 0.00 0.00 0. 0. 0. 0.
4 .1455 2.2670 -.6395 1.1558 0. 0. 0.
.0 .0 1.00 0.00 0.00 0.00 0.00 0. 0. 0. 0.
4 .1455 2.2670 -.6395 1.1558 0. 0. 0.
0.0000 0. 0. 0. 0. 0. 0. 0. 0. 0. 0. 0.
#20|20|20 Kick
1 0. 0. 0.
'MULTIPOL' VKIC DVCL18 985
0 .kicker
0.1000E-03 10. 0.0E+00 0 0 0 0 0 0 0 0 0 0 0 0
.0 .0 1.00 0.00 0.00 0.00 0.00 0. 0. 0. 0.
4 .1455 2.2670 -.6395 1.1558 0. 0. 0.
1.570796327 0. 0. 0. 0. 0. 0. 0. 0. 0. 0. 0.
#20|20|20 Kick
1 0. 0. 0.
'DRIFT' DRIF D2TX 986
32.2485
'MULTIPOL' SBEN L19BD 987
0 .Dip
200.6554 10. 0.11712499 -0.04843927 -0.00050017 0 0 0 0 0 0 0 0
0. 0. 10. 4.0 0.800 0.00 0.00 0.00 0.00 0. 0. 0. 0.
4 .1455 2.2670 -.6395 1.1558 0. 0. 0.
0. 0. 10. 4.0 0.800 0.00 0.00 0.00 0.00 0. 0. 0. 0.
4 .1455 2.2670 -.6395 1.1558 0. 0. 0.
0. 0. 0. 0. 0. 0. 0. 0. 0. 0. 0. 0.
#20|20|20 Dip L19BD
3 0.0000 0.0000 -1.1751150450E-002
'DRIFT' DRIF D2S 988
60.9515
'MULTIPOL' SBEN L20BD 989
0 .Dip
200.6554 10. 0.11712499 -0.04843927 -0.00050017 0. 0. 0. 0. 0. 0. 0 0
0. 0. 10. 4.0 0.800 0.00 0.00 0.00 0.00 0.00 0. 0. 0. 0.
4 .1455 2.2670 -.6395 1.1558 0. 0. 0.
0. 0. 10. 4.0 0.800 0.00 0.00 0.00 0.00 0.00 0. 0. 0. 0.
4 .1455 2.2670 -.6395 1.1558 0. 0. 0.
0.0000 0. 0. 0. 0. 0. 0. 0. 0. 0. 0. 0.
#20|20|20 Dip L20BD
3 0.0000 0.0000 -1.1751150450E-002
'DRIFT' DRIF DSG10 990
31.7339
'MULTIPOL' HKIC SML20 991
0 .kicker
0.2413E+03 10. 0.0E+00 0 0 0 0 0 0 0 0 0 0 0 0
.0 .0 1.00 0.00 0.00 0.00 0.00 0. 0. 0. 0.
4 .1455 2.2670 -.6395 1.1558 0. 0. 0.
.0 .0 1.00 0.00 0.00 0.00 0.00 0. 0. 0. 0.
4 .1455 2.2670 -.6395 1.1558 0. 0. 0.
0.0000 0. 0. 0. 0. 0. 0. 0. 0. 0. 0. 0.
#20|20|20 Kick
1 0. 0. 0.
'DRIFT' DRIF DSG10 992
31.7339
'MARKER' MARK ESUPERL 993
'MATRIX' 994
1 11
'FAISCEAU' 995
'END' 996

```



## B.2 Zgoubi files, $\vec{n}_0$ vector search using FIT

### zgoubi.dat including FIT input :

```

Xing gammaG = 9
'OBJET'
15.4071e3 14.95063e3
2
1 1
-0.64333404 -0.49841318 7.55234854E-02 9.07085314E-02 0.0E+00 1. 'p'
1
'SCALING'
1 3
MULTIPOL VKIC
-1
15.4071 scales the vertical kick
1
MULTIPOL SBEN
-1
15.4071
1
MULTIPOL QUAD
-1
15.4071
1
'PARTICUL'
938.27203d0 1.602176487d-19 1.7928474d0 0. 0.
'FAISCEAU'
'SPNTRK'
4.1
0.3222862708 -0.6092011735 0.7241015089
'MARKER' #Start
'MARKER' MARK BSUPERA
'MULTIPOL' SBEN ALBF
0 .Dip
200.6554 10.00 0.11712499 0.04848519 -0.00050563 0.0 0.0 0.0 0.0 0.0 0.0 0.0
0. 0. 10.00 4.0 0.800 0.00 0.00 0.00 0.00 0. 0. 0. 0.
4 .1455 2.2670 -.6395 1.1558 0. 0. 0.
0. 0. 10.00 4.0 0.800 0.00 0.00 0.00 0.00 0.00 0. 0. 0.
4 .1455 2.2670 -.6395 1.1558 0. 0. 0.
0. 0. 0. 0. 0. 0. 0. 0. 0. 0.
#20|20|20 Dip ALBF
3 0.0000000000000000 0.0000000000000000 -1.175115045000000E-002
'DRIFT' DRIF D2S
60.9515
.....
'DRIFT' DRIF DSG10
31.7339
'MULTIPOL' HKIC SML20
0 .kicker
0.2413E+03 10.00 0.000000E+00 0.000000 0.0 0.0 0.0 0.0 0.0 0.0 0.0 0.0
.0 .0 1.00 0.00 0.00 0.00 0.00 0. 0. 0. 0.
4 .1455 2.2670 -.6395 1.1558 0. 0. 0.
.0 .0 1.00 0.00 0.00 0.00 0.00 0. 0. 0. 0.
4 .1455 2.2670 -.6395 1.1558 0. 0. 0.
0.000000000 0. 0. 0. 0. 0. 0. 0. 0.
#20|20|20 Kick
1 0. 0. 0.
'DRIFT' DRIF DSG10
31.7339
'MARKER' MARK ESUPERL
'MARKER' #End
'SPNPRT'
'FIT'
3 Variables :
5 10 0 2 Sx_0
5 11 0 2 Sy_0
5 12 0 1 Sz_0
3 Constraints :
10.1 1 1 994 0. .3 0 Sx at end
10.1 1 2 994 0. .3 0 Sy at end
10.1 1 3 994 0. 1. 0 Sz at end
'END'

```

### zgoubi.res including FIT output :

```

996 FIT
variable # 1 IR = 5 , ok.
variable # 1 IP = 10 , ok.
variable # 2 IR = 5 , ok.
variable # 2 IP = 11 , ok.
variable # 3 IR = 5 , ok.
variable # 3 IP = 12 , ok.
constraint # 1 IR = 994 , ok.
constraint # 2 IR = 994 , ok.
constraint # 3 IR = 994 , ok.

FIT variables in good order, FIT will proceed.

STATUS OF VARIABLES (Iteration # 0)
LMNT VAR PARAM MINIMUM INITIAL FINAL MAXIMUM STEP
5 1 10 -0.322 0.328 0.3278000720 0.967 9.764E-15
5 2 11 -1.83 -0.606 -0.6064336572 0.609 1.729E-14
5 3 12 0.00 0.724 0.7244206873 1.45 1.081E-14

STATUS OF CONSTRAINTS
TYPE I J LMNT# DESIRED WEIGHT REACHED KI2 * Parameter(s)

```

```

10 1 1 994 0.0000 0.3000 1.2911894E-13 2.0915E-03 * 0 :
10 1 2 994 0.0000 0.3000 1.1151080E-12 0.1560 * 0 :
10 1 3 994 0.0000 1.000 8.6353147E-12 0.8419 * 0 :
    
```

### B.3 Zgoubi files, ring closed orbit search using FIT

#### zgoubi.dat including FIT input :

```

Data generated by searchCO
'OBJET'
 1000.
5
.001 .001 .001 .001 0. .001
-6.431975E-01 -4.982951E-01 0.0E+00 0.0E+00 0.0E+00 1.00000000E+00 'co'
'MARKER' MARK BSUPERA
'MULTIPOL' SBEN ALBF
0 .Dip
200.6554 10.00 0.11712499 0.04848519 -0.00050563 0.0 0.0 0.0 0.0 0.0 0.0 0.0
0.0 0.10.00 4.0 0.800 0.00 0.00 0.00 0.00 0.0 0.0 0.0
4 .1455 2.2670 -.6395 1.1558 0.0 0.0
0.0 0.10.00 4.0 0.800 0.00 0.00 0.00 0.00 0.0 0.0 0.0
4 .1455 2.2670 -.6395 1.1558 0.0 0.0
0.0 0.0 0.0 0.0 0.0 0.0 0.0 0.0
#20|20|20 Dip ALBF
3 0.0000000000000000 0.0000000000000000 -1.175115045000000E-002
'DRIFT' DRIF D2S
60.9515
.....
.....
.....
'MULTIPOL' HKIC SML20
0 .kicker
0.2413E+03 10.00 0.000000E+00 0.000000 0.0 0.0 0.0 0.0 0.0 0.0 0.0 0.0
0.0 0.1.00 0.00 0.00 0.00 0.00 0.0 0.0 0.0
4 .1455 2.2670 -.6395 1.1558 0.0 0.0
0.0 0.1.00 0.00 0.00 0.00 0.00 0.0 0.0 0.0
4 .1455 2.2670 -.6395 1.1558 0.0 0.0
0.000000000 0.0 0.0 0.0 0.0 0.0 0.0
#20|20|20 Kick
1 0.0 0.0
'DRIFT' DRIF DSG10
31.7339
'MARKER' MARK ESUPERL
'MATRIX'
1 11
'FAISCEAU'
'FIT'
3
1 30 0 3
1 31 0 3
1 35 0 .1
3
3.1 1 2 978 0. 1 0 x_co
3.1 1 3 978 0. 1 0 xp_co
3 1 6 978 80707.6 1 0 co length
'END'
    
```

#### zgoubi.res including FIT output :

```

STATUS OF VARIABLES (Iteration # 0)
LMNT VAR PARAM MINIMUM INITIAL FINAL MAXIMUM STEP
1 1 30 -0.256 -7.034E-02 -7.0344865763E-02 = x_co (cm) 0.128 3.098E-13
1 2 31 -0.359 -9.439E-02 -9.4388984947E-02 = x'_co (cm) 0.180 3.926E-13
1 3 35 0.903 1.00 1.002797547 = p/p_0 1.10 2.127E-13
STATUS OF CONSTRAINTS
TYPE I J LMNT# DESIRED WEIGHT REACHED KI2 * Parameter(s)
3 1 2 978 0.0000000E+00 1.0000E+00 1.3279162E-09 6.9766E-01 * 0 :
3 1 3 978 0.0000000E+00 1.0000E+00 8.0138363E-10 2.5409E-01 * 0 :
3 1 6 978 8.0707564E+04 1.0000E+00 8.0707564E+04 4.8257E-02 * 0 :
    
```

Path length of particle 1 : 80707.564 cm

TRANSFER	MATRIX	ORDRE	1 (MKSA units)			
0.732535	-16.3490		0.00000	0.00000	0.00000	2.92379
0.145067	-1.87262		0.00000	0.00000	0.00000	0.118147
0.00000	0.00000	-0.909176		-11.6183	0.00000	0.00000
0.00000	0.00000	0.175032		1.13689	0.00000	0.00000
-0.338693	3.56095	0.00000		0.00000	1.00000	11.6934
0.00000	0.00000	0.00000		0.00000	0.00000	1.00000

First order symplectic conditions (expected values = 0) :

```

-4.5006E-05 -5.9300E-05 0.000 0.000 0.000 0.000
    
```

Beam matrix (beta/-alpha/-alpha/gamma) and periodic dispersion (MKSA units)

19.898601	1.585380	0.000000	0.000000	0.000000	2.059607
1.585380	0.176567	0.000000	0.000000	0.000000	0.145139
0.000000	0.000000	11.694319	-1.029730	0.000000	0.000000
0.000000	0.000000	-1.029730	0.176183	0.000000	0.000000
0.000000	0.000000	0.000000	0.000000	0.000000	0.000000
0.000000	0.000000	0.000000	0.000000	0.000000	0.000000

Betatron tunes  
 NU\_Y = 0.65346381 NU\_Z = 0.76816038